UNIVERSIDAD MICHOACANA DE SAN NICOLÁS DE HIDALGO

DIVISIÓN DE ESTUDIOS DE POSGRADO DE LA FACULTAD DE INGENIERÍA ELÉCTRICA

"A GENERALIZED SHORT-TERM UNIT COMMITMENT METHODOLOGY FOR ANALYZING ELECTRIC POWER AND NATURAL GAS INTEGRATED SYSTEMS"

BY

CECILE ALEJANDRA TOVAR RAMÍREZ

THESIS

REQUERIMENT FOR THE DEGREE OF

DOCTOR IN SCIENCES IN ELECTRICAL ENGINEERING

ADVISOR

DR. CLAUDIO RUBÉN FUERTE ESQUIVEL

MORELIA, MICHOACÁN OCTOBER 2019

A GENERALIZED SHORT-TERM UNIT COMMITMENT METHODOLOGY FOR ANALYZING ELECTRIC POWER AND NATURAL GAS INTEGRATED SYSTEMS

Los Miembros del Jurado de Examen de Grado aprueban la **Tesis de Doctorado en Ciencias en Ingeniería Eléctrica, Opción en Sistemas Eléctricos** de ***Cecile Alejandra Tovar Ramírez.***

Dra. Elisa Espinosa Juárez
Presidente del Jurado

Dr. Claudio Rubén Fuerte Esquivel
Director de Tesis

Dr. Jaime Cerda Jacobo
Vocal

Dr. J. Aurelio Medina Rios
Vocal

Dr. Jonathan Gómez Martínez
Revisor Externo (CENACE)

Dr. Roberto Tapia Sánchez
Jefe de la División de Estudios de Posgrado de la Facultad de Ingeniería Eléctrica. UMSNH
(Por reconocimiento de firmas)

UNIVERSIDAD MICHOACANA DE SAN NICOLÁS DE HIDALGO
Agosto 2019

Acknowledgments

I want to thank deeply to my parents Ma. de la Paz and Horacio, and to my brother Ulises too, who have given me their unconditional love, example and all the necessary support so that I could reach this great goal in my professional career.

Thanks to my husband, José Guadalupe, my children Ismael, Elizabeth and Abigail, with whom I am really grateful for their patience and unconditional love. They are my inspiration and necessary motivation to keep going in difficult times and to improve myself to be a better person.

I would like to thank specially to my advisor PhD. Claudio Rubén Fuerte Esquivel, for his support and the necessary knowledge to be able to develop this Ph.D. research work, as well as experience, friendship and encourage to continue with my research work.

Also, I like to thank the members of the doctoral committee, for their valuable comments and suggestions that help to improve this research work, as well as to the División de Estudios de Posgrado of the FIE from UMSNH for the support to obtain my doctoral degree.

Financial support given by CONACyT, México, through the project CB-256680 and by the Fondo de Sustentabilidad Energética SENER-CONACyT, México, under grant 246949 is gratefully acknowledged.

Lastly, I thank to the Consejo Nacional de Ciencia y Tecnología (CONACyT) of Mexico for the financial support provided, through the grant No. 251698, which facilitated my doctoral studies.

Contents

Acknowledgments……i
Contents…….…… ii
List of figures……..iv
List of tables…….……viii
List of publications…….....ix
Resumen……..x
Abstract ……....xi
Nomenclature……xii
Acronyms……...……..xvi

1 Introduction

1.1 Research Motivation……1
1.2 State of the art……..2
1.3 Objective……..9
1.4 Methodology……9
1.5 Main Contributions…….……...10
1.6 Justification……11
1.7 Organization of the Thesis……12

2 Generalized short-term unit commitment formulation

2.1 Introduction……...…… 13
2.2 Lagrangian Duality……14
2.3 Decomposition Basics……16
2.4 GUC model…….……...18
2.5 Generalized short-term unit commitment solution……..…….. 22
2.5.1 GUC solution algorithm…….…….……...22
2.6 Optimal gas and AC power flow module…….……...24
2.6.1 Objective function……..24
2.6.2 Natural gas network……... 25

2.6.3 Electricity network……28
2.6.4 Coupling thermal units……...32
2.6.5 Set of decision variables……33
2.7 Dynamic programming module for unit commitment……33
2.8 Conclusions……... 35

3 Case Studies

3.1 Introduction……..…… 37
3.2 Base Case study……38
3.3 The effect of voltage control at a specific node…….……..43
3.4 Effect of increased demand for electricity and natural gas.……..……....45
3.5 Co-optimization of the IEEE 118-bus electric system and 15-node gas network……...……...47
3.6 Effect of different wind/load profile data ……56
3.7 Effect of the electricity network modeling ……62
3.8 The effect of considering primary reserves……64
3.9 Conclusions……...…… 75

4 Conclusions and future work

4.1 Conclusions……..……77
4.2 Future work…….……..79

Appendix A……..81
Bibliography……87

List of figures

Figure 2.1 Flow Chart of the proposed GUC formulation ……17

Figure 2.2 Natural gas network model……27

Figure 2.3 Typical system frequency response to primary regulation after a contingency……....30

Figure 2.4 Frequency regulation response of *i*-th unit generator…….……...31

Figure 3.1 Forecast of wind speed and load demand profiles for 24 hours……...38

Figure 3.2 The multi-energy network's infrastructures……..39

Figure 3.3 Active power generation dispatches for 24 hours in advance for base case..40

Figure 3.4 Dynamic behavior of natural gas in pipelines for base case……..…41

Figure 3.5 Dynamic behavior of nodal pressures for base case……41

Figure 3.6 Dynamic behavior of nodal voltage magnitudes in the electric network for base case…….……...……42

Figure 3.7 Reactive power generation support for 24 hours in advance for base case...42

Figure 3.8 Active power generation dispatches for 24 hours in advance for base case..44

Figure 3.9 Dynamic behavior of nodal voltage magnitudes at the electric network with the effect of voltage control at Node 2 …….……..44

Figure 3.10 Reactive power generation support for 24 hours in advance with the effect of voltage control at Node 2……..45

Figure 3.11 Active power generation dispatches for 24 hours in advance for case with load increment……...46

Figure 3.12 Dynamic behavior of natural gas in pipelines for case with load increment……...46

Figure 3.13 Dynamic behavior of nodal pressures for case with load increment…….46

Figure 3.14 15-bus natural gas network.…… ……...47

Figure 3.15 Active power generation dispatches of gas-fired units for 24 hours in advance for the Co-optimization of the IEEE 118-bus electric system and 15-node gas network……..……51

Figure 3.16 Active power generation dispatches of coal-fired units for 24 hours in advance for Co-optimization of the IEEE 118-bus electric system and 15-node gas network……..51

Figure 3.17 Reactive power generation dispatches of gas-fired units for 24 hours in advance for Co-optimization of the IEEE 118-bus electric system and 15-node gas network.…… ……52
Figure 3.18 Reactive power generation dispatches of coal-fired units for 24 hours in advance for Co-optimization of the IEEE 118-bus electric system and 15-node gas network……..52
Figure 3.19 Hourly nodal voltage profiles for Co-optimization of the IEEE 118-bus electric system and 15-node gas network.…….52
Figure 3.20 Hourly gas pressure profiles at nodes with gas-fired units for Co-optimization of the IEEE 118-bus electric system and 15-node gas network …….……53
Figure 3.21 Maximum mismatch between static and dynamic variables for Co-optimization of the IEEE 118-bus electric system and 15-node gas network……..54
Figure 3.22 Hourly system cost for the IEEE 118-bus electric power system and 15-bus natural gas network for Co-optimization of the IEEE 118-bus electric system and 15-node gas network…….……..54
Figure 3.23 Forecast of wind speed and load demand profiles for 24 hours (scenario 4)...57
Figure 3.24 Number of iterations of each OGPF study performed at the last global iteration…….…….…….……...57
Figure 3.25 Hourly system cost for each case study….…….…….……...58
Figure 3.26 Forecast of high/low wind speed profiles for 24 hours……58
Figure 3.27 Active power generation dispatches of gas-fired units for 24 hours in advance with high wind speed profile……...59
Figure 3.28 Active power generation dispatches of gas-fired units for 24 hours in advance with low wind speed profile……60
Figure 3.29 Active power generation dispatches of coal-fired units for 24 hours in advance with high wind speed profile……...60
Figure 3.30 Active power generation dispatches of coal-fired units for 24 hours in advance with low wind speed profile……61

Figure 3.31 Hourly gas pressure profiles at nodes connected to gas-fired units with a high wind speed profile……61
Figure 3.32 Hourly gas pressure profiles at nodes connected to gas-fired units with a low wind speed profile……..61
Figure 3.33 Active power generation dispatches of gas-fired units for 24 hours in advance for Co-optimization of the IEEE 118-bus electric system and 15-node gas network for lossless transmission network ……..…..63
Figure 3.34 Active power generation dispatches of coal-fired units for 24 hours in advance for Co-optimization of the IEEE 118-bus electric system and 15-node gas network for lossless transmission network. ……..….63
Figure 3.35 Hourly system cost for the IEEE 118-bus electric power system and the 15-bus natural gas network.…..…….……..……..…..……64
Figure 3.36 Active power generation dispatches of generation units for 24 hours in advance for base case including reserves.....…..…….……66
Figure 3.37 Reserves provided by generation units for 24 hours in advance for base case including reserves...…….…….…… ….……66
Figure 3.38 Hourly frequency deviations profiles for base case including reserves.....….67
Figure 3.39 Reactive power generation dispatches of thermal units for 24 hours in advance for base case including reserves..…….…….…..67
Figure 3.40 Hourly nodal voltage profiles for base case including reserves……68
Figure 3.41 Active power generation dispatches of generation units for 24 hours in advance for base case including frequency regulation.…..…….69
Figure 3.42 Reserves provided by generation units for 24 hours in advance for base case including frequency regulation...….……..…… 69
Figure 3.43 Hourly frequency deviation profiles for base case including frequency regulation.…..…….…….…… ….…….…….....70
Figure 3.44 Active power generation dispatches of gas-fired units for 24 hours in advance for Co-optimization of the IEEE 118-bus electric system and 15-node gas network including frequency regulation.…..…….…….....71

Figure 3.45 Active power generation dispatches of coal-fired units for 24 hours in advance for Co-optimization of the IEEE 118-bus electric system and 15-node gas network including frequency regulation.…….…….....72
Figure 3.46 Active power generation dispatches of coal-fired units for 24 hours in advance for Co-optimization of the IEEE 118-bus electric system and 15-node gas network including frequency regulation.…….…….....72
Figure 3.47 Active power generation dispatches of coal-fired units for 24 hours in advance for Co-optimization of the IEEE 118-bus electric system and 15-node gas network including frequency regulation.…….…….....73
Figure 3.48 Hourly frequency deviation profiles for Co-optimization of the IEEE 118-bus electric system and 15-node gas network including frequency regulation.…….……. ….…….……73
Figure 3.49 Hourly nodal voltage profiles for Co-optimization of the IEEE 118-bus electric system and 15-node gas network including frequency regulation.…….……. ….…….……....74
Figure 3.50 Reactive power generation dispatches of gas-fired units for 24 hours in advance for Co-optimization of the IEEE 118-bus electric system and 15-node gas network including frequency regulation.…….…….....74
Figure 3.51 Reactive power generation dispatches of coal-fired units for 24 hours in advance for Co-optimization of the IEEE 118-bus electric system and 15-node gas network including frequency regulation.…….…….....75

List of tables

Table I 5-node benchmark system, generators……...39

Table II 15-node gas system, loads and compressor's data……..48

Table III IEEE 118-bus benchmark system, thermal generators……...48

Table IV Energy consumption by thermal generators……...49

Table V Efficiency of thermal generators for 24 hours……50

Table VI Number of OGPF's iterations for Co-optimization of the IEEE 118-bus electric system and 15-node gas network…….……..…54

Table VII Values of Lagrangian multipliers for Co-optimization of the IEEE 118-bus electric system and 15-node gas network……..55

Table VIII Active power generation for Co-optimization of the IEEE 118-bus electric system and 15-node gas network……...55

Table IX Wind/load scenarios …….…….…….…….……..56

Table A 1 5 Nodes electric power system……...81

Table A 2 Lines of 5 nodes electric power system……..81

Table A 3 118 Nodes electric power system……...81

Table A.4 Lines of 118 nodes electric power system……..84

Table A 5 3 Nodes natural gas network……..85

Table A 6 Pipelines of 3 nodes natural gas network……85

Table A 7 15 Nodes natural gas network……85

Table A 8 Pipelines of 15 nodes natural gas network……85

Table A 9 15 Pipelines natural gas network……86

List of publications

Tovar-Ramírez. C.A., Martínez-Mares A. and Fuerte-Esquivel C.R., "Short-Term Unit Commitment for Integrated Natural Gas and Electricity Infraestructures" 2016 IEEE PES T&D Transmission & Distribution Conference and Exposition-Latin America (PES T&D-LA), ISBN: 2472-9639, September 2016, Morelia, Mich., Mex., pp.1-6. DOI: (10.1109/TDC-LA.2016.7805639).

Tovar-Ramírez C.A., Fuerte-Esquivel C.R., Martínez Mares A. and Sánchez-Garduño J.L., "A generalized short-term unit commitment approach for analyzing electric power and natural gas integrated systems" Electric Power Systems Research, ISSN 0378-7796, July 2019, Vol. 172, pp 63-76. DOI: (10.1016/j.epsr.2019.03.005).

Resumen

El creciente uso global del gas natural para la generación de energía eléctrica ha dado lugar a una mayor interdependencia entre las infraestructuras de gas natural y eléctrica que, a su vez, presenta nuevos desafíos para los operadores de sistemas de potencia y gas para lograr una operación diaria confiable y eficiente de ambos sistemas. Esta tesis propone un enfoque generalizado de asignación de unidades a corto plazo para optimizar la asignación horaria de generación térmica considerando la interdependencia existente entre las infraestructuras de gas natural y de electricidad. Este enfoque generalizado está formulado como un problema de optimización no lineal entero-mixto donde es incorporado un modelo óptimo de gas y de flujos de potencia de corriente alterna multi-período al problema de asignación de unidades térmico. Contrario de todas las demás propuestas que ignoran el despacho de potencia reactiva y las restricciones de la red eléctrica de corriente alterna, así como restricciones asociadas con regulación primaria para resolver el problema de asignación de unidades que considera el sistema integrado de electricidad y gas natural, el enfoque de solución propuesto co-optimiza simultáneamente la asignación y el despacho de potencia activa y reactiva, mientras toma en cuenta el conjunto de restricciones físicas y operativas asociadas con cada infraestructura. Este conjunto de restricciones incluye límites de generación de potencia reactiva, de magnitud de voltajes nodales, de desviación de frecuencia y restricciones de la dinámica del flujo de gas. La solución se obtiene al descomponer este problema de optimización generalizado en dos subproblemas de optimización mutuamente conectados: uno espacialmente separable relacionado con el problema de asignación de unidades y el otro temporalmente separable asociado con la co-optimización unificada de ambos sistemas de energía, que se resuelven secuencialmente hasta que el mismo despacho de generación horario en ambos subproblemas es obtenido. Por lo tanto, esta solución es óptima para el problema de asignación de unidades y para el problema de flujos óptimos de gas y de potencia. Se presenta casos de estudio en dos sistemas multi-energéticos para ilustrar numéricamente la idoneidad y las características principales del enfoque propuesto.

Palabras clave: Redes integradas de gas natural y electricidad, programación no lineal entera-mixta, operación de los sistemas de potencia, asignación de unidades con restricciones de seguridad, reserva primaria, regulación de frecuencia primaria.

Abstract

The growing global use of natural gas for electric power generation has lead to a greater interdependence between natural gas and electricity infrastructures, which in turn presents new challenges for power and gas system operators to achieve a reliable and efficient daily operation of both systems. This thesis proposes a generalized short-term unit commitment approach for optimizing the hourly thermal generation scheduling by considering the existing interdependence between natural gas and electricity infrastructures. This generalized approach is formulated as a mixed-integer nonlinear optimization problem where a multi-period optimal gas and alternating current power flow model is incorporated into the thermal unit commitment problem. Contrary to all other proposals that ignore the reactive power dispatch and alternating current electricity network constraints, as well as the constraints associated with primary frequency regulation to solve the unit allocation problem for solving the unit commitment problem that considers the integrated electricity-natural gas system, the proposed solution approach simultaneously co-optimizes the active and reactive power scheduling and dispatch, while taking into account the set of physical and operational constraints associated with each infrastructure. This set of constraints includes reactive power generation limits, nodal voltage magnitude limits, frequency deviation limits and dynamic gas flow constraints. The solution is obtained by decomposing this generalized optimization problem into two mutually connected optimization subproblems: one spatially separable related to the unit commitment problem and the other temporally separable associated with the unified co-optimization of both energy systems, which are sequentially solved until the same hourly generation dispatch in both subproblems is obtained. Hence, this solution is optimal for the unit commitment problem and the optimal gas and power flow problem. Study cases on two multi-energy systems are presented to numerically illustrate the suitability and main characteristics of the proposed approach.

Keywords: integrated gas and electricity networks, mixed-integer nonlinear programming, power systems operation, security-constrained unit commitment, primary reserve, primary frequency regulation.

Nomenclature

Sets and Indices

I	Set of thermal generators.
T	Set of periods of time.
Ω_n	Set of nodes adjacent to node *n* in the natural gas network.
Ω_j	Set of all nodes *j* adjacent to node i in the electric power system.
Ω_i^{on}	Set of time periods that the *i*-th unit must run (hr).
Ω_i^{off}	Set of time periods that the *i*-th unit is not available (hr).
t	Index of time periods.
N_{thg}	Number of thermal generators.
N_{ng}	Number of nodes in the natural gas infrastructure.
N_t	Number of time periods.
Ncs	Number of compressor stations.
N_{ng}^{source}	Number of natural gas sources.
N_{el}	Number of nodes in the electric power system.
N_{el}^{PV}	Number of PV nodes in the electric power system.

Constants

g	32.2178 gravitational constant (ft/s^2).
z_o	Gas compressibility factor at base conditions (dimensionless).
ρ_o	Gas density at base conditions (lb/ft^3).
Π_o	Gas pressure at base conditions (PSIA).
T_o	Gas temperature at base conditions (°R).
γ_b	Time constant for boiler's thermal processes (hr).
ρ	Gas density (lb/ft^3).
GHV_{ng}	Gross heating value of natural gas (BTU/SCF).
D_i	Governor droop of the *i*-th unit (MW/Hz).

Parameters

ρ_p^k	Poljac's step size of iteration *k.*
L_{nm}	Pipeline's length from node *n* to node *m* (Mi).
D_{nm}	Inner diameter of pipeline connecting nodes *n* and *m* (in).
A_{nm}	Cross-sectional area of pipeline connecting nodes *n* and *m* (in^2).
λ_{nm}^{fr}	Friction factor of pipeline connecting nodes *n* and *m* (dimensionless).
∂x	Pipeline's differential length (Mi).
∂h	Pipeline's differential slope (ft).
$G_{n,t}^{source}$	Gas supplied by a source at time *t* (MMSCF).
$\overline{G}_{n,t}^{source}$	Upper natural gas limit injection at node *n* at time *t* (MMSCF).
$\underline{G}_{n,t}^{source}$	Lower natural gas limit injection at node *n* at time *t* (MMSCF).
$G_{n,t}^{load}$	Gas extracted by a non-electrical load at time *t* (MMSCF).
Zc	Average gas compressibility factor (dimensionless).
T_g^n	Gas temperature at node *n* (°R).
E_c	Compressor's parasitic efficiency (dimensionless).
η_c	Compression process efficiency (dimensionless).
C_{cn}	Gas specific heat ratio (dimensionless).
$\overline{\Pi}_{n,t}$	Maximum gas pressure allowed at node *n* at time *t* (PSIA).
$\underline{\Pi}_{n,t}$	Minimum gas pressure allowed at node *n* at time *t* (PSIA).
P_{it}^g	Active power output of the *i*-th base generator at time *t* (pu).
Q_{it}^g	Reactive power output of the *i*-th base generator at time *t* (pu).
$P_{i,t}^{load}$	Active power load at node *i* at time *t* (pu).
$Q_{i,t}^{load}$	Reactive power load at node *i* at time *t* (pu).
G_{ii}, G_{ij}	Conductances of the nodal admittance matrix (pu).
B_{ij}, B_{ij}	Susceptances of the nodal admittance matrix (pu).
sp_{it}^{PFR}	Available active power with primary frequency regulation at time *t* (pu).

$sp_{it}^{\max}$	Maximum output of the *i* unit under primary frequency regulation at time *t* (pu).
$sp_{it}^{P\&R}$	Available active power and reserves without frequency regulation at time *t* (pu).
$SC_i^{\max}$	Cold start fuel cost for generator *i* (USD).
t_d	Cooling time after the unit was shut down (hr).
LT_{it}	Number of time periods that unit *i* has been on or off (hr).
MUT_i	Minimum number of time periods *t* that unit *i* must remain on after it has been turned on (hr).
MDT_i	Minimum number of time periods *t* that unit *i* must remain off after it has been turned on (hr).

Variables

λ	Lagrangian multiplier.
$G_{nm,t}^{in}$	Gas flow at the inlet node *n* of the pipeline at time *t* (MMSCF).
$G_{nm,t}^{out}$	Gas flow at the outlet node *m* of the pipeline at time *t* (MMSCF).
$\Pi_{n,t}$	Pressure at the *n*-th node of the pipeline at time *t* (PSIA).
$z_{\Pi_{n,t}}$	Gas compressibility factor at the *n*-th node of the pipeline at time *t* (dimensionless).
$G_{nm,t}^{C}$	Gas flowing in the compressor at time *t* (MMSCF).
$\tau_{nm,t}^{C}$	Gas extracted by compressor at time *t* (MMSCF).
$BHP_{nm,t}^{C}$	Energy consumption by compressor at time *t* (MMSCF).
$G_{ni,t}^{load}$	Gas extracted at time *t* by an electric generator connected at the *i*-th node of the electrical network (MMSCF).
$R_{nm,t}^{C}$	Compression ratio at time *t* (dimensionless).
$L_{i,t}^{C,nm}$	Active power demanded by the compressor motors (pu).
$V_{i,t}$	Voltage magnitude at node *i* at time *t* (pu).
$\theta_{ij,t}$	Voltage phase angle at node *i* at time *t* (radians).

sp_{it}	Active power output of unit *i* at time *t* given by the optimal gas and AC power flow program (pu).
sq_{it}	Reactive power output of unit *i* at time *t* given by the optimal gas and AC power flow program (pu).
dp_{it}	Active power output of unit *i* at time *t* given by the unit commitment program (pu).
dq_{it}	Reactive power output of unit *i* at time *t* given by the unit commitment program (pu).
$u^{i,t}$	On/off *s*tatus of generator *i* at time *t*.
r_{it}	Active power reserve available for *i* unit generator at time *t* (pu).
Δf_t	System frequency deviation given by the primary regulation control at time *t* (Hz).

Acronyms

RES	Renewable Energy Sources
UC	Unit Commitment
DC	Direct Current
SCUC	Security-Constrained Unit Commitment
AC	Alternating Current
MILP	Mixed-Integer Linear Programming
MINLP	Mixed-Integer Nonlinear Programming
PDEs	Partial Differential Equations
OPF	Optimal Power Flow
AC-OPF	Alternating Current Optimal Power Flow
OGPFs	Optimal Gas and Power Flows
GUC	Generalized Short-Term Unit Commitment
MBAL	Modified Barrier-Augmented Lagrangian
MBTU	Thousand British Thermal Unit.
MMSCF	Million Standard Cubic Feet.
MSCM	Million Standard Cubic Meter.

Chapter 1

Introduction

1.1 Research Motivation

The continuing and increasing use of natural gas as a primary energy source for electricity generation over the last decade [Chaudry 2014], coupled with the facts that the operation of the natural gas system partly depends on electricity and those changes in power outputs from gas-fired generating units represent swing loads affecting natural gas flows in pipelines, has resulted in a greater operational codependency between these two energy infrastructures, creating new challenges for planners and operators of both transmission networks. In the context of this interdependence, the assessment of supplying available natural gas to power plants plays a major role in the operational coordination of gas-fired generators with other types of generating units to satisfy the demand for electricity at the lowest operating cost, while satisfying all operational and physical constraints of both natural gas and electricity networks. Furthermore, with the increasing deployment of renewable energy sources (RES), this coordination has acquired more relevance because of the greater need for operational flexibility in the power dispatch in response to a higher variability of grid-connected renewable energy as well as fluctuations in demand.

The necessity of providing generation flexibility that incorporates limitations from energy transmission systems in order to accommodate short-term power imbalances, together with the fact that gas-fired generators can rapidly change their electric power output to quickly achieve a balance between generation and demand, have produced several proposals associated with the short-term coordination of generation units based on a unit commitment (UC) study that incorporates operational constraints of both natural gas and electricity systems. Generally speaking, this study consists of determining the operating status of electric generators to satisfy the expected electric power demand in a period of time ranging from a few hours to one day in advance.

In order to assess the coordinated scheduling of security-constrained electricity and natural gas infrastructures in the UC context, a number of proposals [Liu 2009, Qadrdan 2014, Alabdulwahab 2015, Zhang 2016, Alabdulwahab 2017, Liu 2010, Biskas 2018, Badakhshan 2015, Liu 2011, Correa-Posada 2015, Damavandi 2011, Zhao 2017, He 2017] have been formulated that consider the relaxed direct current (DC) model for the electricity network, while the natural gas transmission network is represented by a steady-state gas flow model [Liu 2009, Qadrdan 2014, Alabdulwahab 2015, Zhang 2016, Alabdulwahab 2017, Liu 2010, Biskas 2018, Badakhshan 2015] or by a set of dynamic gas flow constraints [Liu 2011, Correa-Posada 2015, Damavandi 2011]. In all these proposals, the short-term scheduling of both infrastructures is sequentially performed by first solving a security-constrained unit commitment (SCUC), which considers only the electric power system. The feasible operation of the gas network is then checked for the fuel demanded by the dispatched gas-fired units.

One of the drawbacks of using a DC model for the electricity network is the inability of incorporating detailed electric device models and nonlinear operational constraints, such as those associated with reactive generation limits or voltage magnitude limits, which implies that the commitment schedules only provide active power dispatches. In practical electrical power system operation, however, these dispatches of active power are unfeasible, and the units must be newly rescheduled by considering the alternating current (AC) electricity network constraints to obtain the dispatches of active and reactive power that satisfy the real operating conditions of the integrated electricity-natural gas system [Godinez-Fernández 2019]. This problem is overcomed in this work by proposing a generalized short-term unit commitment approach where the natural gas and electricity systems are co-optimized in a unified nonlinear framework of analysis to obtain the active and reactive power scheduling and dispatch subject to the constraints associated with the unit commitment and with the integrated AC electricity-natural gas system.

1.2 State of the art

In order to assess the coordinated scheduling of security-constrained electricity and natural gas infrastructures in the UC context, some proposals have been formulated that

consider the relaxed direct current (DC) model for the electricity network [Liu 2009, Qadrdan 2014, Alabdulwahab 2015, Zhang 2016, Alabdulwahab 2017, Liu 2010, Biskas 2018, Badakhshan 2015, Liu 2011, Correa-Posada 2015, Damavandi 2011] and a steady-state nonlinear model of the natural gas system by using the Weymouth equation [Liu 2009, Qadrdan 2014, Alabdulwahab 2015, Zhang 2016, Alabdulwahab 2017, Liu 2010, Biskas 2018, Badakhshan 2015].

An hourly security-constrained unit commitment (SCUC) problem is proposed in [Liu 2009] based on Benders decomposition, which separates the large-scale optimization problem into one master problem and two feasibility check subproblems. A mixed-integer linear programming (MILP) formulation of the master unit commitment (UC) problem is first solved to determine the unit commitment status and power dispatch of generators. Based on this scheduling, a feasible lineal subproblem is solved to check that power transmission flow constraints are satisfied. A sequential solution of both problems is carried out until a feasible power generation dispatch for the electricity network is found, with results that permit determining the fuel demand for the gas-fired units over the entire planning horizon. The next step is then to assess the natural gas supply availability such that a nonlinear natural gas network subproblem is iteratively solved by a successive application of linear programming to check the gas network's operational feasibility according to the amount of fuel demanded by the dispatched gas-fired units. If this subproblem is unfeasible, natural gas consumption constraints for gas-fired units will be formed and added to the master UC problem for a new rescheduling of generators. This iterative process will continue until a feasible generation dispatch which satisfies the operational constraints of both electricity and natural gas networks is obtained. This type of solution approach has been adopted with minor adjustments to assess the impact of the wind forecast uncertainty [Qadrdan 2014], the variability of wind energy [Alabdulwahab 2015] and the hourly response of electricity demand [Zhang 2016] on the interdependency of both energy systems and generators scheduling, where the uncertain data are modeled by using the concept of probabilistic forecast based on scenarios. A similar sequential coordinated solution of both networks is also reported in [Alabdulwahab 2017] by considering random outages of generating units and transmission lines as well as load forecasting inaccuracies; however, unlike [Alabdulwahab 2015] and [Zhang 2016] the nonlinear natural gas flow equations are

piecewise linearized to obtain a set of linear constraints. In all these stochastic SCUC proposals, the natural gas network feasibility is checked for all scenarios.

A coordinated scheduling of both energy infrastructures is proposed in [Liu 2010] and [Biskas 2018] based on the augmented Lagrangian relaxation method, which decomposes the primal optimization problem into two subproblems by relaxing the electricity-natural gas coupling constraints and by adding quadratic penalty terms. One of these subproblems is related to a dual SCUC and the other to the gas allocation. These dual subproblems are sequentially solved using the block descendent coordination technique by first minimizing the augmented Lagrangian with respect to the gas units' hourly commitment status and power production, maintaining units' hourly gas consumption at predetermined values. Next, the augmented Lagrangian is then minimized with respect to these gas consumptions keeping the scheduling of units and their power production at fixed values. The quadratic penalty terms are represented by piecewise linear approximations in [Liu 2010], and after a prespecified number of iterations, the best solution to the dual problem is used to construct a final feasible solution to the primal problem where no violations occur in the coupling constraints. In this case, based on the last solution of the gas allocation dual subproblem, the primal SCUC problem with inequality coupling constraints is solved to obtain the power system schedule. This scheduling is then used to solve the primal natural gas allocation problem with equality coupling constraints. On the other hand, the quadratic terms are not linearized in [Biskas 2018] nor is a second optimization process required to obtain the feasible solution. In this solution approach, the iterative sequential solution of the dual subproblems terminates when the norm between the gas consumption and active power produced by the gas-fired units is lower than a predefined maximum deviation. Otherwise, the vector of Lagrange multipliers of the coupling constraints are updated based on a subgradient method at the start of the next iteration.

A fuzzy max-min optimization problem is formulated in [Badakhshan 2015] for a SCUC by considering the natural gas transmission network, which is solved by a bi-level programming approach. In this case, the first level formulates an optimal gas flow problem for a single period of time by considering the objective function used for the SCUC problem and assuming that all gas-fired generation units are on-line. The minimization of this nonlinear constrained optimization problem is achieved by using a genetic algorithm and

provides the maximum gas consumption of each generation unit; these consumptions are then used to set up a set of fuzzy fuel consumption constraints that is included into the linear SCUC problem. The second level solves the fuzzy SCUC problem for the electricity network by employing a mixed-integer linear programming. This sequential solution of both optimization problems linked by the gas consumption of generation units is repeated until reaching the genetic algorithm convergence.

The representation of the steady-state operation of a gas transmission network assumes that the natural gas flows at the speed of light, like electricity, [Shahidehpour 2005] which is inaccurate because the flow of gas travels at a much slower than that. In practice, this assumption implies that the gas system responds slowly to disturbances in the network, requiring a longer stabilization time than that needed by an electric power system. Hence, some proposals have taken into account this fact by considering dynamic gas flow constraints on the modeling of the gas transmission network, which are associated with the gas traveling velocity and compressibility, in order to better represent the flexibility that power systems demand from gas systems in terms of supplying the required fuel to the gas-fired units over a short-term planning horizon. This is the case of the proposals reported in [Liu 2011] and [Correa-Posada 2015]. In the former proposal, a bi-level coordinated scheduling model of both energy systems is formulated based on a transient state model of natural gas flow described by a set of nonlinear partial differential equations (PDEs). The optimization problem is decomposed into a master problem and two feasibility check subproblems, which are solved as reported in [Liu 2009]. In this case, the implicit finite difference method is used to transform the set of PDEs into a set of algebraic difference equations, which are then included in the formulation of the natural gas network feasibility check problem. In these equations, the pipeline's total length is partitioned into several segments, and the time interval is considered on an hourly basis. On the other hand, a SCUC is formulated in [Correa-Posada 2015] as a MILP problem by representing the nonlinear and non-convex functions associated with the dynamic gas flow constraints by piecewise linear segments. The MILP problem is solved by Benders decomposition, where a master problem solves the UC and dispatch problems providing an operational feasibility solution of the gas transmission network. Based on this solution, a set of subproblems is solved to check the power network operational feasibility for hourly pre- and post-contingency conditions. This iterative solution process

between the master problem and subproblems continues until a feasible UC and generation dispatch is found. Lastly, in [Damavandi 2011] the gas network is considered as a set of gas areas interacting between each other through tie-pipelines. Furthermore, a quasi-dynamic linear model of the gas flow is derived by accounting for the gas velocity and the lengths of tie-pipelines, but disregarding the gas nodal pressures such that the gas flowing through a tie-pipeline only depends on a time delay. In this context, the unit commitment problem is formulated as a mixed-integer linear programming problem which considers the electricity network and natural gas areas constraints on two different time scales: an hourly time scale is used for the equations representing the operation of the electricity network, while a time scale based on minutes is used for the equations related to the natural gas flowing between gas areas.

The integration of a set of constraints associated with natural gas supply into a two-stage mixed-integer linear stochastic unit commitment and dispatch process is reported in [Zhao 2017]. In the first stage a day-ahead unit commitment is determined, while the response of the committed units to real-time natural gas availability is assessed in the second stage through a number of scenarios. In the proposed formulation, the natural gas network is not represented in detail, i.e. it is only modeled by directly considering the gas flows through pipelines. On the other hand, the electricity network is modeled by a DC model.

A robust security-constrained unit commitment of integrated electricity-natural gas system is proposed in [He 2017] by considering random transmission line outages and limited adjustments in natural gas contracts. The whole problem is decomposed into a master problem and a security check subproblem by using a second-order cone-based column and constraint generation approach. The master problem is solved to obtain a unit commitment schedule, which is validated by obtaining the worst contingency scenario in the solution of the security check subproblem. These two problems are sequentially solved until the set of contingency scenarios are considered secure. The electric power network is represented by a DC model, and the natural gas infrastructure is represented by a steady-state model. The natural gas flow functions are relaxed into second-order cone constraints.

Taking into account what has been proposed in the integral analysis of gas and electricity networks considering reserves, a methodology considering different heating scenarios with the aim to quantify the flexibility with which the gas network can provide

primary energy to the power system is reported in [Clegg 2015]. In this proposal both the local active power generation and the contribution of a certain amount of power reserve provided by each generator are obtained. In this case, each generator must fulfil the requirements of system's reserves considering its 30 minute ramp rate and the available generation. The problem is formulated through a multi-stage integrated gas and electrical transmission network model, which is composed of a DC transmission grid and both steady-state and transient model of the gas infrastructure. Lastly, a metric based on the concept zonal linepack is introduced to assess the multi-energy system's flexibility. This metric is used to impose inter-temporal constraints in the optimization problem. On the other hand, a co-optimization of the electricity and gas systems based on a mixed integer non-linear programming model is reported in [Biskas 2014]. The unit commitment problem is solved considering DC power flow constraints, system reserve requirements and a steady-state model of the gas network. The decomposition of the overall problem is based on the Augmented Lagrangian method to obtain two optimization subproblems associated with the electric and natural gas infrastructures, respectively.

A few economic studies have highlighted the importance of accounting for the interdependence between electricity and natural gas markets using an integrated modeling approach. In this context, the work reported in [Rieping 2018] focuses on the effects of gas demand uncertainty on the investments for increasing the capacity of electricity generation. An integrated dynamic model of both the electricity and gas sectors is proposed to determine an optimal investment in the electricity sector and the operational decisions in both sectors. The integration of the electricity and gas sector is provided by a fuel linkage. In [Qiu 2016] an expansion co-planning model for both the electricity and gas networks is proposed, where the electric power and gas networks are linked through gas-fired generators. The aim of this proposal consists of minimizing the total investment and operation cost, subject to a variety of technical constraints, system's reliability and security criteria. Two linearization techniques are introduced to deal with the nonlinear nature of gas and power system models: piecewise linear approximation and the first-order Taylor series approximation. Hence, an iterative process is proposed to simulate the interactions between both infrastructures in a combined gas and electricity market. The solution of this study provides a strategic guidance through which the energy industry can take operating and planning decisions.

As mentioned before, a major drawback of using a DC model for the electricity network is the inability of incorporating detailed models of electric components and nonlinear operational constraints. Since the satisfaction of these operational limits will require a further rescheduling of units because of the inconsistency between the DC-based unit commitment and real operation states, and because these nonlinear constraints can only be accurately modeled considering an alternating current (AC) flow network model for the electricity infrastructure, some researchers have proposed the integration of the AC optimal power flow (AC-OPF) study into the formulation of the unit commitment problem to take into account the voltage magnitude constraints and reactive power generation [Guan 1996, Murillo-Sánchez 1997, Murillo-Sánchez 2000, Murillo-Sánchez 2001, Bragin 2016, Bai 2015, Castillo 2016]. Based on the previous works by [Batut 1992] and [Baldick 1995], a conceptual way of integrating these two problems is suggested but not implemented in [Guan 1996] by using the concept of duplication of variables, the augmented Lagrangian method and the auxiliary problem principle. The proposal consists of separating the UC and OPF problems in terms of spatial and temporal perspectives, respectively, by introducing a set of duplicating variables that coexists in both problems. This decomposition is achieved by representing all these variables in the form of a set of equality constraints which is relaxed by Lagrange multipliers. Furthermore, a capacity reserve constraint is also added to the OPF problem to ensure that the demand is satisfied at each period of time. The proposed approach sequentially solves the UC and OPF problems for given values of Lagrange multipliers associated with those two types of constraints, and these values are updated at the end of each iteration of this sequential solution in order to reweight the amount of active power produced by the generators. This iterative solution process continues until a generation scheduling satisfies all operational constraints. A more comprehensible formulation of this idea as well as its serial and parallel implementation are reported in [Murillo-Sánchez 1997] and [Murillo-Sánchez 2000], where only the active and reactive power outputs of generators are the variables to be duplicated.

Based on the ideas proposed by [Batut 1992] and [Baldick 1995] and the successful application to include the AC-OPF problem into the UC formulation [Murillo-Sánchez 1997], this thesis proposes a generalized unit commitment problem for multi-energy systems where the co-optimization of the natural gas and electricity systems is performed for the short-term generation scheduling. In this case, the problems of unit commitment and multi-

period optimal gas and power flows (OGPFs) are formulated based on the nonlinear modeling of both energy systems and solved in a unified framework analysis.

1.3 Objective

The main objective of this work is to formulate the unit commitment problem in multi-energy systems by considering the co-optimization of the natural gas and electricity infrastructures in a single frame of reference for a unified iterative solution. This solution must provide information to both power and gas systems operators to achieve an efficient and reliable daily operation for both interdependent systems.

1.4 Methodology

This thesis proposes a formulation for a generalized short-term unit commitment (GUC) in order to meet the electric demand forecast, while the physical and operating constraints from the natural gas and electricity infrastructures are satisfied. The proposed formulation decomposes the entire problem into the UC and OGPF subproblems, where the UC consists of the selection of units to be put into operation at each period of time in which the short-term planning horizon is discretized. On the other hand, the OGPF deals with the most economic allocation of the forecasted electric demand among the generators that have been scheduled for each time period. These two separated but mutually connected subproblems involve a mixed-integer non-linear optimization problem, where the concept of duplication of variables is used to integrate both UC and OGPF subproblems. This concept consists of defining two sets of variables that coexist in both subproblems: static variables related to a single period of time, and dynamic variables associated with multiple periods of time. In order to achieve the equivalence between these two types of variables, two sets of artificial constraints have to be added in the problem's formulation, which allows to split the original GUC into two subproblems with only static and dynamic variables, respectively, and their corresponding equality and inequality constraints. These sets of artificial constraints, however, may produce convergence problems on the feasible solution. These problems are overcome by adding convexification terms to the artificial constraints, but the resulting augmented Lagrangian function is non-separable. This last drawback is solved by using the

auxiliary problem principle, which consists of linearizing the convexification terms with respect to their previous iteration to decompose the augmented Lagrangian function into two independent sets of discrete equations depending on static and dynamic variables, respectively.

Once the GUC problem has been mathematically formulated as mentioned above, an iterative sequential solution of the UC and OGPF subproblems is performed aiming to obtain the same generation dispatches at each period of time for each subproblem, while satisfying the corresponding set of constraints. The OGPF subproblem is first solved for each subperiod of time by considering that all generation units are committed. The computed values of Lagrange multipliers associated with the equality constraints of generation buses are then used to set the Lagrange multipliers' values related to the artificial constraints of the UC subproblem. Note that these values are maintained constant during the UC solution process. The UC solution's feasibility is evaluated by using the following test: the dispatch is considered feasible (resp. infeasible) if the total generation scheduling of active power satisfies (resp. does not satisfy) the total demand of active power. The UC solution's feasibility is evaluated by using the following test: the dispatch is considered feasible (resp. infeasible) if the total generation scheduling of active power satisfies (resp. does not satisfy) the total demand of active power. If the UC solution is feasible, the OGPF subproblem is solved for each subperiod of time, but considering only the scheduled units and their corresponding generation limits. This multiperiod optimization problem has a feasible solution if and only if all OGPFs converge to an optimal solution. Otherwise, the Lagrangian multipliers must be updated to perform a new UC study. This iterative solution process of both subproblems is performed until the maximum mismatch associated with the static and dynamic variables is less than or equal to a specified tolerance.

1.5 Main Contributions

The specific contributions of the proposed approach are twofold. On the one hand, there is a generalized unit commitment formulation, and on the other hand, there is its solution methodology. These specific contributions are described below.

1) The proposal integrates for the first time a multi-period nonlinear optimal gas and power flows approach into the unit commitment problem associated with an integrated AC electricity-natural gas system, resulting in a generalized unit commitment approach. This approach simultaneously obtains the active and reactive power scheduling and dispatch, as well as the amount of gas to be supplied to the committed thermal units, while satisfying the operational constraints of the integrated AC electricity-natural gas system and the UC constraints. Hence, the resulting unit commitment and generation schedules must not be corrected to satisfy the operational requirements associated with each energy infrastructure.

2) Instead of decomposing the generation scheduling problem into one subproblem regarding the unit commitment and feasible operation of the electricity network and another subproblem related to the feasible operation of the natural gas problem, the original optimization problem is decomposed into two mutually connected optimization subproblems: one of them associated with the unit commitment and the other with the co-optimization of both energy systems, respectively. Contrary to the sequential optimization of the electricity and natural gas networks for checking their operational feasibility, the proposed co-optimization approach directly determines, based on the multi-period nonlinear optimal gas and power flows formulation, the operation state of both networks by considering their operational and physical constraints as well as their interdependencies.

To the best of the author's knowledge, this way of performing the unit commitment study in multi-energy systems by considering the co-optimization of the natural gas and electricity infrastructures in a single frame of reference for a unified, iterative solution is a newly developed concept that has not been previously proposed.

1.6 Justification

In the daily operation of power systems, major power loads draw a significant amount of reactive power such that the committed units must supply this power to satisfy reactive

power demands and maintain nodal voltage magnitudes within permissible limits. In this context, the major drawback of using a DC model for the electricity network in the context of the UC problem is that the scheduling is performed without the consideration of constraints related to voltage magnitudes and reactive power generation, such that determining the reactive power dispatch is not possible. Added to this, the result of modeling the electricity infrastructure as an ideal network is that the unit commitment and power scheduling may deviate from the real requirements of generation demanded by the power system.

To solve these problems, the power system operator must adjust the original dispatch, which can cause the hourly committed units to change in number and/or power scheduling to maintain nodal voltage magnitudes within specified limits, as well as to supply the correct amount of active and reactive power according to the real operating and physical constraints of the electricity network. Note that these adjustments will also affect how the interdependency between both natural gas and electricity networks takes place such that the operation status of the entire multi-energy system must be newly assessed. In addition to this preventive control action, the reserve of active power must be considered in the formulation of the SCUC problem in order to have enough flexibility to maintain the frequency regulation within limits by following the forecasted time variations of power demand and of renewable-based generation.

1.7 Organization of the Thesis

The proposed methodology is detailed in the rest of this thesis, which is structured as follows. Chapter 2 presents the generalized short-term unit commitment formulation considering integrated multi-energy systems, and details the solution process of this formulation. The application of the proposed approach is presented in Chapter 3, where the impact of considering reactive power sources, voltage magnitude constraints and primary frequency regulation on the generation scheduling is discussed. Finally, the main conclusions and future work of this proposal are summarized in Chapter 4.

Chapter 2

Generalized short-term unit commitment formulation

2.1 Introduction

In the context of this work, the generalized short-term unit commitment (GUC) study regards to economically determine a schedule of the thermal generation units to be put into operation over a period of time, ranging from a few hours to one day in advance, to meet the forecast demand, while satisfying the physical and operating constraints imposed on both natural gas and electricity infrastructures. In practice, operating conditions can violate the operational limits of some electric components, which is permissible for a given period of time. Hence, the operational limits can be relaxed in order to achieve convergence in the iterative solution process of the optimization problem. Because of the physical limitations of the electrical components or specific control actions, however, some state variables are subject to inequality constraints to avoid the optimal solution not making physical sense or not being physically possible. These types of constraints are considered hard constraints and are not relaxed.

The generation scheduling involves the turn on and turn off times as well as the active and reactive power production for each thermal generator. The solution of this mixed-integer optimization problem involves the formulation of two separate but mutually connected optimization subproblems. The first subproblem is the unit commitment or pre-dispatch consisting of the selection of units to be placed in operation at each period of time in which the short-term planning horizon is discretized. The other subproblem is the optimal gas and AC power flows analysis, which deals with the most economic allocation of the forecasted electric demand in each time period among the generation units that have been scheduled for each one of these periods of time. The sequential iterative solution of these two subproblems is then performed in order to obtain the same generation dispatches at each period of time.

2.2 Lagrangian Duality

In order to obtain an optimal solution to the GUC problem, the Lagrangian relaxation technique is used, which is one type of dual optimization. This technique is described in [Knowles 2010] departing from the solution of the following optimization problem:

$$\min\ f_0(x) \tag{2.1}$$

$$\text{such that}\ \ f_i(x) \le 0 \qquad \forall i \in 1,...,m \tag{2.2}$$

A solution of the optimization problem can be achieved by minimizing the following function:

$$J(x) = \begin{cases} f_0(x), & if \quad f_i(x) \le 0 \quad \forall i \\ \infty, & otherwise \end{cases} \tag{2.3}$$

$$= f_0(x) + \sum_i I\left[f_i(x) \right] \tag{2.4}$$

where $I[u]$ is an infinite step function that gives infinite penalty to a constraint being dissatisfied:

$$I[u] = \begin{cases} 0, & if \quad u \le 0 \\ \infty, & otherwise \end{cases} \tag{2.5}$$

The minimization of $J(x)$ is troublesome, however, because $I[u]$ is both non-differentiable and discontinuous, it is necessary to replace $I[u]$ with another function easier to handle. If $I[u]$ is replaced by λu in the function $J(x)$, where λu is a straight line representing a lower limit of $I[u]$ [Knowles 2010], the following Lagrangian function is obtained:

$$L(x,\lambda) = f_0(x) + \sum_i \lambda_i f_i(x) \tag{2.6}$$

If the problem constraints are all satisfied (i. e. $f_i(x) \le 0\ \forall i$) for a particular value of *x*, it is possible to set $\lambda_i(x) = 0\ \forall i$ in order to obtain $L(x,0) = f_0(x)$. On the other hand, if

any of the constraints are not satisfied, then $f_i(x) \geq 0$ for some *i*. In this case, it is possible to make $L(x,\lambda)$ infinite by taking $\lambda_i \to \infty$, which implies that the maximization of $L(x,\lambda)$ with respect to λ results in $J(x)$:

$$\max_{\lambda} L(x,\lambda) = J(x) \tag{2.7}$$

Based on the arguments mentioned above, the problem of minimizing $J(x)$ can then be formulated as

$$\min_{x} \max_{\lambda} L(x,\lambda) \tag{2.8}$$

On the other hand, exchanging the order of maximization over λ and minimization over *x* results in

$$\max_{\lambda} \min_{x} L(x,\lambda) = \max_{\lambda} g(\lambda) \tag{2.9}$$

where $g(\lambda) = \min_{x} L(x,\lambda)$ is known as the dual function, and its maximization is known as the *dual problem*, in contrast to the original *primal problem*. In order to relate both problems, and taking into account that λu is a lower bound on $I[u]$, $L(x,\lambda)$ is a lower bound on $J(x)$ for all $\lambda \geq 0$. Thus,

$$L(x,\lambda) \leq J(x) \qquad \forall \lambda \geq 0 \tag{2.10}$$

$$\Rightarrow \min_{x} L(x,\lambda) = g(\lambda) \leq \min_{x} J(x) =: p^* \tag{2.11}$$

$$\Rightarrow d^* = \max_{\lambda} g(\lambda) \leq p^* \tag{2.12}$$

where p^* and d^* are the optimum of the primal and dual problems, respectively. If for any λ the dual function $g(\lambda)$ gives a lower bound on the optimal problem, the dual problem of maximizing over λ is interpreted as finding the tightest possible lower bound on p^*:

$$\max_{\lambda} \min_{x} L(x,\lambda) \leq \min_{x} \max_{\lambda} L(x,\lambda) \tag{2.13}$$

This property is known as weak duality, and in fact holds for general and smooth functions *L*. The difference between $d^* - p^*$ is known as the optimal duality gap. Strong duality means that we have equality, i. e. the duality gap is zero. Strong duality holds if the optimization problem is convex and a strictly feasible point exist (i.e. a point *x* where all

constraints are strictly satisfied). In that case, the solution of the primal and dual problems is equivalent, i.e. the optimal x^* is given by $\min_x L\left(x, \lambda^*\right)$, where λ^* is the maximizer of $g\left(\lambda\right)$.

Based on the arguments mentioned above, the concept of duality provides an efficient way of solving the original GUC (potentially nonconvex) constrained optimization problem proposed in this thesis.

2.3 Decomposition Basics

For the purpose of this work, the original GUC problem is decomposed into the UC and OGPF subproblems by applying the concepts of the duplication of variables, the augmented Lagrangian relaxation and of the auxiliary problem principle [Batut 1992] and [Baldick 1995] as follows. Note that these two concepts have also been applied in the context of the hydrothermal scheduling problem in [Belloni 2003] and [Takigawa 2012]. The duplication of variables is first applied in reformulating the original GUC problem in terms of two sets of variables that coexist in both subproblems: static variables associated with one single period of time and dynamic variables related to multiple time periods. A set of artificial equality constraints is also formulated to equalize the same type of static and dynamic variables that have been duplicated. By relaxing this set of additional constraints, a set composed of a Lagrangian function as well as equality and inequality constraints is obtained, which in turn is split into two terms that solely depend on static and dynamic variables, respectively. Since the numerical optimization of this set of equations is inherently unstable in terms of convergence to a feasible solution [Batut 1992], the problem is overcome by adding convexification terms to the Lagrangian function, which results in a non-separable augmented Lagrangian function. Lastly, the auxiliary problem principle is used to decompose the augmented Lagrangian function into two independent sets of discrete equations depending on static and dynamic variables, respectively. The resulting set of equations that solely depends on the static variables is temporally separable and corresponds to the OGPF subproblem, while the other set of equations that is only a function on dynamic variables is spatially separable into N_{thg} generators and corresponds to the UC subproblem. The mathematical formulation of the entire process of decomposing the original GUC problem into these two optimization subproblems is mathematically detailed in the following section and is shown in Fig. 2.1.

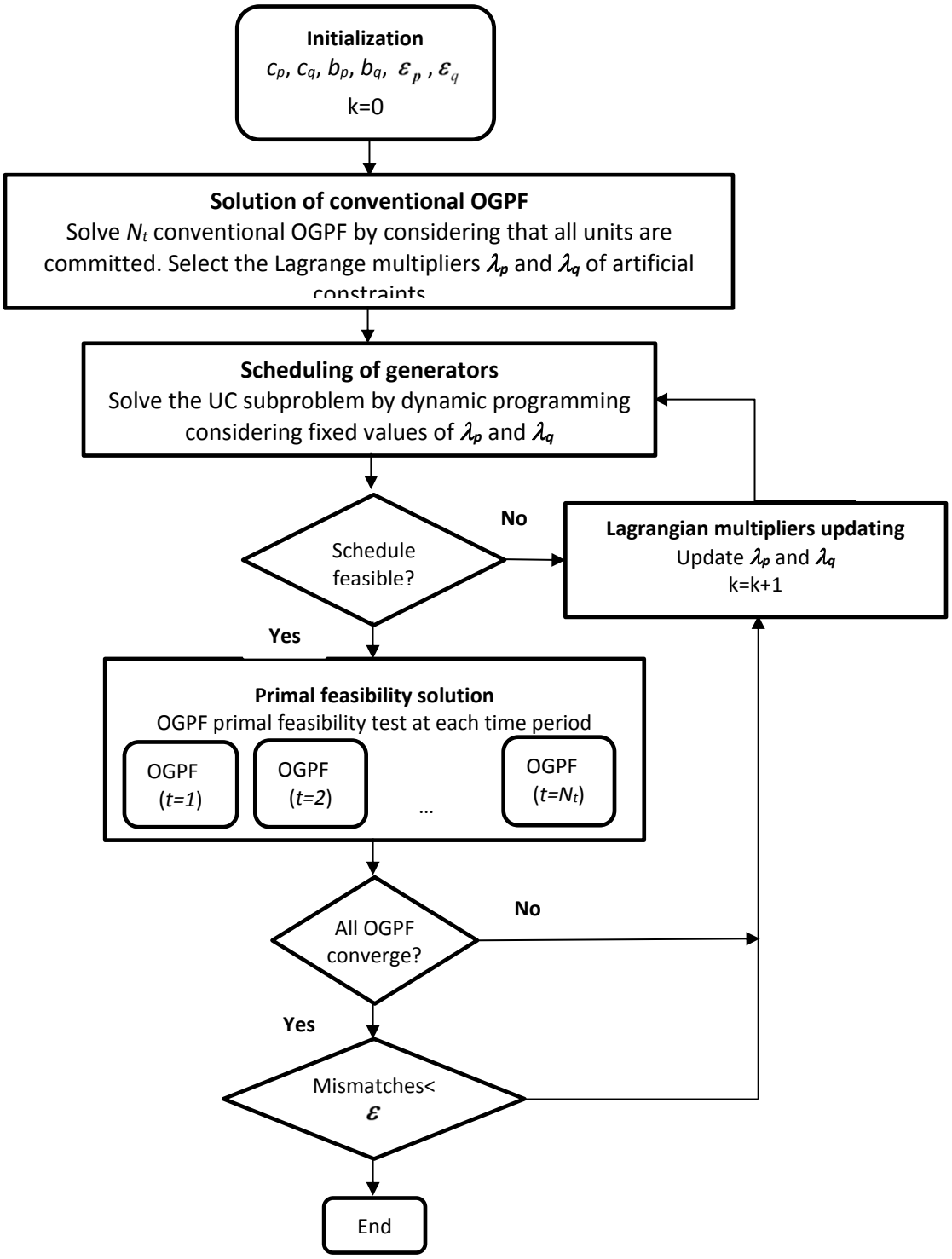

Fig. 2.1. Flow chart of the proposed GUC formulation.

Based on this flow chart, *Nt* conventional OGPFs are first solved with all units committed. The UC is then formulated and solved by considering fixed values for the Lagrange

multipliers $\boldsymbol{\lambda_p}$ and $\boldsymbol{\lambda_q}$ of artificial constraints. These values were obtained by the conventional OGPF solution. The UC solution determines the units to be placed in operation at each time period as well as their corresponding generation of active power. Based on the UC solution, the multiperiod OGPF subproblem is solved by only considering the dispatched units at each period of time. If the OGPF is infeasible for some time periods, the dispatch of units given by the UC solution is considered infeasible and the values of Lagrangian multipliers $\boldsymbol{\lambda_p}$ and $\boldsymbol{\lambda_q}$ must be updated to perform a new UC study. The iterative solution process between both subproblems stops when the mismatch of duplicated variables is less than or equal to a specified tolerance error $\boldsymbol{\varepsilon}$.

Lastly, the algorithm's computational burden to reach the convergence, in terms of cpu time, depends on the size of both electricity and natural gas networks as well as the number of gas-fired generators composing the power system. Generally speaking, the solution of the conventional OGPF, UC and dispatch-constrained OGPF problems requires 35.04%, 0.34%, and 64.62%, respectively, of the total cpu time.

2.4 GUC model

The GUC problem is formulated by considering a set I of N_{thg} thermal generators, $I=\{1,2,..N_{thg}\}$, that can be scheduled over a short-term planning horizon discretized in a set of T periods of time $T=\{t_1,t_2,..N_t\}$. For each period of time t there is a vector of decision variables $\boldsymbol{x}_t$, which are also referred as static decision variables, with lower and upper limits $\underline{\boldsymbol{x}}_t$ and $\overline{\boldsymbol{x}}_t$, respectively, associated with the natural gas and electricity systems: $\boldsymbol{x}_T = \boldsymbol{x}_t\big|_{t\in T} = \left[\boldsymbol{x}_t^{ng}\ \boldsymbol{x}_t^{el}\right]_{t\in T}$. From this set of variables, the active and reactive power outputs of the i-th generator during the time period t are denoted as sp_{it} and sq_{it}, respectively, and the discrete-valued variable $u_{it}\in\{1,0\}$ indicates its corresponding on/off status. Based on this notation, the active power output of each scheduled unit at the t-th period of time corresponds to the elements of the vector $\boldsymbol{sp}_{It} = \left[sp_{it}\right]_{i\in I}$. Similarly, the active power produced by the i-th generator at each time period of the planning horizon are collected together into the vector $\boldsymbol{sp}_{iT} = \left[sp_{it}\right]_{t\in T}$. Lastly, the elements of the vector $\boldsymbol{sp} = \left[sp_{it}\right]_{i\in I,t\in T}$

correspond to the active power produced by each generator at every period of time [He 2017]. All other decision variables can be similarly represented over the whole period of study; for example, the commitment status of all generators during the planning horizon is given by $\boldsymbol{u} = [u_{it}]_{i\in I, t\in T}$.

Based on the information mentioned above, the GUC problem is mathematically formulated as a mixed-integer nonlinear optimization problem given by

$$\min_{x,u} \left\{ \begin{array}{l} F(\boldsymbol{sp},\boldsymbol{u}) + K(\boldsymbol{u}) + C_r(\boldsymbol{r}) \,\big|\, \boldsymbol{h}(\boldsymbol{x}) = \boldsymbol{0}, \boldsymbol{g}(\boldsymbol{x}) \le \boldsymbol{0}, \boldsymbol{R}(\boldsymbol{sp},\boldsymbol{u}) \le \boldsymbol{0}, \\ \boldsymbol{M}(\boldsymbol{sp},\boldsymbol{sq},\boldsymbol{u}) \le \boldsymbol{0}, \boldsymbol{C}(\boldsymbol{u}) \le \boldsymbol{0} \end{array} \right\} \tag{2.14}$$

where the total cost of producing the active power required over the entire planning horizon is the scalar function $F(\boldsymbol{sp},\boldsymbol{u})$, which is spatially and temporally separable. The spatially separable scalar function $K(\boldsymbol{u})$ represents the startup and shutdown costs. The reserve cost offered by each generator in order to supply primary frequency regulation reserve r_{it}, is represented by $C_r(\boldsymbol{r})$ [Restrepo 2005], which is also spatially and temporally separable.

The set of operational constraints $\boldsymbol{h}(\boldsymbol{x}) = \left\{ \boldsymbol{h}_t^{ng}(\boldsymbol{x}_t)\, \boldsymbol{h}_t^{el}(\boldsymbol{x}_t) \right\}_{t\in T}$ and physical constraints $\boldsymbol{g}(\boldsymbol{x}) = \left\{ \boldsymbol{g}_t^{ng}(\boldsymbol{x}_t)\, \boldsymbol{g}_t^{el}(\boldsymbol{x}_t) \right\}_{t\in T}$ imposed on the natural gas and electricity networks is temporally separable. The two sets of intertemporal, spatially separable constraints $\boldsymbol{R}(\boldsymbol{sp},\boldsymbol{u}) = \left\{ \boldsymbol{R}_i(\boldsymbol{sp}_{iT}, \boldsymbol{u}_{iT}) \right\}_{i\in I}$ and $\boldsymbol{C}(\boldsymbol{u}) = \left\{ \boldsymbol{C}_i(\boldsymbol{u}_{iT}) \right\}_{i\in I}$ are associated with the ramping and total fuel constraints as well as the minimum up time/down time constraints, respectively. Lastly, the set of operation constraints related to thermal generators is $\boldsymbol{M}(\boldsymbol{sp},\boldsymbol{sq},\boldsymbol{u}) = \left[\boldsymbol{M}_{it}(sp_{it}, sq_{it}, u_{it}) \right]_{i\in I, t\in T}$, which is spatially and temporally separable. Note that these constraints also include the active and reactive powers of those generators that are not included in the unit commitment but are considered in the OGPF subproblem.

The set of variables representing active and reactive power outputs of thermal units are duplicated such that $\boldsymbol{dp}=\boldsymbol{sp}$ and $\boldsymbol{dq}=\boldsymbol{sq}$, where the "$\boldsymbol{d}$" variables correspond to a dynamic copy of the static variables "$\boldsymbol{s}$" to reformulate the GUC problem (2.14) by the equivalent optimization problem (2.15). Note that in order to achieve this equivalence two additional sets of artificial constraints have been added to the optimization problem (2.15) to insure that

each set of variables, those associated with the active and reactive power generated by the scheduled units at each period of time, will have the same values at the optimal solution: if $\boldsymbol{x}$ solves (2.14), then $\boldsymbol{x}$ solves (2.15), and if ($\boldsymbol{x}$, $\boldsymbol{dp}$, $\boldsymbol{dq}$) is a solution of (2.15), then ($\boldsymbol{dp}$=$\boldsymbol{sp}$$\in$$\boldsymbol{x}$, $\boldsymbol{dq}$=$\boldsymbol{sq}$$\in$$\boldsymbol{x}$, $\boldsymbol{x}$) is a solution of (2.14) [He 2017]

$$\min_{\substack{\boldsymbol{x},\boldsymbol{u},\\ \boldsymbol{dp},\boldsymbol{dq}}} \left\{ \begin{array}{l} F(\boldsymbol{dp},\boldsymbol{u}) + K(\boldsymbol{u}) + C_r\left(\boldsymbol{r}\right) \\ \boldsymbol{R}(\boldsymbol{dp},\boldsymbol{u}) \le \boldsymbol{0}, \boldsymbol{M}(\boldsymbol{dp},\boldsymbol{dq},\boldsymbol{u}) \le \boldsymbol{0}, \boldsymbol{C}(\boldsymbol{u}) \le \boldsymbol{0}, \boldsymbol{dp} = \boldsymbol{sp}, \boldsymbol{dq} = \boldsymbol{sq} \end{array} \middle| \begin{array}{l} \boldsymbol{h}(\boldsymbol{x}) = \boldsymbol{0}, \boldsymbol{g}(\boldsymbol{x}) \le \boldsymbol{0}, \\ \end{array} \right\}. \tag{2.15}$$

The Lagrangian optimization problem (2.16) is obtained by relaxing the set of artificial constraints $\boldsymbol{dp}$=$\boldsymbol{sp}$ and $\boldsymbol{dq}$=$\boldsymbol{sq}$, resulting the max-min dual optimization problem (2.17) with a decomposable structure:

$$\min_{\substack{\boldsymbol{x},\boldsymbol{u},\\ \boldsymbol{dp},\boldsymbol{dq}}} \left\{ \begin{array}{l} F(\boldsymbol{dp},\boldsymbol{u}) + K(\boldsymbol{u}) + C_r\left(\boldsymbol{r}\right) + \boldsymbol{\lambda}_p^{\mathrm{T}}\left(\boldsymbol{sp} - \boldsymbol{u} \circ \boldsymbol{dp}\right) + \boldsymbol{\lambda}_q^{\mathrm{T}}\left(\boldsymbol{sq} - \boldsymbol{u} \circ \boldsymbol{dq}\right) \\ \boldsymbol{g}(\boldsymbol{x}) \le \boldsymbol{0}, \boldsymbol{R}(\boldsymbol{dp},\boldsymbol{u}) \le \boldsymbol{0}, \boldsymbol{M}(\boldsymbol{dp},\boldsymbol{dq},\boldsymbol{u}) \le \boldsymbol{0}, \boldsymbol{C}(\boldsymbol{u}) \le \boldsymbol{0} \end{array} \middle| \boldsymbol{h}(\boldsymbol{x}) = \boldsymbol{0}, \right\} \tag{2.16}$$

$$\max_{\boldsymbol{\lambda}_p,\boldsymbol{\lambda}_q} \left\{ \begin{array}{l} \min_{\boldsymbol{x}} \left\{ \boldsymbol{\lambda}_p^{\mathrm{T}}\,\boldsymbol{sp} + \boldsymbol{\lambda}_q^{\mathrm{T}}\,\boldsymbol{sq} \;\middle|\; \boldsymbol{h}(\boldsymbol{x}) = \boldsymbol{0}, \boldsymbol{g}(\boldsymbol{x}) \le \boldsymbol{0} \right\} + \\ \min\limits_{\boldsymbol{dp},\boldsymbol{dq},\boldsymbol{u}} \left\{ \begin{array}{l} F(\boldsymbol{dp},\boldsymbol{u}) + K(\boldsymbol{u}) + C_r\left(\boldsymbol{r}\right) \\ -\boldsymbol{\lambda}_p^{\mathrm{T}}\left(\boldsymbol{u} \circ \boldsymbol{dp}\right) - \boldsymbol{\lambda}_q^{\mathrm{T}}\left(\boldsymbol{u} \circ \boldsymbol{dq}\right) \end{array} \middle| \boldsymbol{R}(\boldsymbol{dp},\boldsymbol{u}) \le \boldsymbol{0}, \boldsymbol{M}(\boldsymbol{dp},\boldsymbol{dq},\boldsymbol{u}) \le \boldsymbol{0}, \boldsymbol{C}(\boldsymbol{u}) \le \boldsymbol{0} \right\} \end{array} \right\}. \tag{2.17}$$

The difficulty to obtain a feasible solution of the dual optimization problem (2.17), since the solution process may exhibit a numerical oscillatory performance, is overcome by adding two convexification terms of artificial constraints to the objective function in the primal optimization problem (2.16), which results in (2.18). In this case, $\|\cdot\|$ is the inner product norm, and the scalar penalty parameters c_p and c_q are chosen and adjusted as discussed in [Batut 1992], where both parameters usually correspond to a large value bigger than 0. According to [Birgin 2010], however, the subproblem associated with the minimization of the augmented Lagrangian may be very difficult to solve when the penalty

parameter has a very large value. This is due to the Newton-based iterative solution process does not decrease the augmented Lagrangian's value. Based on the abovementioned, a value of the order of $1x10^6$ has been chosen for these penalty terms, which provides enough good results in the minimization of the augmented Lagrangian function. Since the augmented Lagrangian relaxation problem (2.18) is not separable because the duplicated variables are mixed in the convexification terms, the auxiliary problem principle is used to linearize these terms with respect to their values of a previous iteration, rendering these convexification terms separable [Cohen 1980]. Hence, the resulting dual problem decomposed into two independent minimization subproblems at the *k*-th iteration of the solution process is given by (2.19), where the index *k*-1 indicates known values at the (*k*-1)-th iteration and the scalar penalty factors b_p and b_q are chosen as discussed in [Batut 1992], where $b_p \geq 2c_p$ and $b_q \geq 2c_q$.

$$\min_{\substack{\boldsymbol{x},\boldsymbol{u},\\ \boldsymbol{dp},\boldsymbol{dq}}} \left\{ \begin{array}{l} F(\boldsymbol{dp},\boldsymbol{u}) + K(\boldsymbol{u}) + C_r(\boldsymbol{r}) + \boldsymbol{\lambda}_p^{\mathrm{T}}(\boldsymbol{sp} - \boldsymbol{u} \circ \boldsymbol{dp}) + \boldsymbol{\lambda}_q^{\mathrm{T}}(\boldsymbol{sq} - \boldsymbol{u} \circ \boldsymbol{dq}) \\ + \dfrac{c_p}{2}\left\|\boldsymbol{sp} - \boldsymbol{u} \circ \boldsymbol{dp}\right\|^2 + \dfrac{c_q}{2}\left\|\boldsymbol{sq} - \boldsymbol{u} \circ \boldsymbol{dq}\right\|^2 \\ \left| \boldsymbol{h}(\boldsymbol{x}) = \boldsymbol{0}, \boldsymbol{g}(\boldsymbol{x}) \leq \boldsymbol{0}, \boldsymbol{R}(\boldsymbol{dp},\boldsymbol{u}) \leq \boldsymbol{0}, \boldsymbol{M}(\boldsymbol{dp},\boldsymbol{dq},\boldsymbol{u}) \leq \boldsymbol{0}, \boldsymbol{C}(\boldsymbol{u}) \leq \boldsymbol{0} \right. \end{array} \right\} \tag{2.18}$$

$$\max_{\boldsymbol{\lambda}_p,\boldsymbol{\lambda}_q} \left\{ \begin{array}{l} \min\limits_{\boldsymbol{x}} \left\{ \begin{array}{l} \boldsymbol{\lambda}_{\boldsymbol{p},k-1}^{\mathrm{T}}\boldsymbol{sp} + \boldsymbol{\lambda}_{\boldsymbol{q},k-1}^{\mathrm{T}}\boldsymbol{sq} \\ + \dfrac{b_p}{2}\left\|\boldsymbol{sp} - \boldsymbol{sp}_{k-1}\right\|^2 + \dfrac{b_q}{2}\left\|\boldsymbol{sq} - \boldsymbol{sq}_{k-1}\right\|^2 \\ + c_p \boldsymbol{sp}^{\mathrm{T}}\left(\boldsymbol{sp}_{k-1} - \boldsymbol{u}_{k-1} \circ \boldsymbol{dp}_{k-1}\right) \\ + c_q \boldsymbol{sq}^{\mathrm{T}}\left(\boldsymbol{sq}_{k-1} - \boldsymbol{u}_{k-1} \circ \boldsymbol{dq}_{k-1}\right) \\ + \dfrac{b_p}{2}\left\|\boldsymbol{u}_{k-1} \circ \boldsymbol{dp}_{k-1}\right\|^2 + \dfrac{b_q}{2}\left\|\boldsymbol{u}_{k-1} \circ \boldsymbol{dq}_{k-1}\right\|^2 \end{array} \right| \boldsymbol{h}(\boldsymbol{x}) = \boldsymbol{0}, \boldsymbol{g}(\boldsymbol{x}) \leq \boldsymbol{0} \right\} + \\ \min\limits_{\boldsymbol{dp},\boldsymbol{dq},\boldsymbol{u}} \left\{ \begin{array}{l} F(\boldsymbol{dp},\boldsymbol{u}) + K(\boldsymbol{u}) + C_r(\boldsymbol{r}) \\ - \boldsymbol{\lambda}_{\boldsymbol{p},k-1}^{\mathrm{T}}(\boldsymbol{u} \circ \boldsymbol{dp}) - \boldsymbol{\lambda}_{\boldsymbol{q},k-1}^{\mathrm{T}}(\boldsymbol{u} \circ \boldsymbol{dq}) \\ + \dfrac{b_p}{2}\left\|\boldsymbol{u} \circ \boldsymbol{dp}\right\|^2 + \dfrac{b_q}{2}\left\|\boldsymbol{u} \circ \boldsymbol{dq}\right\|^2 \\ - b_p(\boldsymbol{u} \circ \boldsymbol{dp})^{\mathrm{T}}(\boldsymbol{u} \circ \boldsymbol{dp}_{k-1}) - b_q(\boldsymbol{u} \circ \boldsymbol{dq})^{\mathrm{T}}(\boldsymbol{u} \circ \boldsymbol{dq}_{k-1}) \\ - c_p(\boldsymbol{u} \circ \boldsymbol{dp})^{\mathrm{T}}\left(\boldsymbol{sp}_{k-1} - \boldsymbol{u}_{k-1} \circ \boldsymbol{dp}_{k-1}\right) \\ - c_q(\boldsymbol{u} \circ \boldsymbol{dq})^{\mathrm{T}}\left(\boldsymbol{sq}_{k-1} - \boldsymbol{u}_{k-1} \circ \boldsymbol{dq}_{k-1}\right) \end{array} \right| \begin{array}{c} \boldsymbol{R}(\boldsymbol{dp},\boldsymbol{u}) \leq \boldsymbol{0}, \\ \boldsymbol{M}(\boldsymbol{dp},\boldsymbol{dq},\boldsymbol{u}) \leq \boldsymbol{0}, \\ \boldsymbol{C}(\boldsymbol{u}) \leq \boldsymbol{0} \end{array} \end{array} \right\}. \tag{2.19}$$

2.5 Generalized short-term unit commitment solution

The two independent minimization subproblems given in (2.19) are sequentially solved in a coordinated fashion until both solutions simultaneously converge to a single optimum dispatch at each period of time, while satisfying the corresponding set of constraints. In this formulation, the first minimization problem of (2.19) is temporally separable into N_t optimal gas and power flow problems: one OGPF problem for each time period t. On the other hand, the second minimization problem is spatially separable into N_{thg} single generator scheduling problems over the entire planning horizon. The coordinated solution of both subproblems is performed through the values of all Lagrange multipliers $\boldsymbol{\lambda_p}$ and $\boldsymbol{\lambda_q}$ associated with the artificial constraints, as described below, which directly affect the active and reactive power outputs of generators.

2.5.1 GUC solution algorithm

The proposed solution algorithm for the GUC problem proceeds as follows:

Step 1. [Initialization.]

$k = 1$, c_p, c_q, b_p, b_q, $\boldsymbol{\varepsilon_p}$, $\boldsymbol{\varepsilon_p}$.

Step 2. [Solution of conventional OGPF problems.]

Solve N_t conventional OGPF problems of the form (2.20) by considering all the units committed as well as their corresponding generation limits. The resulting values of the Lagrange multipliers associated with the power flow equality constraints at the generator buses are used to set the fixed values of $\boldsymbol{\lambda}_{\boldsymbol{p},iT}^{k-1}$ and $\boldsymbol{\lambda}_{\boldsymbol{q},iT}^{k-1}$ $\forall i \in N_{thg}$ to be used in the scheduling of generators, step 3, and the solution of N_t independent OGPF problems, described in step 5. Note that these values of $\boldsymbol{\lambda}_{\boldsymbol{p},iT}^{k-1}$ and $\boldsymbol{\lambda}_{\boldsymbol{q},iT}^{k-1}$ $\forall i \in N_{thg}$ remain fixed during the solution process of each subproblem: the scheduling of generators and the OGPF,

$$\min_{\boldsymbol{x}} \left\{ \sum_{i=1}^{N_g} C_i(Pg_i) \middle| \boldsymbol{h}(\boldsymbol{x}) = \boldsymbol{0}, \boldsymbol{g}(\boldsymbol{x}) \le \boldsymbol{0} \right\} \quad \forall t \in T \ . \tag{2.20}$$

Step 3. [Scheduling of generators.]

Solve N_{thg} individual generator scheduling problems of the form (2.21), which corresponds to the second minimization problem of (2.19), by dynamic programming:

$$\underset{\boldsymbol{dp}_{iT},\boldsymbol{dq}_{iT},\boldsymbol{u}_{iT}}{\arg\min}\left\{\begin{array}{l|l} F_i(\boldsymbol{dp}_{iT},\boldsymbol{u}_{iT})+K(\boldsymbol{u}_{iT})+C_{r,i}\left(r_{iT}\right)+\dfrac{b_p}{2}\left\|\boldsymbol{u}_{iT}\circ\boldsymbol{dp}_{iT}\right\|^2+\dfrac{b_q}{2}\left\|\boldsymbol{u}_{iT}\circ\boldsymbol{dq}_{iT}\right\|^2 & \\ -\left(\left(\boldsymbol{\lambda}_{\boldsymbol{p},iT}^{k-1}\right)+c_p\left(\boldsymbol{sp}_{iT}^{k-1}-\boldsymbol{u}_{iT}^{k-1}\circ\boldsymbol{dp}_{iT}^{k-1}\right)+b_p\left(\boldsymbol{u}_{iT}^{k-1}\circ\boldsymbol{dp}_{iT}^{k-1}\right)\right)^{\mathrm{T}}\left(\boldsymbol{u}_{iT}\circ\boldsymbol{dp}_{iT}\right) & \boldsymbol{R}(\boldsymbol{dp},\boldsymbol{u})\le\boldsymbol{0},\ \boldsymbol{M}(\boldsymbol{dp},\boldsymbol{dq},\boldsymbol{u})\le\boldsymbol{0},\ \boldsymbol{C}(\boldsymbol{u})\le\boldsymbol{0} \\ -\left(\left(\boldsymbol{\lambda}_{\boldsymbol{q},iT}^{k-1}\right)+c_q\left(\boldsymbol{sq}_{iT}^{k-1}-\boldsymbol{u}_{iT}^{k-1}\circ\boldsymbol{dq}_{iT}^{k-1}\right)+b_q\left(\boldsymbol{u}_{iT}^{k-1}\circ\boldsymbol{dq}_{iT}^{k-1}\right)\right)^{\mathrm{T}}\left(\boldsymbol{u}_{iT}\circ\boldsymbol{dq}_{iT}\right) & \end{array}\right\}. \quad (2.21)$$

$\forall i\in I$

Step 4. [Feasibility test of generation.]

If the commitment schedule u at the k-th iteration is not in the database of tested commitments, perform a feasibility test of the generation capacity dispatch for each $t\in T$. The simple test consists of checking if the total active power dispatched at each time period is bigger than the corresponding total demand; if at least one schedule does not satisfy its demanded active power, store the unit commitment in the database as infeasible and go to step 7. Otherwise, the commitment is stored as feasible and go to step 5.

Step 5. [Primal feasibility solution.]

Perform the test of primal feasible solution by solving N_t independent OGPF problems of the form (2.22), which corresponds to the first minimization problem of (2.19), considering only the scheduled units and their corresponding generation limits. If and only if all OGPFs converge to an optimal solution, store the commitment in the database as feasible; otherwise, the schedule is stored as infeasible and go to step 7.

$$\underset{\boldsymbol{x}_{It}}{\arg\min}\left\{\begin{array}{l|l} \dfrac{b_p}{2}\left\|\boldsymbol{sp}_{It}\right\|^2+\left(\left(\boldsymbol{\lambda}_{\boldsymbol{p},It}^{k-1}\right)+c_p\left(\boldsymbol{sp}_{It}^{k-1}-\boldsymbol{u}_{It}^{k-1}\circ\boldsymbol{dp}_{It}^{k-1}\right)-b_p\boldsymbol{sp}_{It}^{k-1}\right)^{\mathrm{T}}\boldsymbol{sp}_{It} & \\ +\dfrac{b_q}{2}\left\|\boldsymbol{sq}_{It}\right\|^2+\left(\left(\boldsymbol{\lambda}_{q,It}^{k-1}\right)+c_q\left(\boldsymbol{sq}_{It}^{k-1}-\boldsymbol{u}_{It}^{k-1}\circ\boldsymbol{dq}_{It}^{k-1}\right)-b_q\boldsymbol{sq}_{It}^{k-1}\right)^{\mathrm{T}}\boldsymbol{sq}_{It} & \boldsymbol{h}_t(\boldsymbol{x}_t)=\boldsymbol{0},\ \boldsymbol{g}_t(\boldsymbol{x}_t)\le\boldsymbol{0} \\ +\dfrac{b_p}{2}\left(\left\|\boldsymbol{sp}_{It}^{k-1}\right\|^2+\left\|\boldsymbol{u}_{It}^{k-1}\circ\boldsymbol{dp}_{It}^{k-1}\right\|^2\right)+\dfrac{b_q}{2}\left(\left\|\boldsymbol{sq}_{It}^{k-1}\right\|^2+\left\|\boldsymbol{u}_{It}^{k-1}\circ\boldsymbol{dq}_{It}^{k-1}\right\|^2\right) & \end{array}\right\}. \quad (2.22)$$

$\forall t\in T$

Step 6. [Check the stopping criterion.]

For values of $\boldsymbol{\varepsilon_p} = \boldsymbol{\varepsilon_q} = 1\text{x}10^{-3}$, the iterative process stops if the mismatches $\boldsymbol{sp} - \boldsymbol{dp} < \boldsymbol{\varepsilon_p}$ and $\boldsymbol{sq} - \boldsymbol{dq} < \boldsymbol{\varepsilon_q}$ are satisfied. The primal-dual solution has been achieved.

Step 7. [Dual variables updating.]

Update the Lagrangian multipliers $\boldsymbol{\lambda}^k_{\boldsymbol{p},iT} = \boldsymbol{\lambda}^{k-1}_{\boldsymbol{p},iT} + \rho^k_p \left(\boldsymbol{sp}^k_{iT} - \boldsymbol{u}^k_{iT} \circ \boldsymbol{dp}^k_{iT} \right)$ and $\boldsymbol{\lambda}^k_{\boldsymbol{q},iT} = \boldsymbol{\lambda}^{k-1}_{\boldsymbol{q},iT} + \rho^k_q \left(\boldsymbol{sq}^k_{iT} - \boldsymbol{u}^k_{iT} \circ \boldsymbol{dq}^k_{iT} \right) \forall i \in N_{thg}$, with $\rho^k_p = \left(c_p \big/ \left(1 + \alpha_p k \right) \right) \le c_p$ and $\rho^k_q = \left(c_q \big/ \left(1 + \alpha_q k \right) \right) \le c_q$.

Step 8. Set k=k+1 and go back to step 3.

2.6 Optimal gas and AC power flow module

2.6.1 Objective function

The minimization of the total generation cost of electric power in thermal units is considered as the objective function in the conventional OGPF problem. The production cost associated with the i-th thermal unit is represented by the convex function $C_i \left(P_{thg,i} \right) = a_i + b_i P_{thg,i} + c_i P^2_{thg,i}$, where the parameters a_i, b_i and c_i are the cost curve coefficients. On the other hand, the objective function to be minimized in each independent OGPF problem, described in Step 5 of the GUC solution algorithm, is given by

$$\sum_{i \in I} \left\{ \begin{array}{l} \frac{b_p}{2} \left(sp_{it} \right)^2 + \left(\lambda^{k-1}_{p,it} + c_p \left(sp^{k-1}_{it} - u^{k-1}_{it} dp^{k-1}_{it} \right) - b_p sp^{k-1}_{it} \right) sp_{it} \\ + \frac{b_p}{2} \left(\left(sp^{k-1}_{it} \right)^2 + \left(u^{k-1}_{it} dp^{k-1}_{it} \right)^2 \right) \\ + \frac{b_q}{2} \left(sq_{it} \right)^2 + \left(\lambda^{k-1}_{q,it} + c_q \left(sq^{k-1}_{it} - u^{k-1}_{it} dq^{k-1}_{it} \right) - b_q sq^{k-1}_{it} \right) sq_{it} \\ + \frac{b_q}{2} \left(\left(sq^{k-1}_{it} \right)^2 + \left(u^{k-1}_{it} dq^{k-1}_{it} \right)^2 \right) \end{array} \right\} \forall t \in T \qquad (2.23)$$

2.6.2 Natural gas network

Since the optimization problem is formulated in a multi-period basis, the gas flow dynamics through the pipeline must be considered to obtain an accurate assessment of the interdependence between the natural gas and electricity networks. The transient model adopted in this thesis is the one reported in [Moritz 2007], where the pipeline is represented by a two-port network having only two nodes representing the beginning and end of the pipe, which are referred to as "*in*" and "*out*" nodes, respectively.

The two nonlinear equations for the gas flow through the pipeline connected between nodes *n* and *m* are given by (2.24) and (2.25), which represent the continuity equation and momentum equation, respectively. Assuming a unidirectional gas flow from node *n* to node *m*, the variables $G_{nm,t}^{in}$ and $G_{nm,t}^{out}$ denote the gas flow at the inlet node *n* and the outlet node *m* of the pipeline, respectively, at time period *t*. Furthermore, $\Pi_{n,t}$ and $\Pi_{m,t}$ are the nodal pressures at nodes *n* and *m*, respectively, at the period of time *t*, while $z_{\Pi n,t}$ and $z_{\Pi m,t}$ are the compressibility factors that depend on the gas pressure computed at nodes *n* and *m*, respectively, at the time period *t*. Assuming a constant gas temperature T_g^{nm} along the pipe, $z_{\Pi n,t} = 1 + \alpha_g \Pi_{n,t}$ where $\alpha_g < 0$ and hence $0 < z_{\Pi n,t} < 1$. The values of all variables with subindex *t*-Δ*t* were calculated at the previous time period. Regarding the pipeline parameters L_{nm} is the length, D_{nm} is the inner diameter, λ_{nm}^{fr} is a friction factor, *g* is the gravity constant acceleration and A_{nm} is the cross-section area. In addition, the following parameters are defined at base conditions: z_0 is the compressibility factor, ρ_0 is the gas density, Π_0 is the pressure and T_0 is the gas temperature.

$$\frac{G_{nm,t}^{out} - G_{nm,t}^{in}}{L_{nm}} + A_{nm} \frac{z_0 T_0}{\Pi_0 T_g^{nm}} \frac{\dfrac{\Pi_{m,t}}{z_t} - \dfrac{\Pi_{m,(t-\Delta t)}}{z_{(t-\Delta t)}}}{\Delta t} = 0, \quad \forall \{n,m\} \in N_{ng} \tag{2.24}$$

$$\frac{\Pi_{m,t}-\Pi_{n,t}}{L_{nm}}+g\frac{\rho_0 z_0 T_0}{\Pi_0 T_g^{nm}}\frac{\partial h}{\partial x}\frac{\Pi_{m,t}}{z_{\Pi m,t}}+\frac{\lambda_{nm}^{fr}}{2D_{nm}}\frac{\rho_0\Pi_0 T_g^{nm}}{\left(A_{nm}\right)^2 z_0 T_0}\frac{\left(G_{nm,t}^{out}\right)^2 z_{\Pi m,t}}{\Pi_{m,t}}$$
$$+\frac{\rho_0}{A_{nm}}\frac{G_{nm,t}^{out}-G_{nm,(t-\Delta t)}^{out}}{\Delta t}+\frac{\rho_0\Pi_0 T_g^{nm}}{\left(A_{nm}\right)^2 z_0 T_0}\frac{\dfrac{\left(G_{nm,t}^{out}\right)^2 z_{\Pi m,t}}{\Pi_{m,t}}-\dfrac{\left(G_{nm,t}^{in}\right)^2 z_{\Pi n,t}}{\Pi_{n,t}}}{L_{nm}} \qquad (2.25)$$
$$\forall\{n,m\}\in N_{ng}.$$

Note from (2.24) that the difference of nodal pressures depends on the mass of gas stored in the pipeline, referred to as linepack, at the time periods t and t-Δt: $LP_{nm,t}$ and $LP_{nm,t-\Delta t}$. This linepack provides the flexibility to cover gas imbalances of demand and supply in the short-term. As a consequence, (2.24) can also be expressed in terms of the linepack as $G_{nm,t}^{out}-G_{nm,t}^{in}=LP_{nm,t}-LP_{nm,t-\Delta t}$.

The set of operating constraints $\left\{\boldsymbol{h}_t^{ng}\left(\boldsymbol{x}_t\right)\right\}_{t\in T}=\mathbf{0}$ is composed as follows. In addition to the momentum equation constraint (2.25), the nodal gas flow mismatch equation constraint at the n-th node at time t is given by (2.26), where $G_{nm,t}^{in}$ and $G_{jn,t}^{out}$ denote the gas flowing from the inlet node n and the gas injected into the outlet node n, $G_{nm,t}^{C}$ is the gas flowing in the compressor, $\tau_{nm,t}^{C}$ is the gas extracted by the compressor, $G_{n,t}^{source}$ is the gas supplied by a source, $G_{n,t}^{load}$ is the gas extracted by a load, $G_{ni,t}^{load}$ is the gas extracted to drive an electric generator connected at the i-th node of the electrical network. Fig. 2.2 shows a representative scheme of the natural gas network model described in this section

$$\begin{aligned}&\Delta G_n=\sum_{m\in\Omega_n}G_{nm,t}^{in}-\sum_{j\in\Omega_n}G_{jn,t}^{out}+\sum_{m\in\Omega_n}G_{nm,t}^{C}+\sum_{m\in\Omega_n}\tau_{nm,t}^{C}\\&-G_{n,t}^{source}+G_{n,t}^{load}+G_{ni,t}^{load}=0,\quad\forall\{n,m,j\}\in N_{ng},\forall t\in T\end{aligned}. \qquad (2.26)$$

Note that the gas $G_{jn,t}^{out}$ injected at node n can be expressed as a function of $G_{jn,t}^{in}$, and the resulting (2.27) substitutes $G_{jn,t}^{out}$ in (2.26) in order to have an expression only in terms of the gas flowing from the inlet nodes. On the other hand, the gas extracted by the compressor depends on its energy consumption $BHP_{nm,t}^{C}$ as given by (2.28), with coefficients α_C, β_C and

γ_C that define the efficiency in the energy conversion process: from the thermal energy contained in the gas to the HP required by the compressor. Finally, $G_{ni,t}^{load}$ is computed as reported in Section 2.6.4.

$$G_{jn,t}^{out} = G_{jn,t}^{in} - A_{jn} \frac{z_0 T_0}{\Pi_0 T_g^{jn}} \frac{\frac{\Pi_{n,t}}{z_t} - \frac{\Pi_{n,(t-\Delta t)}}{z_{(t-\Delta t)}}}{\Delta t} L_{jn}, \quad \forall \{j,n\} \in N_{ng}\ ,\ \forall t \in T \tag{2.27}$$

$$\tau_{nm,t}^{C} = \alpha_C^{nm} + \beta_C^{nm}\ BHP_{nm,t}^{C} + \gamma_C^{nm} \left(BHP_{nm,t}^{C}\right)^2\ \ ,\ \forall \{n,m\} \in N_{ng}, \forall C \in N_{cs}\ ,\ \forall t \in T \tag{2.28}$$

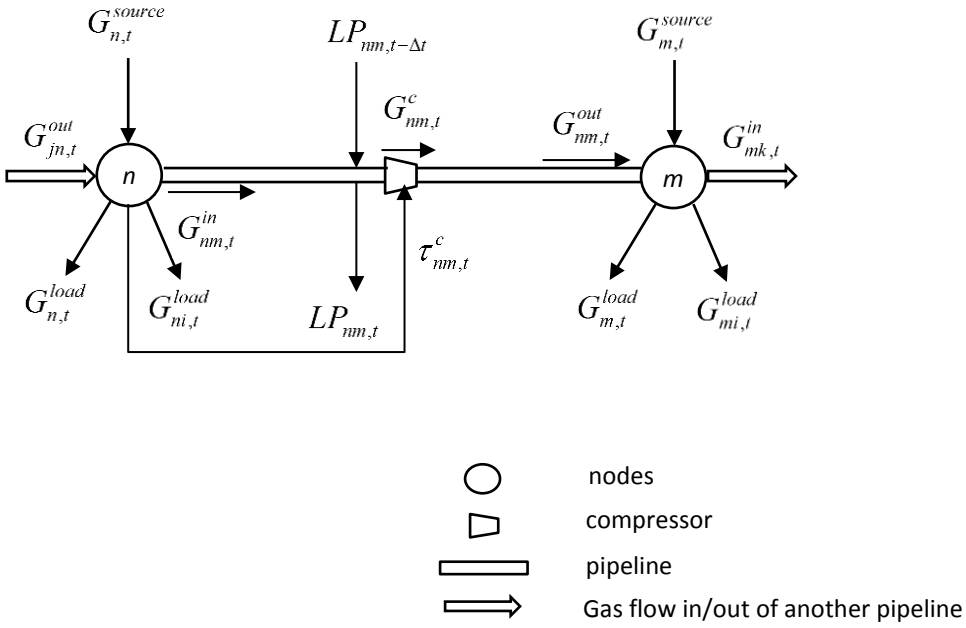

Fig. 2.2. Natural gas network model.

The energy consumption and compression ratio associated with each compressor station are represented by the equality constraints (2.29) and (2.30), respectively, at each time period *t*. In this case, Z_c is the average compressibility factor, $T_{g,t}^{n}$ is the gas temperature at the compressor's inlet node, E_C and η_C represent the parasitic and compression process efficiencies, respectively, c_{cn} is the specific heat ratio for the gas, $R_{nm,t}^{C}$ is the compression ratio and N_{cs} is the set of compressor stations.

$$\Delta HP_{nm,t}^{C} = BHP_{nm,t}^{C} - 0.0854\, Z_c \left(\frac{G_{nm,t}^{C}\, T_{g,t}^{n}}{E_C\, \eta_C} \right) \left(\frac{c_{cn}}{c_{cn}-1} \right) \left(\left(\frac{\Pi_{m,t}}{\Pi_{n,t}} \right)^{\frac{c_{cn}-1}{c_{cn}}} - 1 \right) = 0 \,, \tag{2.29}$$

$\forall \{n,m\} \in N_{ng}, \forall C \in N_{cs}\,,\ \forall t \in T$

$$\Delta R_{nm,t}^{C} = \frac{\Pi_{m,t}}{\Pi_{n,t}} - R_{nm,t}^{C} = 0 \quad , \quad \forall \{n,m\} \in N_{ng}, \forall C \in N_{cs}\,,\ \forall t \in T \qquad . \tag{2.30}$$

Lastly, the physical constraints $\left\{ \boldsymbol{g}_t^{ng}\left(\boldsymbol{x}_t\right) \right\}_{t\in T} \le \mathbf{0}$ imposed on the natural gas are those associated with the gas supplied from each gas source (2.31) and the nodal gas pressures (2.32):

$$\underline{G}_{n,t}^{source} \le G_{n,t}^{source} \le \bar{G}_{n,t}^{source}, \quad \forall source \in N_{ng}^{source}, \forall t \in T \tag{2.31}$$

$$\underline{\Pi}_{n,t} \le \Pi_{n,t} \le \bar{\Pi}_{n,t} \ , \quad \forall n \in N_{ng}\,,\ \forall t \in T\,. \tag{2.32}$$

2.6.3 Electricity network

The operation of the electricity network is represented by the nodal power flow and the primary frequency regulation equality constraints $\left\{ \boldsymbol{h}_t^{el}\left(\boldsymbol{x}_t\right) \right\}_{t\in T} = \mathbf{0}$ given by (2.33) and (2.34) [Martinez-Mares 2012], and (2.38)-(2.42) [Restrepo 2005]. On the other hand, $L_{i,t}^{C,nm}$ is computed by (2.35) and corresponds to the energy supplied to the compressor connected between gas nodes *n* and *m* from the *i*-th node of the electric power system, while the active and reactive powers flowing from the *i*-th node through all transmission components connected to it are computed by (2.36) and (2.37), respectively,

$$\Delta P_{i,t} = sp_{it} + P_{it}^{g} - P_{i,t}^{load} - P_{i,t}^{cal} - L_{i,t}^{C,nm} = 0 \quad , \qquad \forall i \in N_{el} \tag{2.33}$$

$$\Delta Q_{i,t} = sq_{it} + Q_{it}^{g} - Q_{i,t}^{load} - Q_{i,t}^{cal} = 0 \quad , \qquad \forall i \in \left(N_{el} - N_{el}^{PV} \right) \tag{2.34}$$

where

$$L_{i,t}^{C,nm} = BHP_{nm,t}^{C} \left(\frac{0.000007457}{3600} \right) \ , \forall t \in T \tag{2.35}$$

$$P_{i,t}^{cal} = \sum_{j \in i} \left\{ V_{i,t}^2 G_{ii} + V_{i,t} V_{j,t} \left[G_{ij} \cos\left(\theta_{i,t} - \theta_{j,t}\right) + B_{ij} \sin\left(\theta_{i,t} - \theta_{j,t}\right) \right] \right\} \quad , \forall t \in T \qquad (2.36)$$

$$Q_{i,t}^{cal} = \sum_{j \in i} \left\{ -V_{i,t}^2 B_{ii} + V_{i,t} V_{j,t} \left[G_{ij} \sin\left(\theta_{i,t} - \theta_{j,t}\right) - B_{ij} \cos\left(\theta_{i,t} - \theta_{j,t}\right) \right] \right\} \quad , \forall t \in T \, . \qquad (2.37)$$

To have enough flexibility to maintain the frequency deviation within limits, the reserve of active power must be considered [Wood 1996, Alvarez 2002]. When the primary frequency regulation is performed based on this reserve, the available active power sp_{it}^{PFR} of unit *I* is given by (2.38), which is composed of the active power sp_{it} injected to the system plus the power reserve $D_i \Delta f_t$ that can be used to minimize mismatches between power generation and load demand:

$$sp_{it}^{PFR} = sp_{it} - D_i \Delta f_t \quad , \forall i \in I, \;\; t \in T \qquad , \qquad (2.38)$$

where the parameter D_i is the frequency regulation constant or governor droop of the *i*-th unit in MW/Hz, while Δf_t is the system frequency deviation associated with the primary regulation control at sub-period *t*, which is obtained as a consequence of imbalances between generation and demand. Note that the value of this frequency deviation corresponds to the steady state value after the oscillation has been damped out, as shown in Fig. 2.3 [Restrepo 2005].

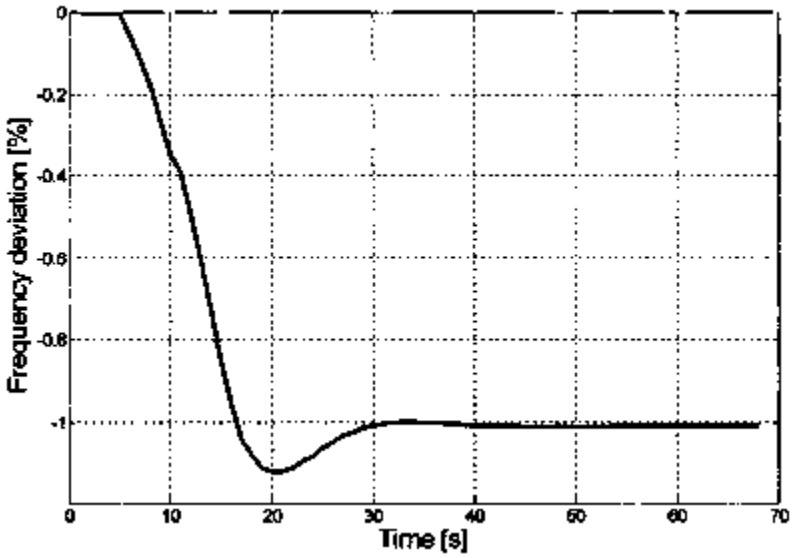

Fig. 2.3. Typical system frequency response to primary regulation after a contingency.

On the other hand, the maximum output of the *i*-th unit under primary frequency regulation is defined by the minimum value between the maximum capacity limit $\overline{sp}_{it}$ and the frequency regulation ramp limit $\Delta sp_i^{\max}$, as given by

$$sp_{it}^{\max} = \min\left\{\overline{sp}_{it},\ sp_{it} + \Delta sp_i^{\max}\right\},\ \forall i \in I,\ \ t \in T\ . \tag{2.39}$$

The ramp limit $\Delta sp_i^{\max}$ constraints the rate at which the output power level of a given generator can be modified in a given period of time and must be consistent with the short time constants of primary frequency regulation, which is typically narrower than the ramp limits associated with the slower secondary and tertiary regulations. The primary frequency deviation response of the *i*-th unit generator is depicted in Fig. 2.4 [Restrepo 2005], where Δf_{bi} corresponds to the break-frequency deviation at which *i*-th unit generator saturates at $sp_{it}^{\max}$ and could be computed by (2.40) at sub-period *t*. If there is an available active power $sp_{it}^{P\&R}$, which includes active power and reserves without frequency regulation, and satisfies $sp_{it}^{P\&R} < sp_{it}^{\max}$,the frequency deviation at which the *i*-th unit generator provides $sp_{it}^{P\&R}$ is

obtained by (2.41). This means that each *i*-th generator deploys the required reserves power at a different given value of system's frequency deviation. Lastly, when the primary frequency regulation is implemented, only one frequency deviation value exists: $-\Delta f_t$ and corresponds to the frequency deviation of the system at which each *i*-th unit generator must provide its available active power under regulation sp_{it}^{PFR}, as given by (2.42).

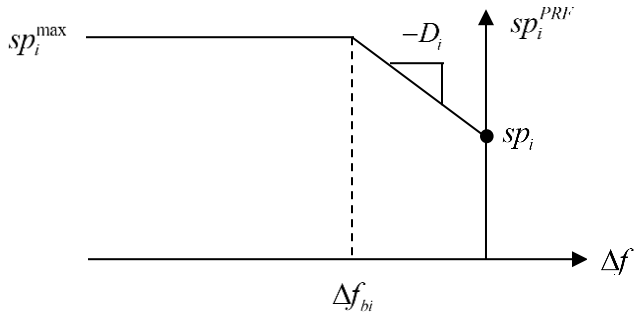

Fig. 2.4. Frequency regulation response of *i*-th unit generator.

$$\Delta f_{bi,t} = \frac{sp_{it} - sp_{it}^{\max}}{D_i} \quad ,\forall i \in I, \;\; t \in T \tag{2.40}$$

$$\Delta f_{it} = \frac{sp_{it} - sp_{it}^{P\&R}}{D_i} \quad ,\forall i \in I, \;\; t \in T \tag{2.41}$$

$$\Delta f_t = \frac{sp_{it} - sp_{it}^{PFR}}{D_i} \quad ,\forall i \in I, \;\; t \in T \tag{2.42}$$

Finally, the set of inequality constraints $\left\{ \boldsymbol{g}_t^{el}\left(\boldsymbol{x}_t\right)\right\}_{t\in T} \le \mathbf{0}$ corresponding to the limits of active and reactive power generations, as well as those associated with nodal voltage magnitudes are represented by (2.43)-(2.46). The limit associated with the active power generation, including its respective active power reserve r_{it} available for *i-th* unit generator, is given by (2.47). The upper and lower bounds of scheduled primary regulation reserve r_{it} available for generators, are represented by (2.48), where this reserve must be equal or bigger than the maximum deviation of active power generation relative to an imbalance between generation and demand, and also must be equal or lower to the upper limit ramp $\Delta sp_i^{\max}$. In addition, the total primary regulation reserves available must be equal or bigger than the

maximum capacity value from all thermal generators of the system, as shown in (2.49), and the maximum frequency deviation of the system is represented by (2.50). Lastly, line flow limits constraints are not included in the formulation.

$$\underline{sp}_{it} \le sp_{it} \le \overline{sp}_{it} \quad , \ \forall i \in I \ , t \in T \tag{2.43}$$

$$\underline{sq}_{it} \le sq_{it} \le \overline{sq}_{it} \quad , \ \forall i \in I \ , t \in T \tag{2.44}$$

$$\underline{Q}_{it}^{g} \le Q_{it}^{g} \le \overline{Q}_{it}^{g} \quad , \ \forall i \in I \ , t \in T \tag{2.45}$$

$$\underline{V}_{i,t} \le V_{i,t} \le \overline{V}_{i,t} \quad , \ \forall i \in \left(N_{el} - N_{el}^{PV} \right) , t \in T \tag{2.46}$$

$$sp_{it} + r_{it} \le \overline{sp}_{it} \quad , \ \forall i \in I \ , t \in T \tag{2.47}$$

$$sp_{it}^{PFR} - sp_{it} \le r_{it} \le \Delta sp_{i}^{\max}, \quad \forall i \in I, \ \ t \in T \tag{2.48}$$

$$sp_{\max} \le \sum_{i \in I} r_{it}, \quad t \in T \tag{2.49}$$

$$-\Delta f_t \le \Delta \overline{f}, \quad t \in T \tag{2.50}$$

2.6.4 Coupling thermal units

The coupling between the electricity and natural gas networks is given through the gas-fired units that act as converters in the energy conversion process of transforming the thermal energy contained in natural gas into electric power. If a thermal unit links the *n*-th node of the gas network to the *i*-th node of the electricity system, the energy conversion process is formulated at time *t* by the heat rate curve $HR_{ni,t}$ (2.51), where the polynomial coefficients define the efficiency of the conversion process. Furthermore, the amount of natural gas $G_{ni,t}^{load}$ required for this energy transformation is given by (2.52), where GHV_{ng} is the natural gas gross heating value. Additionally, the plant efficiency is represented by $\eta_{i,t}$, which is equal to the output energy divided by the input energy and is inversely proportional to the heat rate curve $HR_{ni,t}$, as shown in equation (2.53). To express the efficiency of a generator as a percentage is necessary to divide the equivalent Btu content of each MWh, depending on the type of fuel used, by the heat rate curve. Lastly, this formulation is also applied to other types of thermal units, such as coal-fired generators which are also considered in the reported case studies:

$$HR_{ni,t} = \alpha_{ni} + \beta_{ni}\, sp_{it} + \gamma_{ni}\left(sp_{it}\right)^2 \quad , \forall n \in N_{ng}, \forall i \in N_{el} \ , \forall t \in T \tag{2.51}$$

$$G_{ni,t}^{load} = \frac{HR_{ni,t}}{GHV_{ng}} \ , \forall n \in N_{ng}, \forall i \in N_{el} \ , \forall t \in T \quad . \tag{2.52}$$

$$\eta_{i,t} = \frac{1}{HR_{ni,t}} \ , \forall n \in N_{ng}, \forall i \in N_{el} \ , \forall t \in T \tag{2.53}$$

Finally, the power output of wind generators is considered as a base generation, which is directly injected into the multi-energy system to assess how the wind speed profile affects the schedule and power dispatches of thermal generators. The output power of wind generators is computed as shown in (3.2) and (3.3) of Chapter 3.

2.6.5 Set of decision variables

Finally, the set of decision variables for the optimal power flow module is defined by $\left[\boldsymbol{x}\right] = \left[\boldsymbol{x}^{ng}, \boldsymbol{x}^{el}\right]^{\mathrm{T}}$, where $\boldsymbol{x}^{ng} \in \left\{\boldsymbol{\Pi} \in \Re^{\left(N_{ng} - N_{ng}^{sources}\right)}, \boldsymbol{BHP}^{C} \in \Re^{N_{CS}}, \boldsymbol{G}_{nm}^{C} \in \Re^{N_{CS}}, \boldsymbol{G}_{nm}^{in} \in \Re^{N_{ng}}\right\}$ is the vector of decision variables associated with the natural gas system and $\boldsymbol{x}^{el} \in \left\{\boldsymbol{sp} \in \Re^{I}, \boldsymbol{r} \in \Re^{I}, \boldsymbol{V} \in \Re^{\left(N_{el} - N_{el}^{PV}\right)}, \boldsymbol{\theta} \in \Re^{\left(N_{el}-1\right)}, \boldsymbol{\Delta f} \in \Re^{I}\right\}$ is the one related to the electric power system.

Lastly, the optimal power flow solution method adopted in this thesis is based on the modified barrier-augmented Lagrangian (MBAL) formulation reported in [Goldfarb 1999].

2.7 Dynamic programming module for unit commitment

This module determines the status on, off or banking for each thermal generator at each time period of the planning horizon. In order to schedule generators, the augmented

Lagrangian function that is minimized in the optimization problem described in step 3 of the GUC solution algorithm is given by

$$\sum_{t\in T}\left\{\begin{array}{l} F_i\left(dp_{it},u_{it}\right)+K_{it}\left(u_{it}\right)+C_{r,it}\left(r_{it}\right) \\ +\frac{b_p}{2}u_{it}\left(dp_{it}\right)^2-\left(\lambda_{p,it}^{k-1}+c_p\left(sp_{it}^{k-1}-u_{it}^{k-1}dp_{it}^{k-1}\right)+b_p u_{it}^{k-1}dp_{it}^{k-1}\right)u_{it}dp_{it} \\ +\frac{b_q}{2}u_{it}\left(dq_{it}\right)^2-\left(\lambda_{q,it}^{k-1}+c_q\left(sq_{it}^{k-1}-u_{it}^{k-1}dq_{it}^{k-1}\right)+b_q u_{it}^{k-1}dq_{it}^{k-1}\right)u_{it}dq_{it} \end{array}\right\}\ \forall i\in I\cdot \qquad (2.54)$$

In this case, the cost of active power production over the entire planning horizon $F_i\left(dp_{it},u_{it}\right)$ is a quadratic function similar to the one used in the conventional OPF. On the other hand, the startup cost, which depends on the temperature of the boiler, is computed by $K_{it}\left(u_{it}\right)=SC_i^{\max}\left(1-e^{-\gamma_i t_d}\right)u_{it}\left(1-u_{i(t-\Delta t)}\right),\forall t\in T$ [Wood 1996], where $SC_i^{\max}$ corresponds to the cold start fuel cost, γ_i denotes the time constant associated with the thermal processes inside the boiler and t_d is the cooling time after the unit was shut down.

In addition, the reserve cost is a cost offered by each generator in order to supply primary frequency regulation reserve r_{it}, and is computed by $C_{r,it}\left(r_{it}\right)=rc_i r_{it},\forall t\in T$ [Restrepo 2005], where rc_i is the reserve cost specified by each unit as part of the overall offer.

The set of ramping constraints $\boldsymbol{R}(\boldsymbol{dp},\boldsymbol{u})\le\boldsymbol{0}$ representing the maximum allowable change in active power generation between two consecutive time periods is given by (2.55), while the unit capacity constraints $\boldsymbol{M}(\boldsymbol{dp},\boldsymbol{dq},\boldsymbol{u})\le\boldsymbol{0}$ are formulated by (2.56). The set of constraints $\boldsymbol{C}(\boldsymbol{u})\le\boldsymbol{0}$ are divided into minimum up time and down time constraints (2.57), must-run constraints (2.58) and unavailability constraints (2.59), while the state transition equation is given in (2.60). In this case, LT_{it} is the number of time periods that unit i has been on or off, $LT_{it}\le 0$, at time t. The minimum up time MUT_i corresponds to the minimum number of periods unit i must remain on after it has been turned on, and the minimum down time MDT_i denotes the minimum number of periods unit i must remain off after it has been

shut down. In addition, Ω_i^{on} and Ω_i^{off} are the set of time periods in which the *i*-th unit must run or is not available, respectively,

$$-\Delta dp_i^{\min} \le u_{it}\left(dp_{it} + r_{it}\right) - u_{i(t-\Delta t)} dp_{i(t-\Delta t)} \le \Delta dp_i^{\max} \ , \ \forall t \in T \ \ , \ \forall i \in I \tag{2.55}$$

$$\left.\begin{aligned} & u_{it}\underline{dp}_i \le u_{it} dp_{it} \le u_{it}\overline{dp}_i \\ & u_{it}\underline{dq}_i \le u_{it} dq_{it} \le u_{it}\overline{dq}_i \\ & u_{it}\left(dp_{it} + r_{it}\right) \le u_{it}\overline{dp}_i \end{aligned}\right\}, \ \forall t \in T \ \ , \ \forall i \in I \tag{2.56}$$

$$u_{it} = \left\{\begin{array}{l} 1, \quad if \ \ 1 \le LT_{it} \le MUT_i \\ 0, \quad if \ \ -1 \ge LT_{it} > -MDT_i \\ 0 \ or \ 1, \quad if \ \ MUT_i \le LT_{it} \ \ or \ \ LT_{it} \le -MDT_i \end{array}\right\} \ , \ \forall t \in T \ \ , \ \forall i \in I \tag{2.57}$$

$$u_{it} = 1 \ , \ \forall t \in \Omega_i^{on} \ \ , \ \forall i \in I \tag{2.58}$$

$$u_{it} = 0 \ , \ \forall t \in \Omega_i^{off} \ \ , \ \forall i \in I \tag{2.59}$$

$$LT_{it} = \left\{\begin{array}{l} \max\left(LT_{i(t-\Delta t)}, 0\right) + 1, \quad if \ \ u_{it} = 1 \\ \min\left(LT_{i(t-\Delta t)}, 0\right) - 1, \quad if \ \ u_{it} = 0 \end{array}\right\} \ , \ \forall t \in T \ \ , \ \forall i \in I \ \ . \tag{2.60}$$

2.8 Conclusions

A generalized short-therm unit commitment formulation and the solution methodology have been described in this chapter. The mathematical model represents a realistic natural gas and AC electricity systems in an unified framework of analysis including their operational and physical constraints, with the aim to illustrate the interdependence between both energy systems. Furthermore, the integration of the unit commitment problem

to the OGPF results in a better representation of this interdependence. In order to obtain a feasible solution of this optimization problem, this proposal is based on the concepts of duplication of variables, the augmented Lagrangian relaxation and the auxiliary problem principle. Then, the original problem is decomposed into two mutually connected subproblems: the UC problem (master problem) and the OGPF (subproblem) as described in Section 2.3. Then, the proposed approach could allow to directly determine the operation state of both energy networks considering their operational and physical constraints, as well as the coupling constraints given by the gas-fired units.

The concept of Lagrangian relaxation has been explained in Section 2.2, in order to illustrate more clearly the dual problem used to solve the original GUC constrained optimization problem, which provides a formulation with optimal conditions for constrained optimization problems.

Chapter 3

Case Studies

3.1 Introduction

The proposed methodology described in Chapter 2 is applied to the solution of two multi-energy networks containing wind generators in order to assess the optimal scheduling of generators that simultaneously will meet the forecast demand and all operation constraints in the electric and natural gas systems over a planning horizon of one day ahead. All case studies were performed considering the demand and wind speed variation profiles shown in Fig. 3.1 as a function of time. Note that in some periods of time the fluctuation of wind power has a reverse trend to electricity demand. For the sake of simplicity, the same load variation profile has been considered in both networks in such a way that the demand of natural gas or electricity at any *j*-th node is given by (3.1) as a fraction of the maximum load $Load_{jt}^{\max}$, and the corresponding time-varying factor is given by f_{jt}^{load} for each period time *t* contained in *T*. On the other hand, all wind generators are exposed to the same wind speed, with a variation profile for 24 hours in advance that has been adopted from [Kariniotakis 2006] and are driven by the same wind power curve characteristic that is approximated by the eight-degree polynomial function (3.2) as a function of the wind speed ω_{sp}. Since (3.2) provides the active power output in per unit (pu) of each wind generator's rated power, the amount of active power in MW injected into the network is given by (3.3). Note that this power is considered as a base generation. Note also that variability of power produced by wind generators and demanded by loads is transferred to the operation of the natural gas network via changes in the gas-fired units dispatch:

$$Load_{jt} = f_{jt}^{load} Load_{jt}^{\max} \quad \forall j \in \left\{ N_{ng}, N_{el} \right\} \ , \ t \in T \tag{3.1}$$

$$P_{it}^{wind} = a_{\omega} + b_{\omega}\,\omega_{sp}^{it} + c_{\omega}\left(\omega_{sp}^{it}\right)^{2} + d_{\omega}\left(\omega_{sp}^{it}\right)^{3} + e_{\omega}\left(\omega_{sp}^{it}\right)^{4} + f_{\omega}\left(\omega_{sp}^{it}\right)^{5} + g_{\omega}\left(\omega_{sp}^{it}\right)^{6} + h_{\omega}\left(\omega_{sp}^{it}\right)^{7} + i_{\omega}\left(\omega_{sp}^{it}\right)^{8} \quad (3.2)$$

$$\forall i \in N_{gen}^{wind},\ \forall t \in T$$

$$P_{it}^{g\omega} = P_{i,rate}^{g\omega}\ P_{it}^{wind} \quad \forall i \in N_{gen}^{wind},\ \forall t \in T\ . \quad (3.3)$$

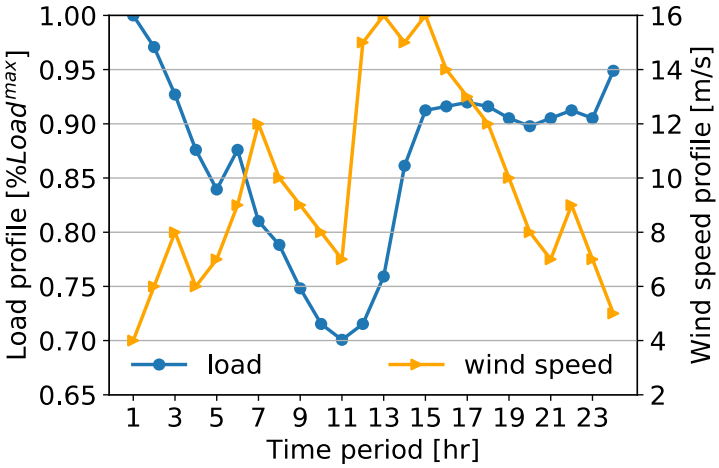

Fig.3.1 Forecast of wind speed and load demand profiles for 24 hours.

3.2 Base case study

In this study case, the GUC is applied to a multi-energy system composed of a 5-bus electricity network and a 3-node natural gas network with a maximum load of 165 MW [Stagg 1968] and 8.8 MSCM, respectively. The topology of this integrated energy system is shown in Fig. 3.2, while the generators' parameters for the dispatch are shown in Table I. Systems' data are given in [Stagg 1968] and [Tao 1998], respectively. The generators are scheduled for 24 hours in advance considering the security constraints for the voltage magnitudes and gas pressures given by $0.96 \leq V \leq 1.06$ pu and $30 \leq \Pi \leq 60$ Mpa, respectively. The following prices are considered for this case: 40 USD/MSCF (1.13 USD/MSCF) for the natural gas and 30 USD/Ton for coal. To assess the interdependencies between both infrastructures, a coal generator is connected at node South and a wind generator at node Main of the electric power system. Furthermore, the natural gas required by the generator embedded at node North is provided from node 3 of the natural gas network. Based on this information, clearly the wind speed in the first hours of analysis is not sufficient to producing

the maximum capacity of the wind generator, as shown in Fig. 3.1, while the natural gas-fired unit has enough capacity to supply the load during the entire planning period. Despite these observations, that may indicate how the demand can be satisfied, the operation of the whole multi-energy system is subjected to the security constraints that determine how the optimization process looks for the most economical generation scheduling to meet the load in each time period of study.

TABLE I. 5-NODE BENCHMARK SYSTEM, GENERATORS

Electric Node	Type	Energy bus	$\overline{sp}$ (MW)	$\underline{sp}$ (MW)	α_i [MBTU/hr]	β_i [MBTU/MWhr]	γ_i [MBTU/MW^{2}hr]	LT_{i1}	MDT	MUT	ΔP_i^{max}	ΔP_i^{min}
North	Gas	NG-3	200.0	30.0	540	0.043	0.007	3	2	3	0.3	0.3
South	Coal	-	65.0	30.0	504	0.43	0.007	1	2	3	0.4	0.4
Main	Wind	-	50.0	0.0	a_ω =1.27 b_ω =-0.806 c_ω =0.245 d_ω =-0.043 e_ω =5.09e-3 f_ω =-3.8e-4 g_ω =1.66e-5 h_ω =-3.85e-7 i_ω = 3.65e-9							

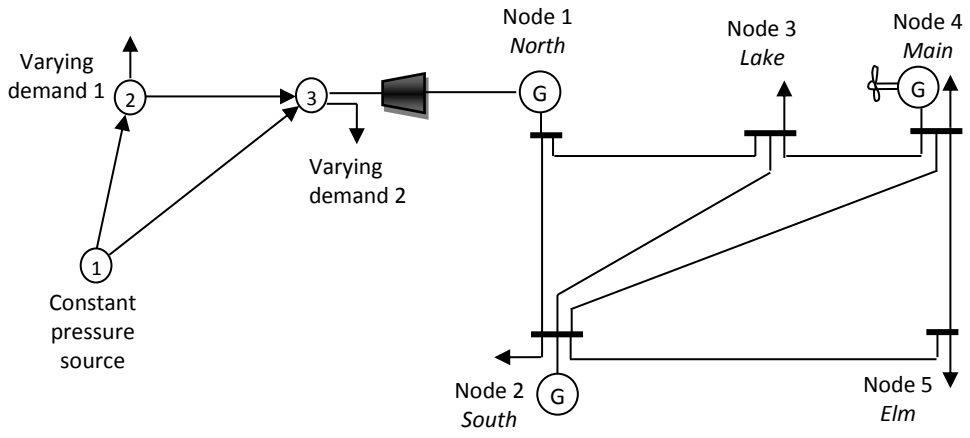

Fig. 3.2. The multi-energy network's infrastructures.

The resulting active power dispatch profile is shown in Fig. 3.3, where it is clear how the scheduling of active power delivered by the fossil fuel generators tries to follow the hourly electric load behavior. Note, however, that in between 12 and 16 hours of study the coal-fired generator is shut down: the algorithm computes a more expensive scenario of operation when this unit is kept on-line during that period of time. Note also that although

the lower demand of electric power occurs at the 11th hour, the gas-based generation cannot supply all the remaining net load not served by the wind generation, so that the coal-based generator must remain on at this hour to accommodate the imbalance between generation and load.

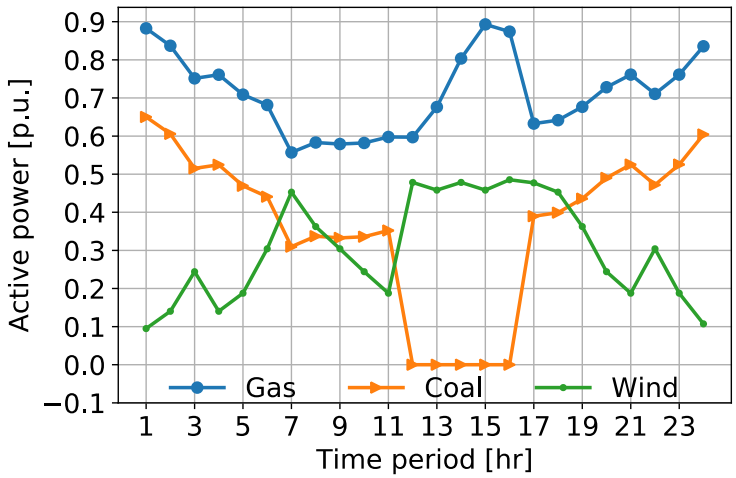

Fig. 3.3 Active power generation dispatches for 24 hours in advance for base case.

The dynamic behavior of the natural gas flows $G^{in}_{nm,t}$ and $G^{out}_{nm,t}$ $\forall\{n,m\}\in N_{ng}$ and $\forall t\in T$, which varies according to the amount of gas demanded by the electric generator and natural gas loads, is shown in Fig. 3.4. As expected, the amount of gas demanded by the generator increases at those hours in which the coal-based generator has been turned off, and this explains why the mass of natural gas flowing in the pipelines also increases during these hours. Note that the gap between $G^{in}_{nm,t}$ and $G^{out}_{nm,t}$ depends on the difference between pressures $\Pi_{m,t}$ and $\Pi_{m,(t-\Delta t)}$ as given by (2.24), and if this difference is very small, the values of $G^{out}_{nm,t}$ and $G^{in}_{nm,t}$ will be very close to each other. The nodal pressures profiles as a function of time are depicted in Fig. 3.5, where the gas pressure at reference node 1 is kept at a fixed value. Note that the pressures at outlet nodes decrease according to the required increase of gas flow in order to meet the gas demand.

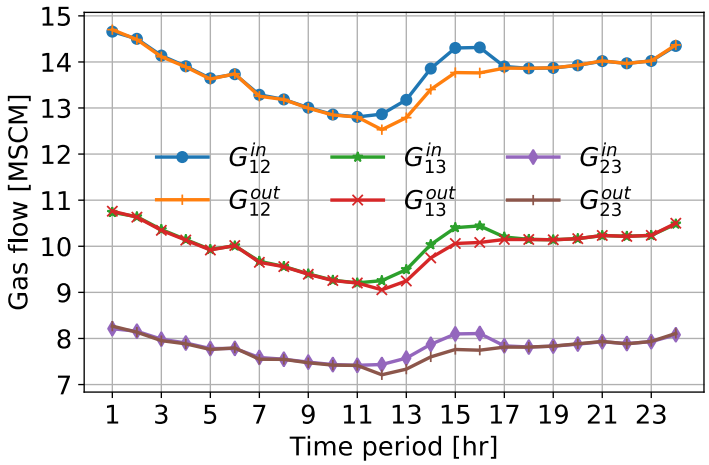

Fig. 3.4. Dynamic behavior of natural gas in pipelines for base case.

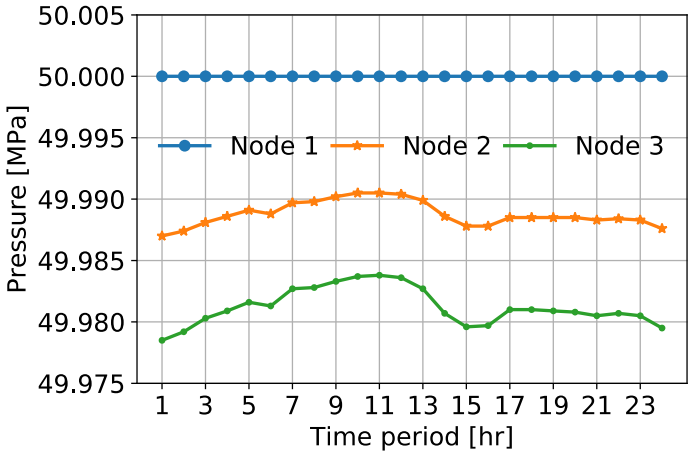

Fig. 3.5. Dynamic behavior of nodal pressures for base case.

Lastly, Fig. 3.6 shows the transient behavior of nodal voltage magnitudes in the electricity network. A sudden change in the nodal voltage magnitudes of all nodes, except in node North, occurs after the 11th hour in which the coal-based generator has been turned off, i.e., there exists a reduction in the support of reactive power. Nevertheless, the nodal voltage magnitude constraints are satisfied, and the electric load is supplied only with the natural gas and wind generators remaining on-line in the electric power system. On the other hand, the voltage magnitude at node North hits its upper limit during the time period in which the coal-based generator is shut down because the gas-fired unit directly embedded at this node must

increase its reactive power generation, as shown in Fig. 3.7, in order to maintain the nodal reactive power balance in the electricity network.

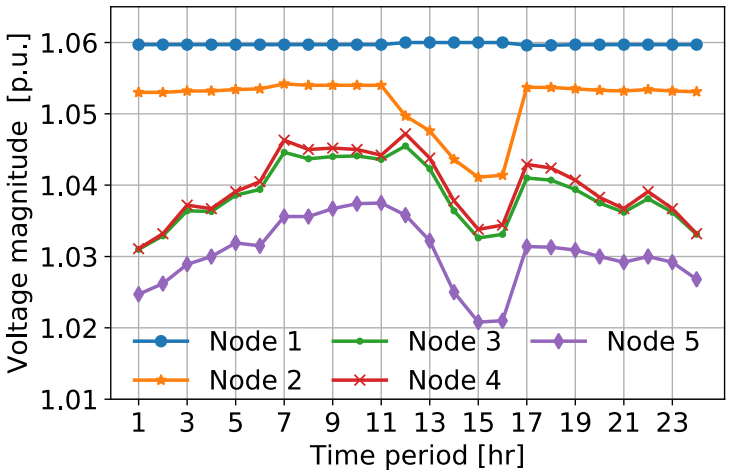

Fig. 3.6. Dynamic behavior of nodal voltage magnitudes in the electric network for base case.

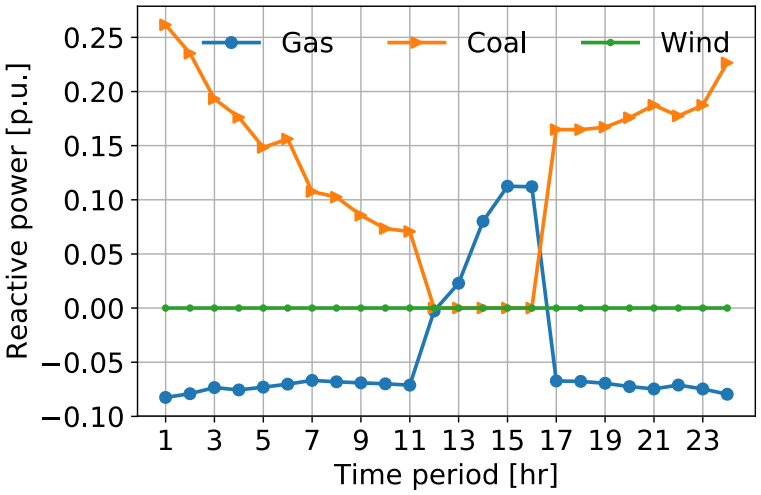

Fig. 3.7. Reactive power generation support for 24 hours in advance for case A.

3.3 The effect of voltage control at a specific node

The case study reported in the previous section is repeated, but the upper and lower bounds of the voltage magnitude at node South are changed to $1.05 \leq V \leq 1.06$ pu. The selection of these bounds aims to show how the need for providing reactive power support to meet voltage magnitude constraints affects the unit commitment solution. Figure 3.8 shows the hourly generation scheduling for each unit considering this new operational constraint. A comparison of these results with the ones reported in Fig. 3.3 shows that the scheduled generators and their active power outputs are equal in each time period until the 13th hour. In the next time period, the natural gas generator is unable to provide the required reactive power support to maintain the voltage control at node South; hence, the coal-based unit has to be turned on from the 14th hour to achieve the target control. Note also that from the 17th hour the power outputs of generators are newly equal to those reported in Fig. 3.3. The nodal voltage magnitude profiles as well as the hourly reactive power generation for this case study are shown in Figs. 3.9 and 3.10, respectively. The former clearly shows that the voltage magnitude at node South is within $1.05 \leq V_{south} \leq 1.06$ pu during the entire planning horizon, which does not occur between 13th and 16th hour for the base case study as shown in Fig. 6. On the other hand, the gas-fired unit must provide reactive power support at the 12th hour to maintain the voltage magnitude within limits, compared with the null support provided at this hour in the base case study. Lastly, note that in both case studies the generation of reactive power reverses between both thermal generators.

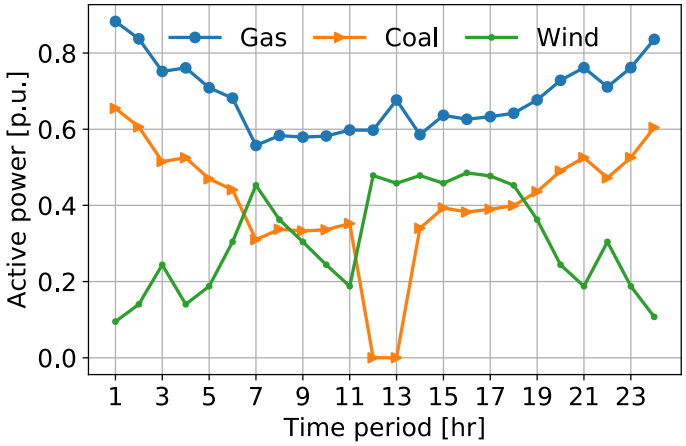

Fig. 3.8. Active power generation dispatches for 24 hours in advance for case with voltage control at Node 2.

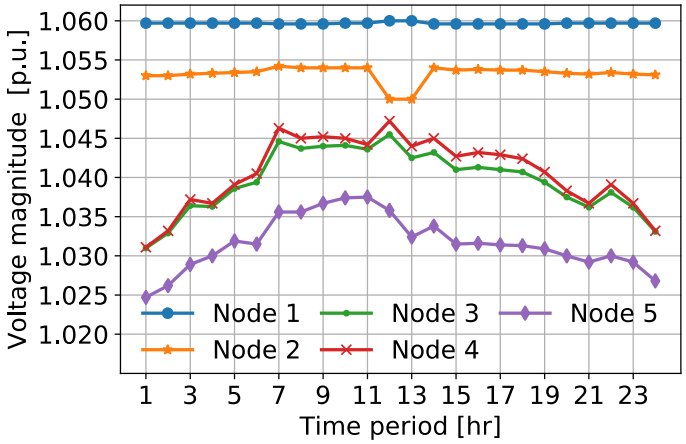

Fig. 3.9. Dynamic behavior of nodal voltage magnitudes at the electric network for case with voltage control at Node 2.

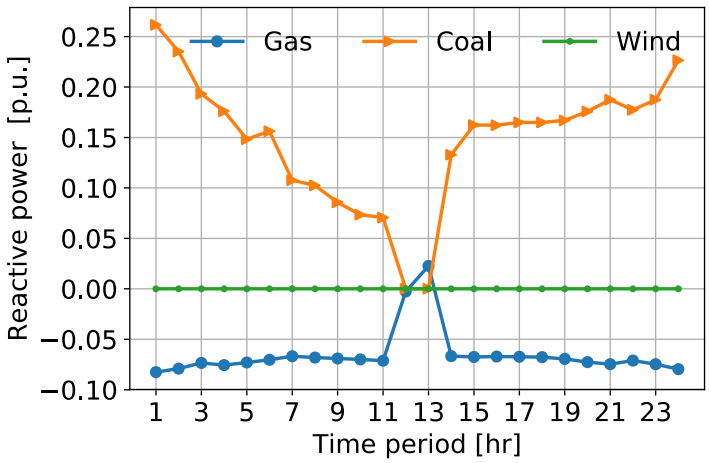

Fig. 3.10. Reactive power generation support for 24 hours in advance for case with voltage control at Node 2.

3.4 Effect of increased demand for electricity and natural gas.

The base case study reported in 3.2 is repeated, but considering a more stressed operational point for the coupled energy system. To achieve this goal, the total amount of electric load is increased by 5% at a constant power factor, while the demand of natural gas by nonelectric loads has increased by 50%. Figure 3.11 shows that the hourly generation scheduling differs from the 14th to the 16th hours, where the coal-based unit is turned on to provide the required active and reactive powers demanded by loads as well as to provided reactive power support to maintain the profile of nodal voltage magnitudes along the electric network between $0.96 \leq V \leq 1.06$. Note also that this profile of generation dispatch and scheduling is similar to the one reported in Fig. 3.8, where the nodal voltage magnitude at node South was constrained to the range of $1.05 \leq V \leq 1.06$.

On the other hand, the dynamic behavior of natural gas flows is shown in Figure 3.12. As expected, there is a greater flow of natural gas through the pipelines with respect to the gas flow associated with the base case, which is shown in Figure 3.4. This is due to the increased demand for natural gas by both the gas-fired generator and nonelectric loads. This increment in the demand of natural gas also provokes a decrement in the nodal gas pressures at nodes 2 and 3, as shown in Fig. 3.13, compared with the existing nodal pressures at these nodes for the base case scenario, which are shown in Fig. 3.5.

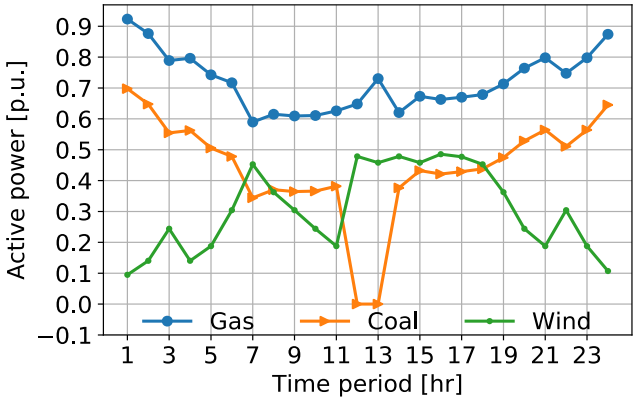

Fig. 3.11. Active power generation dispatches for 24 hours in advance for case with load increment.

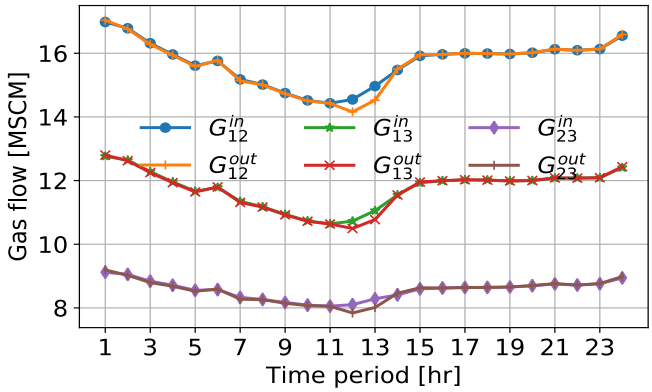

Fig. 3.12. Dynamic behavior of natural gas in pipelines for case with load increment.

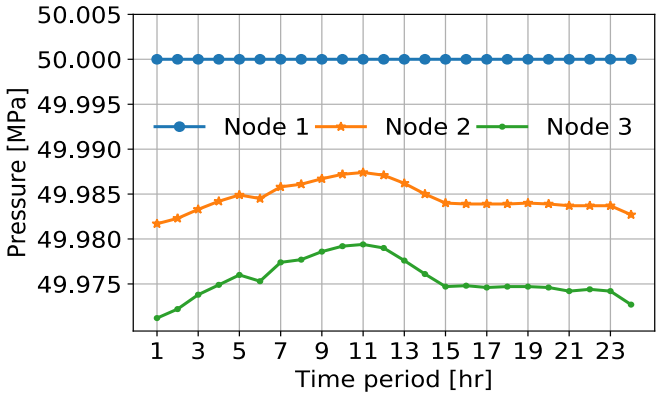

Fig. 3.13. Dynamic behavior of nodal pressures for case with load increment.

3.5 Co-optimization of the IEEE 118-bus electric system and 15-node gas network

A multi-energy infrastructure composed of the 54-machine, IEEE 118-bus electric power system [Power System Test Case Archive on-line] coupled via six gas-fired generators to a 15-node natural gas network [An 2003], shown in Fig. 3.14, is used in this section to demonstrate the application of the proposed approach to a larger system. The gas network has four gas nonelectric loads and four compressors, as reported in Table II, as well as two sources and 12 pipelines. The four compressors are driven by gas turbines, with the gas tapped from the inlet node of the compressor station. The gas pressure at the reference node 1 is kept at a fixed value. On the other hand, the type of primary energy driving the thermal units, the electric nodes at which these units are connected, their active and reactive power generation limits, as well as their corresponding cost curve coefficients, are reported in Table III. Five conventional generators are replaced by wind generators at nodes 61, 65, 66, 69 and 80 with the coefficients of the wind power characteristic shown in Table III. The remaining conventional units are considered as base generation for the entire planning horizon. Finally, the nodal voltage magnitude profile throughout the electric power system is constrained to $0.96 \leq V_k \leq 1.06$ $\forall k \in N_{el}$. Lastly, the fuel costs for the natural gas and coal are 141.3 USD/MSCM and 65 USD/Ton, respectively.

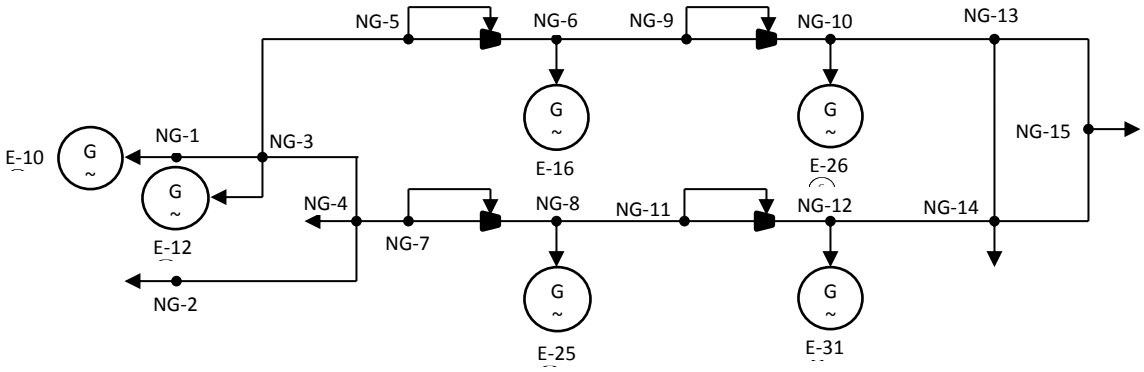

Fig. 3.14. 15-bus natural gas network.

TABLE II. 15-NODE GAS SYSTEM, LOADS AND COMPRESSORS' DATA

Loads		Compressor		
Natural gas node	MMSCF	Inlet node	Outlet node	Ratio
2	1.25	5	6	1.6
4	2.75	7	8	1.8
14	1.58	9	10	1.3
15	4.66	11	12	1.8

TABLE III. IEEE 118-BUS BENCHMARK SYSTEM, THERMAL GENERATORS

Electric node	Primary energy	Primary energy node	$\overline{Sp}$ [pu]	$\overline{Sq}$ [pu	$\underline{Sp}$ [pu	$\underline{Sq}$ [pu]	α_i [MBTU/hr]	β_i [MBTU/MWhr]	γ_i [MBTU/MW^{2}hr]
10	Natural gas	1	6	0.8	2	-2	540	4.3	0.014
12	Natural gas	3	6	0.8	2	-2	540	4.3	0.014
16	Natural gas	6	6	0.8	2	-2	504	5.04	0.018
25	Natural gas	8	6	0.8	2	-2	504	5.04	0.018
26	Natural gas	10	6	0.8	2	-2	504	5.04	0.018
31	Natural gas	12	6	0.8	2	-2	504	5.04	0.018
40	Coal	-	6	0.8	2	-2	1008	6.48	0.032
46	Coal	-	6	0.8	2	-2	1008	6.48	0.032
49	Coal	-	6	0.8	2	-2	1008	6.48	0.032
54	Coal	-	6	0.8	2	-2	540	4.3	0.025
59	Coal	-	6	0.8	2	-2	648	4.3	0.025
61	Wind	-	2.8	0.0	2	-2	a_ω=1.27 b_ω=-0.806 c_ω=0.245 d_ω=-0.043 e_ω=5.1x10^{-3} f_ω=3.8x10^{-4} g_ω=1.67x10^{-5} h_ω=3.9x10^{-7} i_ω=3.7x10^{-9}		
65	Wind	-	2.8	0.0	2	-2			
66	Wind	-	2.8	0.0	2	-2			
69	Wind	-	2.8	0.0	2	-2			
80	Wind	-	2.8	0.0	2	-2			

The generalized unit commitment approach converges to a feasible solution in six iterations to a mismatch tolerance of 1x10^{-3}. The schedule and power generations of thermal units considering the load and wind speed variation profiles depicted in Fig. 3.1 are reported in Figs. 3.15 to 3.18, where several coal units have been turned off within the period of minimum load demand: generators E40 and E46 are shut down in between the 9th and 13th hour. The voltage magnitude profiles at all electric nodes are shown in Fig. 3.19, where these magnitudes are clearly kept within limits. The variation of gas pressures at those nodes delivering this fossil fuel to thermal units is shown in Fig. 3.20. Note that node 1 corresponds to a pressure controlled node, maintaining the specified pressure during the planning horizon. On the other hand, nodes

10 and 12 present the largest gas pressure variations during the study period. Additionally, the results of hourly energy consumption and efficiency associated with thermal generators according to (2.53) are reported in Tables IV and V, respectively. The maximum consumption of fuel corresponds to coal-fired generators E-40, E-46 and E-49, which have the larger coefficient values in their corresponding heat rate curves. Furthermore, these units are turned off during the hours of lower demand because of their low efficiency.

TABLE IV. ENERGY CONSUMPTION BY THERMAL GENERATORS

Generator	Amount of energy consumed by thermal generators per hour (MBTU/MWh)											
	1	2	3	4	5	6	7	8	9	10	11	12
E-10	10.531	10.221	9.899	9.980	9.901	9.922	10.106	10.223	10.172	10.444	10.095	10.444
E-12	10.543	10.236	9.901	9.988	9.899	9.915	10.084	10.194	10.149	10.410	10.080	10.410
E-16	11.437	11.216	11.081	11.076	11.121	11.175	11.471	11.633	11.567	11.929	11.461	11.929
E-25	11.557	11.276	11.074	11.091	11.107	11.161	11.458	11.623	11.553	11.924	11.438	11.924
E-26	11.572	11.285	11.073	11.094	11.105	11.158	11.453	11.617	11.546	11.916	11.431	11.916
E-31	11.547	11.278	11.070	11.093	11.101	11.147	11.425	11.581	11.521	11.875	11.418	11.875
E-40	18.627	18.141	18.035	17.912	18.163	18.348	19.168	19.589	0	0	0	0
E-46	18.485	18.056	18.141	17.912	18.287	18.534	19.479	19.951	0	0	0	0
E-49	17.960	17.178	16.569	16.683	16.608	16.718	17.273	17.585	17.382	18.071	17.118	18.071
E-54	14.494	13.454	12.019	12.586	11.905	11.792	11.703	11.743	11.720	11.870	11.698	11.870
E-59	14.974	13.884	12.548	13.051	12.477	12.413	12.492	12.606	12.554	12.857	12.461	12.857
Generator	Amount of energy consumed by thermal generators per hour (MBTU/MWh)											
	13	14	15	16	17	18	19	20	21	22	23	24
E-10	10.107	9.945	9.897	9.897	9.897	9.897	9.899	9.902	9.929	9.897	9.929	10.291
E-12	10.088	9.935	9.897	9.898	9.899	9.898	9.897	9.899	9.935	9.897	9.935	10.303
E-16	11.476	11.221	11.098	11.093	11.089	11.093	11.110	11.123	11.064	11.098	11.064	11.263
E-25	11.460	11.206	11.089	11.084	11.080	11.084	11.099	11.111	11.066	11.089	11.066	11.339
E-26	11.454	11.202	11.087	11.083	11.079	11.083	11.097	11.109	11.067	11.087	11.067	11.349
E-31	11.433	11.188	11.082	11.079	11.075	11.079	11.091	11.102	11.067	11.082	11.067	11.336
E-40	0	18.483	18.102	18.084	18.067	18.084	18.142	18.186	17.928	18.102	17.928	18.248
E-46	0	18.694	18.230	18.206	18.183	18.206	18.281	18.336	17.970	18.230	17.970	18.152
E-49	17.212	16.800	16.592	16.585	16.579	16.585	16.609	16.630	16.581	16.592	16.581	17.379
E-54	11.702	11.750	11.943	11.961	11.980	11.961	11.908	11.876	12.289	11.943	12.289	13.732
E-59	12.493	12.402	12.495	12.508	12.520	12.508	12.473	12.453	12.773	12.495	12.773	14.183

TABLE V. EFFICIENCY OF THERMAL GENERATORS FOR 24 HOURS

Generator	Thermal generators efficiency per hour (%)											
	1	2	3	4	5	6	7	8	9	10	11	12
E-10	32.4	33.4	34.5	34.2	34.5	34.4	33.8	33.4	33.5	32.7	33.8	32.7
E-12	32.4	33.3	34.5	34.2	34.5	34.4	33.8	33.5	33.6	32.8	33.8	32.8
E-16	29.8	30.4	30.8	30.8	30.7	30.5	29.7	29.3	29.5	28.6	29.8	28.6
E-25	29.5	30.3	30.8	30.8	30.7	30.6	29.8	29.4	29.5	28.6	29.8	28.6
E-26	29.5	30.2	30.8	30.8	30.7	30.6	29.8	29.4	29.5	28.6	29.8	28.6
E-31	29.5	30.3	30.8	30.8	30.7	30.6	29.9	29.5	29.6	28.7	29.9	28.7
E-40	18.3	18.8	18.9	19.0	18.8	18.6	17.8	17.4	0	0	0	0
E-46	18.5	18.9	18.8	19.0	18.7	18.4	17.5	17.1	0	0	0	0
E-49	19.0	19.9	20.6	20.4	20.5	20.4	19.7	19.4	19.6	18.9	19.9	18.9
E-54	23.5	25.4	28.4	27.1	28.7	28.9	29.2	29.1	29.1	28.7	29.2	28.7
E-59	22.8	24.6	27.2	26.1	27.3	27.5	27.3	27.1	27.2	26.5	27.4	26.5
Generator	Thermal generators efficiency per hour (%)											
	13	14	15	16	17	18	19	20	21	22	23	24
E-10	33.8	34.3	34.5	34.5	34.5	34.5	34.5	34.5	34.4	34.5	34.4	33.2
E-12	33.9	34.3	34.5	34.5	34.5	34.5	34.5	34.5	34.3	34.5	34.3	33.1
E-16	29.7	30.4	30.7	30.6	30.8	30.8	30.7	30.7	30.9	30.7	30.8	30.3
E-25	29.8	30.4	30.8	30.8	30.8	30.8	30.7	30.7	30.8	30.8	30.8	30.1
E-26	29.8	30.5	30.8	30.8	30.8	30.8	30.7	30.7	30.8	30.8	30.8	30.1
E-31	29.8	30.5	30.8	30.8	30.8	30.8	30.8	30.7	30.8	30.8	30.8	30.1
E-40	0	18.5	18.9	18.9	18.9	18.9	18.8	18.8	19.0	18.8	19.0	18.7
E-46	0	18.2	18.7	18.7	18.8	18.7	18.7	18.6	19.0	18.7	19.0	18.8
E-49	19.8	20.3	20.6	20.6	20.6	20.6	20.5	20.5	20.6	20.6	20.6	19.6
E-54	29.2	29.0	28.6	28.5	28.5	28.5	28.6	28.7	27.8	28.6	27.8	24.8
E-59	27.3	27.5	27.3	27.3	27.2	27.3	27.4	27.4	26.7	27.3	26.7	24.1

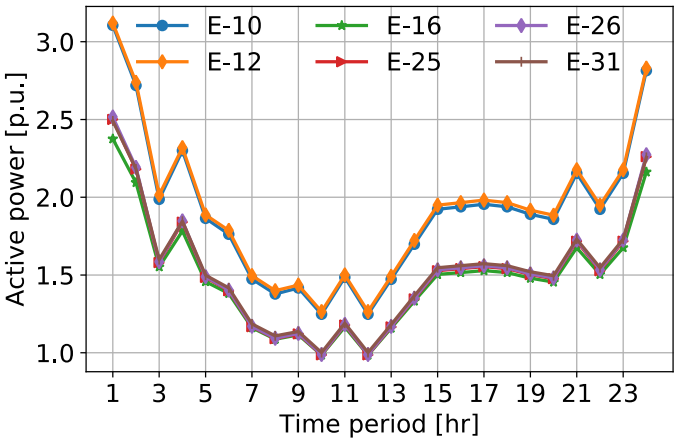

Fig. 3.15. Active power generation dispatches of gas-fired units for 24 hours in advance for the co-optimization of the IEEE 118-bus electric system and 15-node gas network.

.

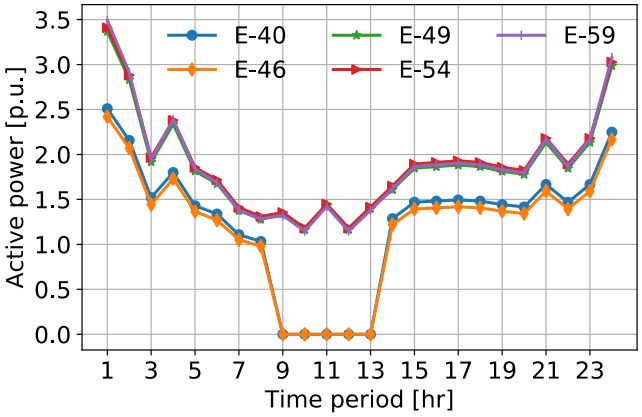

Fig. 3.16. Active power generation dispatches of coal-fired units for 24 hours in advance for the co-optimization of the IEEE 118-bus electric system and 15-node gas network.

.

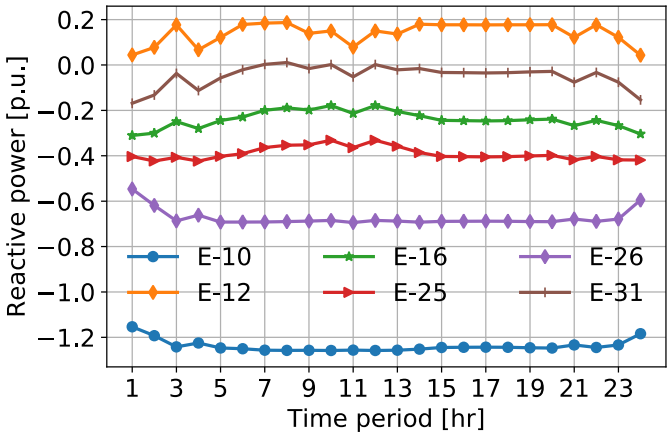

Fig. 3.17. Reactive power generation dispatches of gas-fired units for 24 hours in advance for the co-optimization of the IEEE 118-bus electric system and 15-node gas network.

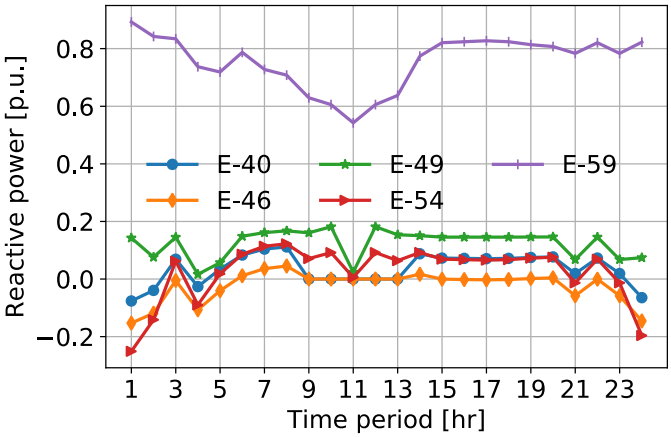

Fig. 3.18. Reactive power generation dispatches of coal-fired units for 24 hours in advance for the co-optimization of the IEEE 118-bus electric system and 15-node gas network.

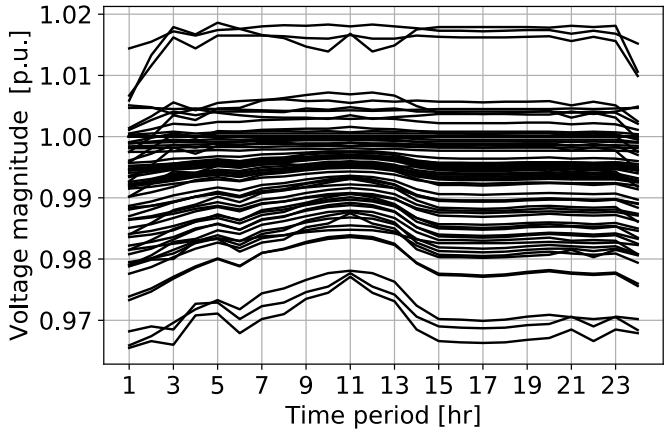

Fig. 3.19. Hourly nodal voltage profiles for the co-optimization of the IEEE 118-bus electric system and 15-node gas network.

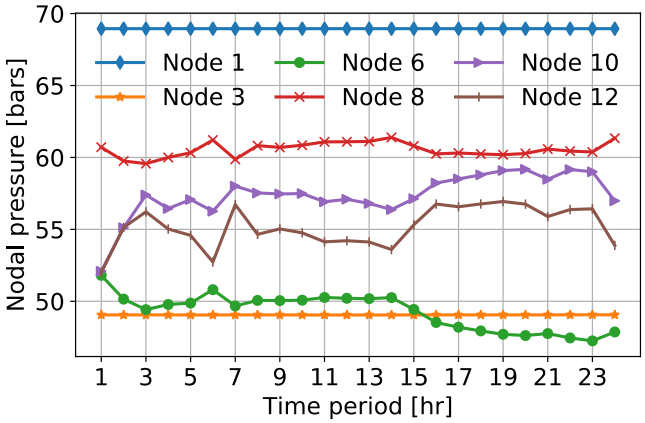

Fig. 3.20. Hourly gas pressure profiles at nodes with gas-fired units for the co-optimization of the IEEE 118-bus electric system and 15-node gas network.

This case study took 27 minutes of simulation. The numerical test was performed using a MATLAB R2014a platform in Windows on a PC with Intel(R) Xeon(R) CPU E5-1650 v3 @ 3.50 GHz and 8.00 GB of RAM memory. Since the proposal is aimed toward the scheduling of thermal units over the period ranging from a few hours in advance to one day ahead, the CPU time required in the study does not affect the validity of our proposal in terms of its applicability and of its results. On the other hand, our firsthand experience with the GUC problem indicates that the conventional optimal gas and power flow solutions described in step 2 of Section 2.5.1 are necessary for initializing the Lagrangian multipliers to be used in the scheduling of the generators. In this context, we have observed a linear convergence toward the solution of the GUC problem, as shown in Fig. 3.21 for case study C reported in this work. The evolution of the total hourly cost as a function of global iterations is shown in Fig. 3.22.

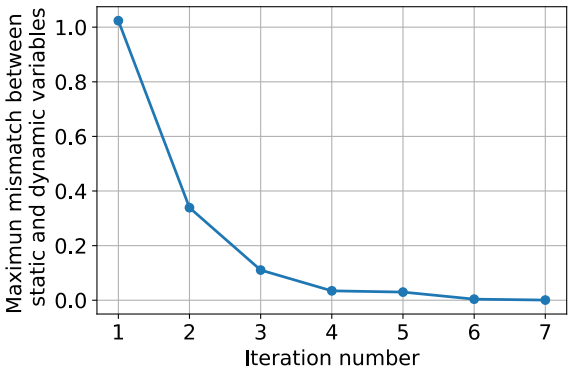

Fig. 3.21. Maximum mismatch between static and dynamic variables for Co-optimization of the IEEE 118-bus electric system and 15-node gas network.

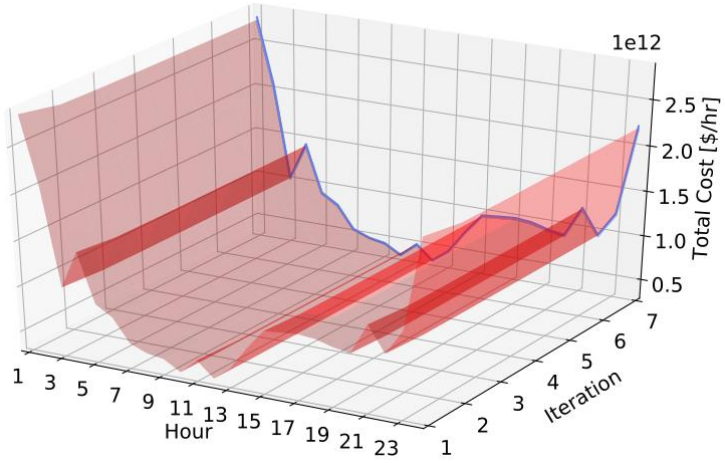

Fig. 3.22. Hourly system cost for Co-optimization of the IEEE 118-bus electric system and 15-node gas network

.

On the other hand, the number of iterations required by the OGPF at each hour of the last global iteration of the solution process is reported in Table VI, where the increase in the number of iterations associated with the co-optimization of both energy networks is greater than that required by the optimization of the electric system due to the amount of constraints associated with the formulation of each optimization problem.

TABLE VI. Number of OGPF's iterations for case study C

Hour	1	2	3	4	5	6	7	8	9	10	11	12
Iter.	46	42	36	38	35	34	31	31	38	37	38	37
Hour	13	14	15	16	17	18	19	20	21	22	23	24
Iter.	38	33	35	35	35	35	35	34	37	35	37	43

The metric used to assess whether the algorithm is converging or not corresponds to the mismatches of the duplicated variables, as stated in step 6 of Section 2.5.1. These mismatches based on active and reactive powers have a great engineering significance and indicate the "closeness" to a primal feasible solution [Murillo-Sánchez 1997], [Murillo-Sánchez 2001]. Furthermore, in this solution the values of multipliers of the artificial constraints associated with both subproblems are as shown in Table VII for the gas-fired units dispatched at three different hours, where Lagrangian multipliers $\lambda^{k}_{\boldsymbol{p},iT}$ have the same value for both UC and OGPF subproblems, thus satisfying the condition of the problem that they must remain fixed during the entire iteration k^{th}. In addition, Table VIII reports the active power generation associated with these Lagrangian multipliers.

TABLE VII. Values of Lagrangian multipliers for case study C

Electrical node	Hour					
	5th hour		10th hour		20th hour	
	UC ($1x10^3$ USD/MWh)	OPF ($1x10^3$ USD/MWh)	UC ($1x10^3$ USD/MWh)	OPF ($1x10^3$ USD/MWh)	UC ($1x10^3$ USD/MWh)	OPF ($1x10^3$ USD/MWh)
E-10	2.1332	2.1332	1.4335	1.4335	2.1260	2.1260
E-12	2.1579	2.1579	1.4530	1.4530	2.1557	2.1557
E-16	2.0876	2.0876	1.4176	1.4176	2.0838	2.0838
E-25	2.1257	2.1257	1.4197	1.4197	2.1143	2.1143
E-26	2.1328	2.1328	1.4230	1.4230	2.1211	2.1211
E-31	2.1456	2.1456	1.4406	1.4406	2.1410	2.1410

TABLE VIII. Active power generation for case study C

Electrical node	Hour					
	5th hour		10th hour		20th hour	
	UC (p.u.)	OPF (p.u.)	UC (p.u.)	OPF (p.u.)	UC (p.u.)	OPF (p.u.)
E-10	1.8663	1.8655	1.2492	1.2490	1.8600	1.8592
E-12	1.8881	1.8872	1.2664	1.2662	1.8861	1.8853
E-16	1.4593	1.4584	0.9865	0.9862	1.4566	1.4557
E-25	1.4862	1.4853	0.9879	0.9876	1.4781	1.4772
E-26	1.4911	1.4903	0.9903	0.9900	1.4829	1.4821
E-31	1.5002	1.4993	1.0027	1.0024	1.4970	1.4961

3.6 Effect of different wind/load profile data

In order to assess how different wind/load profile data affect the convergence and optimality of the solution, the results associated with four different wind/load scenarios are reported in this section. These scenarios are obtained by combining the wind/load profile data shown in Fig. 3.1 with the profiles shown in Fig. 3.23, as reported in Table IX. The number of global iterations and the CPU time required to solve the GUC problem are also reported for each case study. Note that the former is maintained almost constant independently of the type of scenario under study, while the CPU time does not vary greatly. On the other hand, the number of iterations associated with each hourly OGPF study performed in the last global iteration is shown in Fig. 3.24 for all scenarios. Lastly, the hourly system cost for each case study is shown in Fig. 3.25. As expected, the wind/load profile data clearly affect the optimality of the solution because the generators' dispatch patterns are different for each case study.

TABLE IX. Wind/load scenarios

Scenario	Wind Data	Load Data	Global Iterations	CPU Time (sec)
1	Fig. 3.1	Fig. 3.1	7	1620.34
2	Fig. 3.1	Fig. 3.23	6	1522.38
3	Fig. 3.23	Fig. 3.1	6	1907.25
4	Fig. 3.23	Fig. 3.23	7	1980.22

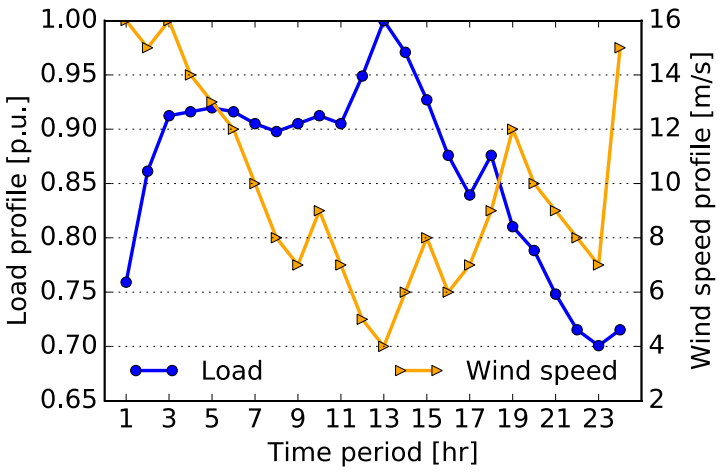

Fig. 3.23. Forecast of wind speed and load demand profiles for 24 hours (scenario 4).

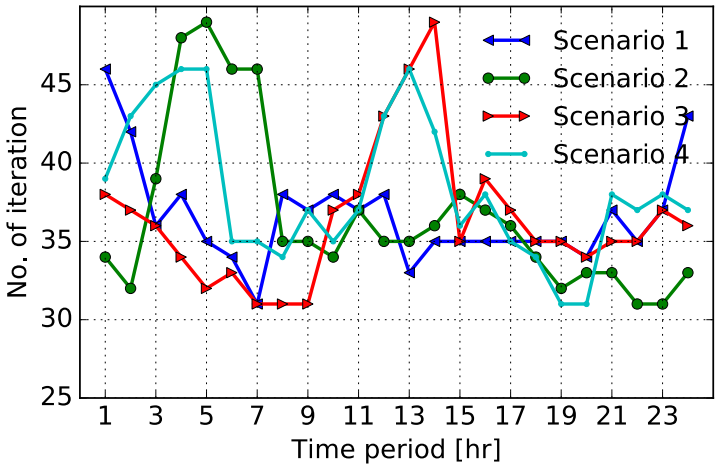

Fig. 3.24. Number of iterations of each OGPF study performed at the last global iteration.

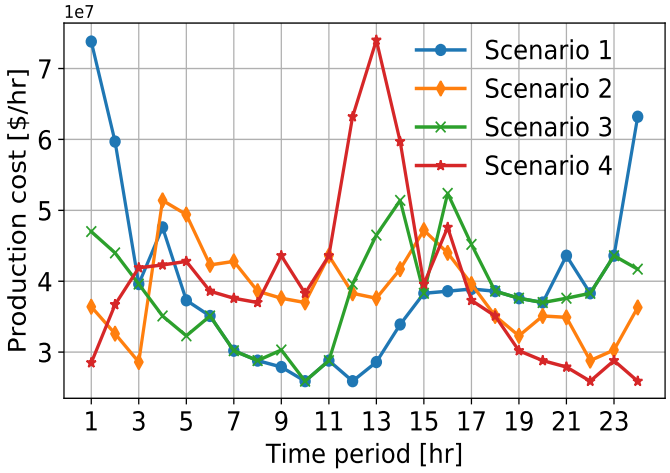

Fig. 3.25. Hourly system cost for each case study.

Finally, it is analyzed the way in which the co-optimization of both energy infrastructures is affected by only varying the wind speed profile. For this purpose, the base wind speed profile is perturbed in ±10%, as shown in Fig. 3.26, while the profiles of both electric and gas loads are the ones reported in Fig. 3.1.

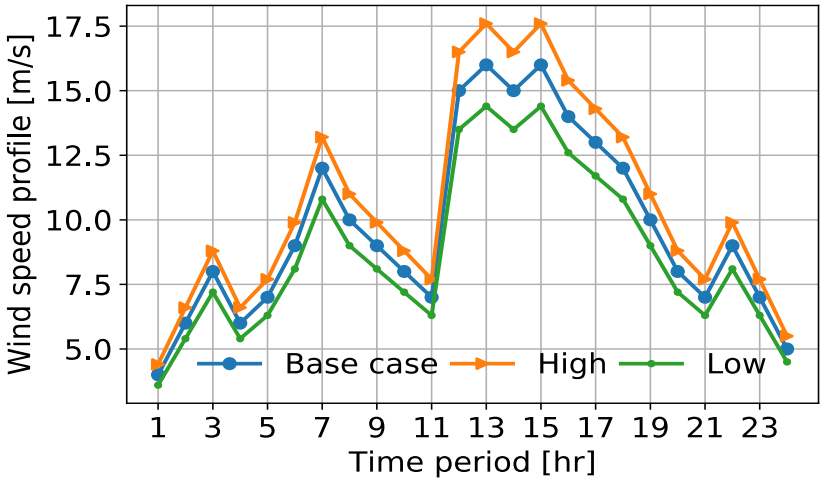

Fig. 3.26. Forecast of high/low wind speed profiles for 24 hours.

Fig. 3.27 and Fig. 3.28 show the active power scheduling and dispatches for gas-fired generators when considering the high and low wind speed profiles, respectively. The active power scheduling associated with the high speed profile is similar to the base schedule of

active power reported in Fig. 3.15, except at hours 11th and 21th, 22th and 24th. At these hours there is a reduction of the active power generated by the gas-fired units because the higher production of active power of the wind generator. The opposite occurs when the co-optimization is performed by considering the low wind speed profile, as demonstrated by comparing the results reported in Figs. 3.18 and 3.15. On the other hand, the same operating performance abovementioned is observed for the coal-fired units, with their scheduling of active power reported in Figs. 3.29 and 3.30 for the high and low wind speed profiles, respectively. Note also that the dispatches of thermal generators are not affected by the changes in the wind speed profiles, which could be due to the operation constraints associated with both energy networks.

Due to the existing interdependency between the electricity and natural gas network, changes in the active power generated by gas-fired units will change nodal gas pressures and the amount of gas flowing through the pipelines composing the natural gas network. For example, Fig. 3.31 shows the gas pressures at nodes from which the natural gas is supplied to thermal generators in the presence of a high wind speed profile. Note that the values of nodal gas pressures is similar to the ones obtained for the base case, but with a slight increase of pressure for some hours (like node 6) in some nodes. This is due to the gas flow through the pipelines supplying to the gas-fired units must be decreased to cut down the generation of active power of these units. As expected, the opposite takes place when the low wind speed profile is considered for the GUC, as shown in Fig.3.32. These results show that the gas pressure decreases at node 12, with respect to its value in the base case, to increase the amount of natural gas supplied to gas-fired units.

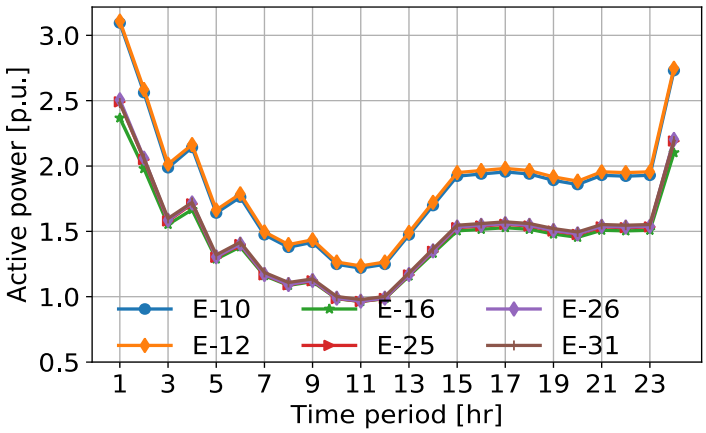

Fig. 3.27. Active power generation dispatches of gas-fired units for 24 hours in advance with high wind speed profile.

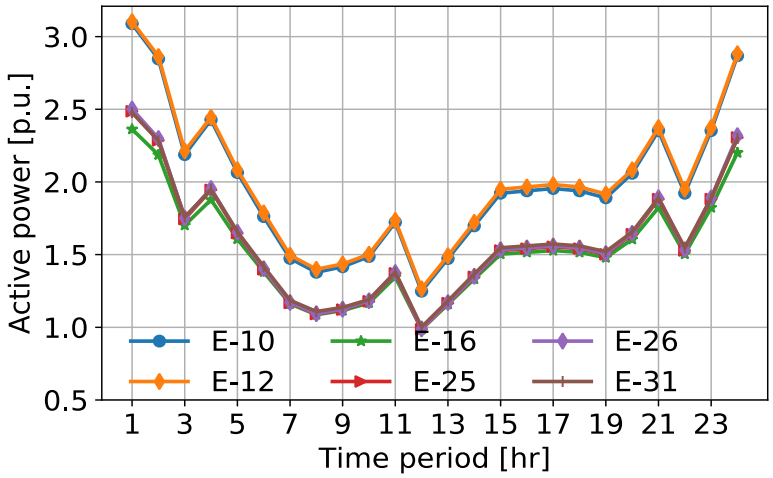

Fig. 3.28. Active power generation dispatches of gas-fired units for 24 hours in advance with low wind speed profile.

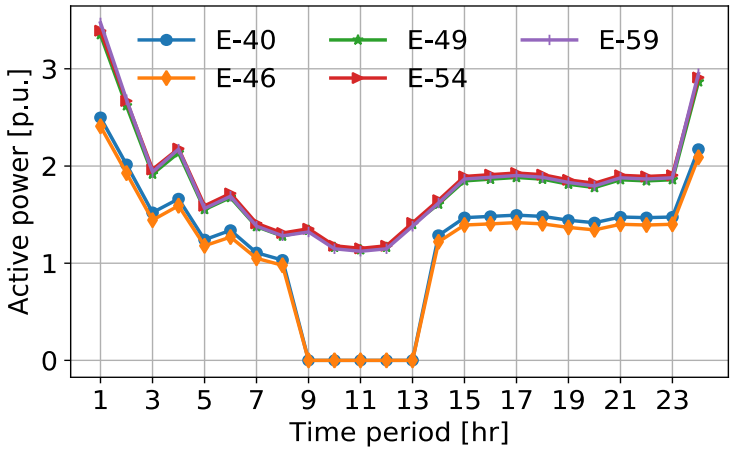

Fig. 3.29. Active power generation dispatches of coal-fired units for 24 hours in advance with high wind speed profile.

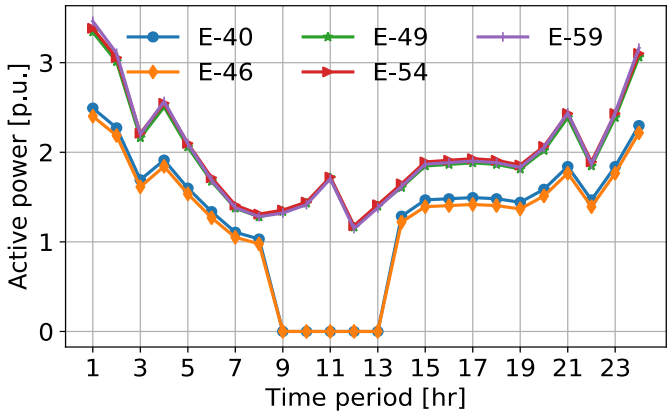

Fig. 3.30. Active power generation dispatches of coal-fired units for 24 hours in advance with low wind speed profile.

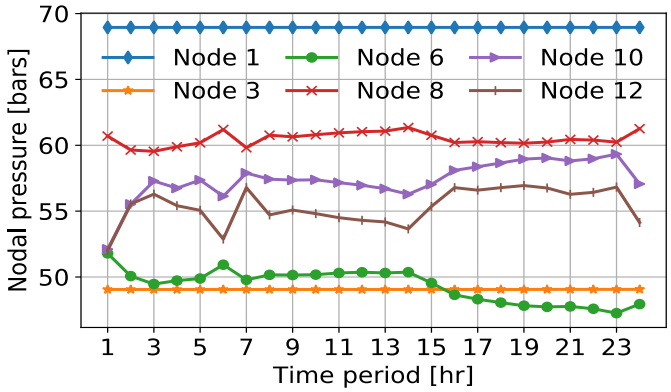

Fig. 3.31. Hourly gas pressure profiles at nodes connected to gas-fired units with a high wind speed profile.

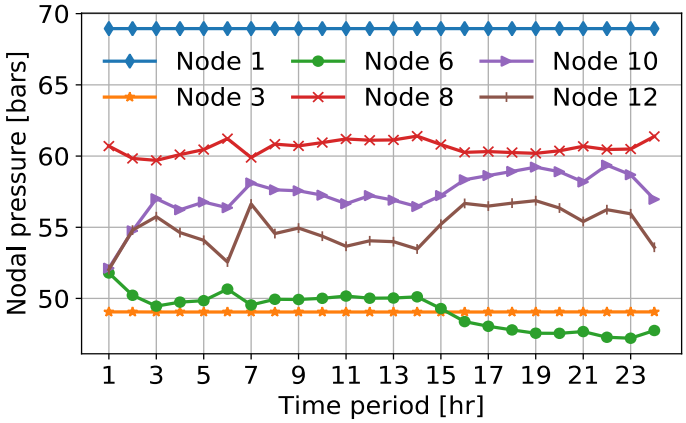

Fig. 3.32. Hourly gas pressure profiles at nodes connected to gas-fired units with a low wind speed profile.

3.7 Effect of the electricity network modeling

The numerical example reported in Section 3.3 demonstrates how the optimal scheduling of generators is affected by the constraints associated with reactive power generation and nodal voltage magnitudes, which validates the importance of considering AC constraints in the UC problem. On the other hand, to numerically demonstrate that the unit commitment outcome is also affected by the way in which the network is modeled, the case study reported in Section 3.5 has been repeated but now considers a lossless electric transmission network, without shunt capacitive effects and only active power loads. The dispatches and active power scheduling for the gas-fired and coal-fired units are shown in Figs. 3.33 and 3.34, respectively. A comparison of these results with the ones reported in Figs. 3.15 and 3.16 clearly shows the changes in both unit dispatches and power schedules, which have a direct impact on the hourly generation costs as shown in Fig. 3.35. Even though the total system cost over the entire planning horizon is reduced by 2% relative to the case study that considers electric losses, this cost is higher in time periods 10 through 14. This is explained as follows. Unlike the gas-fired unit's commitment reported in Section 3.5, units E-16, E-25, E-26 and E-31 are not committed at hours 10 through 14. Hence, the power scheduling of the most expensive gas-fired units E-10 and E-12 increases by approximately 53% during these hours. On the other hand, the same commitment of coal-fired units is obtained in both case studies, but units E-49, E-54 and E-59 increased their active power generation to about 56% for hours 10 through 14.

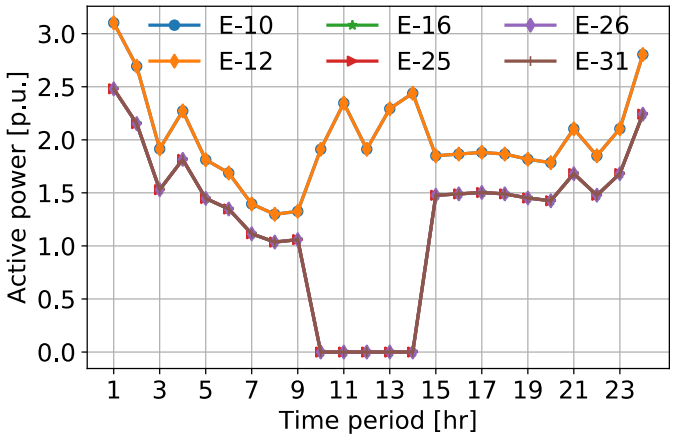

Fig. 3.33. Active power generation dispatches of gas-fired units for 24 hours in advance for lossless transmission network.

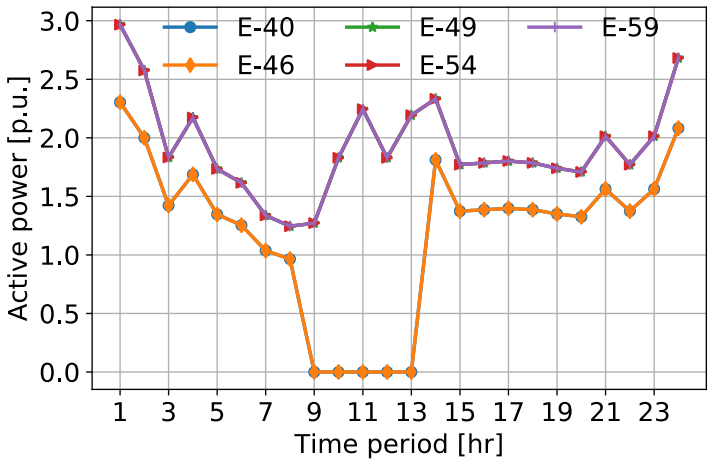

Fig. 3.34. Active power generation dispatches of coal-fired units for 24 hours in advance for lossless transmission network.

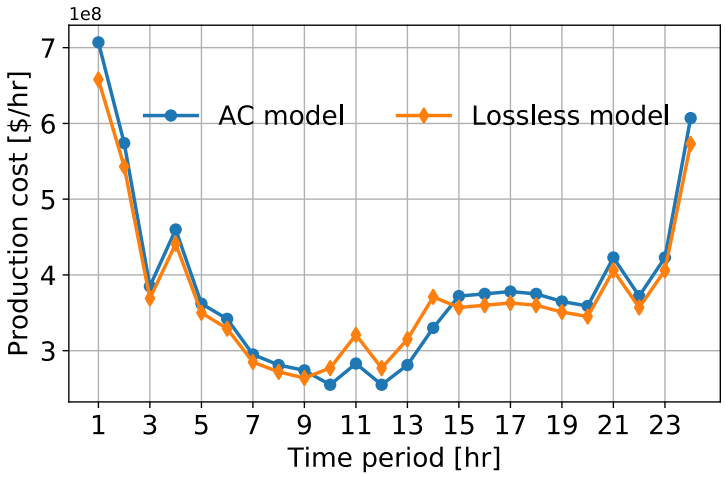

Fig. 3.35. Hourly system cost for the IEEE 118-bus electric power system and the 15-bus natural gas network.

3.8 The effect of considering primary reserves

In order to numerically demonstrate how optimal scheduling of generators is affected by the constraints associated with primary frequency regulation, the case study reported in Section 3.2 has been repeated considering the following two operating scenarios: i) electric power reserves in order to provide more flexibility to the system, including (2.41), (2.43)-(2.47), the upper limit given by (2.48) and (2.49), and ii) security constraints associated with primary frequency regulation that includes (2.38), (2.39), and (2.43) to (2.50). Unlike the base case, the $\bar{sp}$ limit of the thermal generators, defined in (2.43), has now a value of 165 MW and 170 MW for the coal-fired generator and gas-fired generator, respectively. The lower and upper limits considered by (2.44) and (2.45) correspond to the same values adopted for base case. Regarding the nodal voltage magnitude profile throughout the electric power system, given by (2.46), it is constrained to $0.95 \leq V_k \leq 1.05 \ \forall k \in N_{el}$. On the other hand, the values of ramps $\Delta sp_i^{\max}$ and $\Delta sp_i^{\min}$ were increased in both generators to a value of 0.9 pu because the upper limit of r_{it} must be lower than or equal to $\Delta sp_i^{\max}$, according to (2.48). The $\bar{sp}$ values have been modified such that the amount of total reserves available for all thermal generators, as given by (2.49), could be equal to or greater than $sp_{\max}$, which corresponds to the gas-fired generator with the maximum capacity, i.e. :170 MW. On the other hand, the maximum system frequency

deviation $\Delta\overline{f}$, defined in (2.50), has a value of -0.6 Hz, with a system frequency of 60 Hz, while the regulation drop of each unit has a value of 4%. Lastly, the reserve costs are 3 USD/MW for both generator units.

The dispatches and active power scheduling obtained for the gas-fired and coal-fired units without primary frequency regulation are reported in Fig. 3.36. Note that the unit commitment and power schedules are different with respect to the ones obtained without considering reserves, which are reported in Fig. 3.3 of Section 3.2. This is explained as follows. Unlike the coal-fired unit commitment reported in Section 3.2, this unit is now committed at the 15th and 16th hours. Note that the same commitment for the gas-fired generator is obtained in both case studies, but the unit decreased its active power generation for both the 15th and 16th hours because the coal-fired generator is turned on during these hours.

On the other hand, the reserves that each thermal unit could provide for minimizing mismatches between power generation and load demand are shown in Fig. 3.37. The total available reserves are equal to the maximum capacity of the gas-fired generator, which has the greatest capacity value of all thermal generators of the system: 170 MW. If the gas-fired generator provides its total active power reserve, however, the frequency deviation Δf_{1t} , computed by (2.41), would be equal to the frequency deviation profile shown in Fig. 3.38. Note that this value is less than the maximum system frequency deviation $\Delta\overline{f}$ of -0.6 during the entire planning period. The same situation occurs for the coal-fired generator, which could provide its scheduled reserves only if the system frequency deviation is equal to the profile values presented in Fig. 3.38. In this case, the frequency deviation value is also less than the maximum system frequency. On the other hand, the active power reserves available for the gas-fired generator decrease, while its amount of active power dispatched increases in the hours when the coal-fired generator is off-line. The reason behind this operating strategy is associated with the maximum active power available from each *i*-th thermal generator, which is composed of the dispatched active power generation sp_{it} and its available active power reserve r_{it}, as given by (2.47).

The hourly reactive power generation is shown in Fig. 3.39. Note that unlike case A and case B the gas-fired unit provides reactive power support during the entire planning

period in order to maintain nodal voltage magnitudes within limits: $0.95 \leq V_k \leq 1.05 \ \forall k \in N_{el}$. The nodal voltage magnitude profiles are shown in Fig. 3.40, where the nodal voltage magnitude at node 1 is fixed at its upper bound of 1.05 pu during the whole planning period, which also occurs when no reserves are considered, such as in Fig. 3.6 of the base case, but at 1.06 pu.

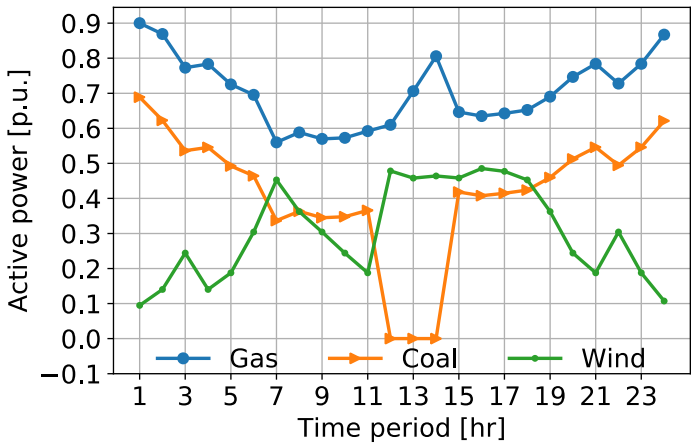

Fig. 3.36. Active power generation dispatches of generation units for 24 hours in advance including reserves.

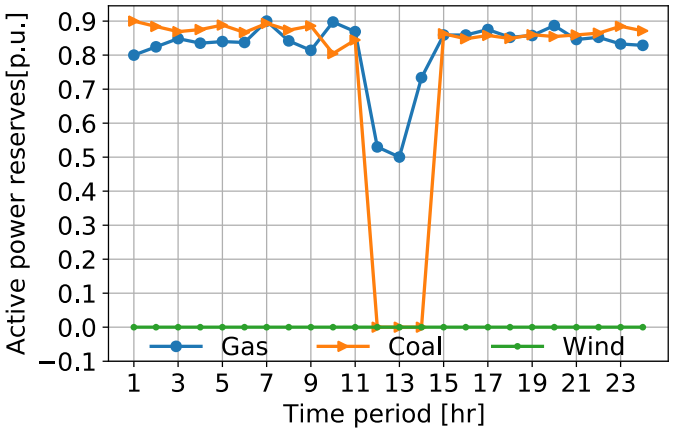

Fig. 3.37. Reserves provided by generation units for 24 hours in advance including reserves.

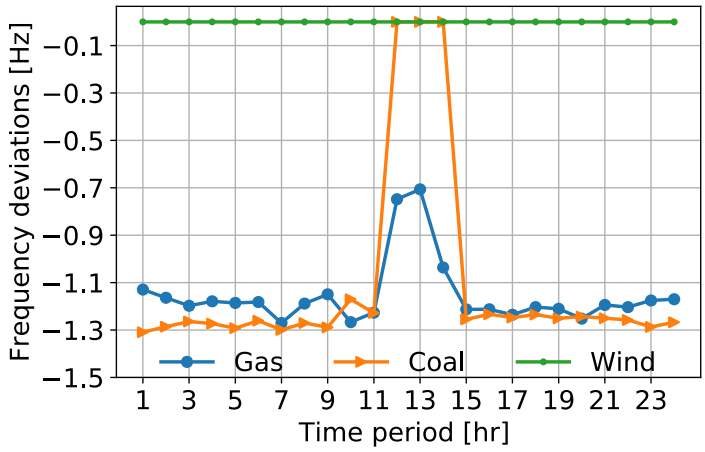

Fig. 3.38. Hourly frequency deviations profiles including reserves.

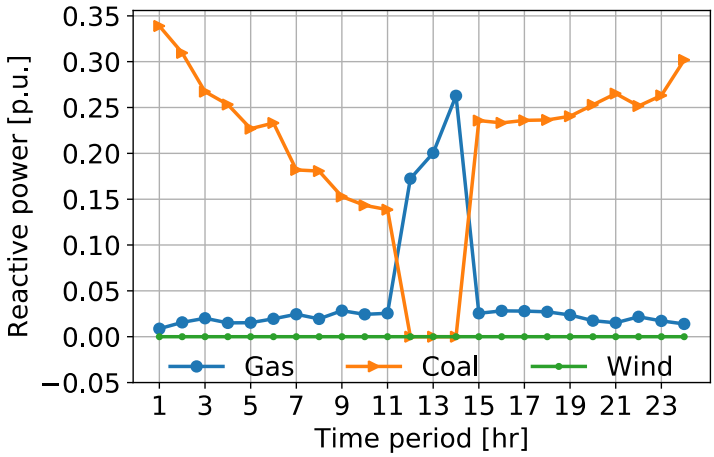

Fig. 3.39. Reactive power generation dispatches of thermal units for 24 hours in advance including reserves.

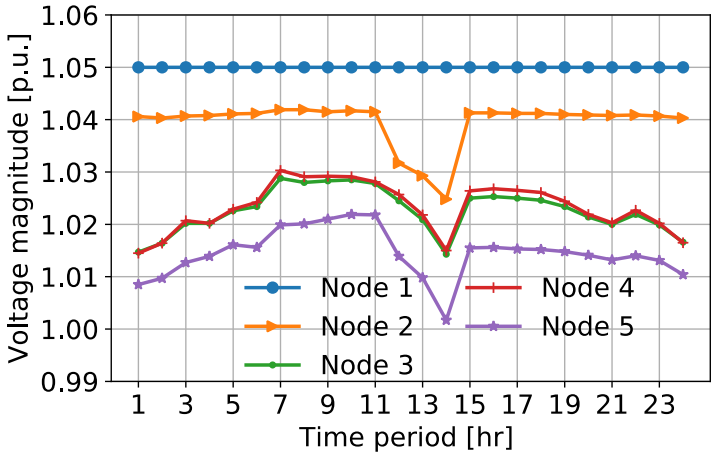

Fig. 3.40. Hourly nodal voltage profiles including reserves.

On the other hand, Fig. 3.41 shows the dispatches and active power scheduling for the same system but considering frequency regulation constraints represented by (2.38), (2.39), and (2.43) to (2.50). As expected, the comparison of these results with the ones reported in Fig. 3.36 shows that the active power dispatches and generation scheduling at each hour are equal, with barely perceptible changes. Unlike values reported in Fig. 3.37, however, Fig. 3.42 shows lower values of available reserves r_{it} during the entire planning period. This is due to the inclusion of the security constraints (2.38), (2.39), (2.48) and (2.50) to maintain the system's frequency deviation within the limit of -0.6 Hz, as schematically reported in Fig. 3.43. It is important to mention that in this new operating context the $sp_{\max}$ value given by (2.49) does not correspond to the maximum capacity of the gas-fired generator because the maximum available reserves for each unit thermal generator are constrained by $\Delta\overline{f}$, as shown in Fig. 3.42. This also implies that the total available reserves will never reach the value of the maximum capacity of thermal generators. Lastly, if the constraint (2.50) is included and the maximum system frequency deviation $\Delta\overline{f}$ has a value of -0.6 Hz, the only option that satisfies (2.49) and (2.50) is when the value of $sp_{\max}$ corresponds to the maximum capacity of the wind generator: 0.5 pu.

On the other hand, the nodal voltage magnitude profiles as well as the hourly reactive power generation have the same behavior compared to Figs. 3.40 and 3.39, respectively.

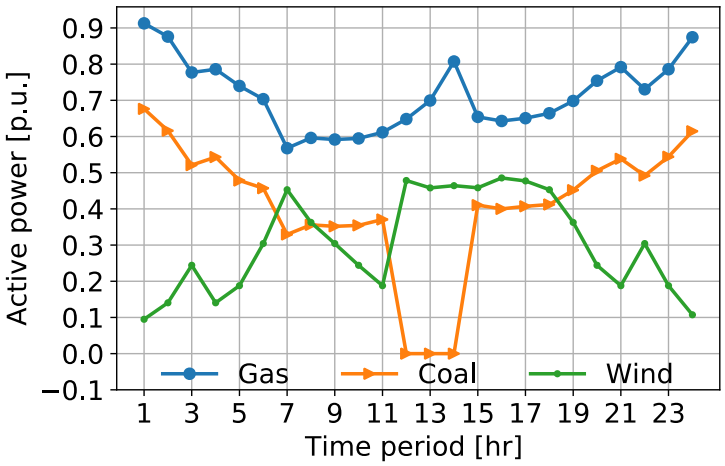

Fig. 3.41. Active power generation dispatches of generation units for 24 hours in advance including frequency regulation.

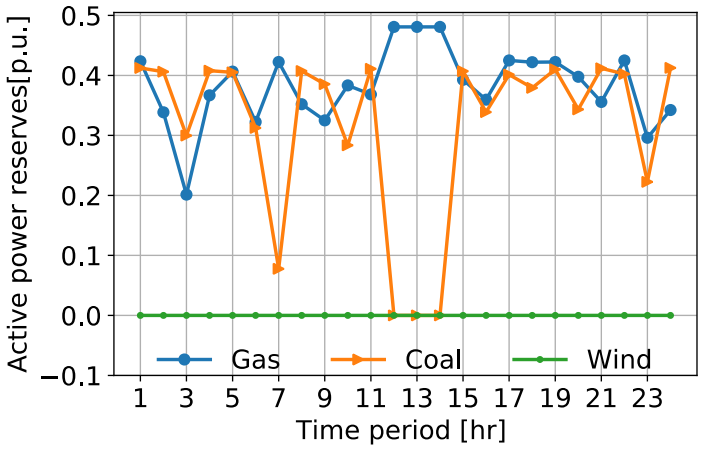

Fig. 3.42. Reserves provided by generation units for 24 hours in advance including frequency regulation.

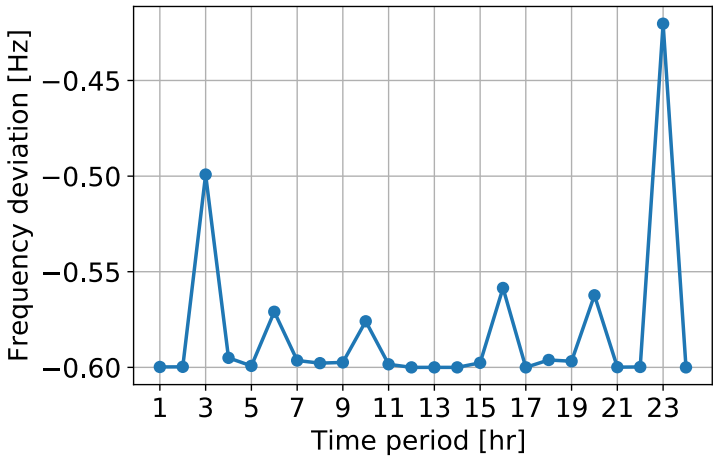

Fig. 3.43. Hourly frequency deviation profiles including frequency regulation.

The generalized unit commitment approach described in Section 3.5, is repeated but considers primary frequency regulation with the aim of illustrating how the scheduling of generators of a large system is affected. In this context, the maximum system frequency deviation $\Delta\overline{f}$, defined in (2.50), has a value of -0.6 Hz, with a system frequency of 60 Hz, while the regulation drop of each unit has a value of 4%. Lastly, the cost of primary reserves is 8 USD/MW.

The hourly generation scheduling for gas-fired and coal-fired units is shown in Figs. 3.44 and 3.45, respectively, considering these new operational constraints. These results clearly show different unit commitments compared with the ones obtained when generation reserves are not considered: Figs. 3.15 and 3.16. By way of example, and unlike the commitment of generator E-46 reported in Section 3.5, this unit E-46 is not committed in between 1 and 5 hours, as well as at hours 17 through 22. Similarly, in this new operating scenario constrained by the frequency regulation, E-40 is scheduled for 24 hours, while E-49 is turned off in between the 18th and 22nd hours.

On the other hand, the total available reserves, given by (2.49), are larger than or equal to the $\boldsymbol{s\bar{p}}$ value of the thermal generator with the highest capacity: 600 MW. According to (2.47), Fig. 3.46 shows that gas-fired generators E-12 and E-16 do not have available reserves for the first hours because the active power delivered at these periods of time is equal to their maximum capacity. Furthermore, Fig. 3.47 shows that the coal-fired generators E-46 and E-49 do not have available reserves during the periods that they are turned off, as given

by (2.55). Regarding to the frequency deviation Δf_t, computed by (2.42), Fig. 3.48 clearly shows that the frequency deviation during the entire planning period is equal to or larger than -0.6 in case the thermal generators must provide their total available reserves because of an imbalance between load demand and power generation. This result differs from the one reported in case A under frequency regulation, in which thermal units do not have enough total available reserves to reach the $\bar{sp}$ value of the unit generator with the highest capacity. This means that in the presence of a large imbalance between power generation and load demand, such as the loss of a generating unit, the probability of providing sufficient reserves from the generators is higher if there is a larger number of generators connected to the electric system.

Lastly, the nodal voltage magnitude profiles at all electric nodes are reported in Fig. 3.49, where these magnitudes are clearly kept within limits, while the hourly reactive power support provided by each thermal generator is shown in Figs. 3.50 and 3.51 for the gas-fired and coal-fired generators, respectively.

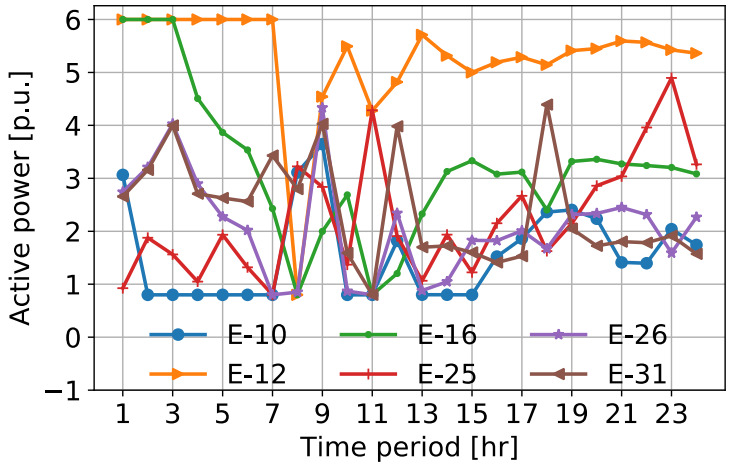

Fig. 3.44. Active power generation dispatches of gas-fired units for 24 hours in advance including frequency regulation.

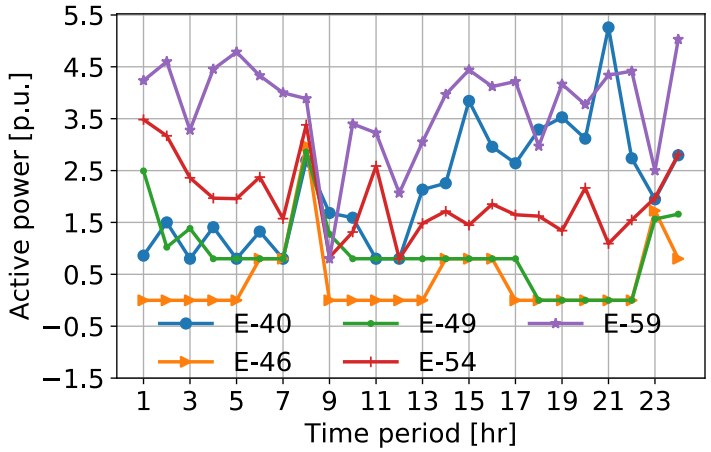

Fig. 3.45. Active power generation dispatches of coal-fired units for 24 hours in advance including frequency regulation.

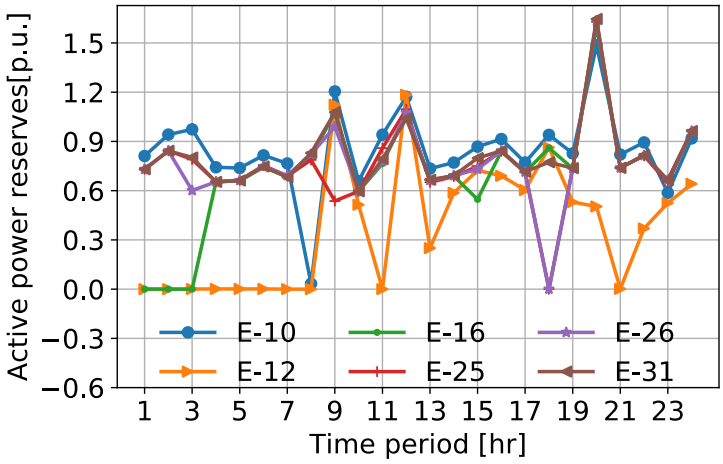

Fig. 3.46. Reserves provided by gas-fired units for 24 hours in advance including frequency regulation.

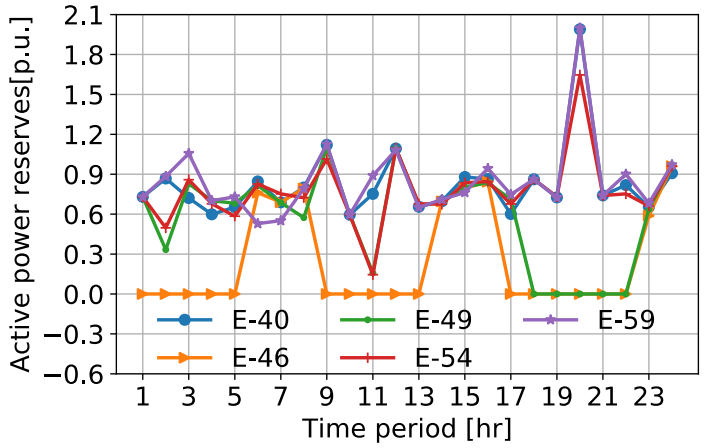

Fig. 3.47. Reserves provided by coal-fired units for 24 hours in advance including frequency regulation.

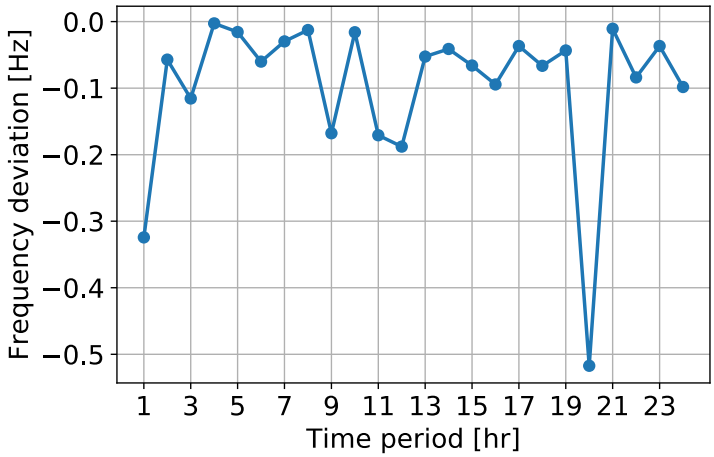

Fig. 3.48. Hourly frequency deviation profiles including frequency regulation.

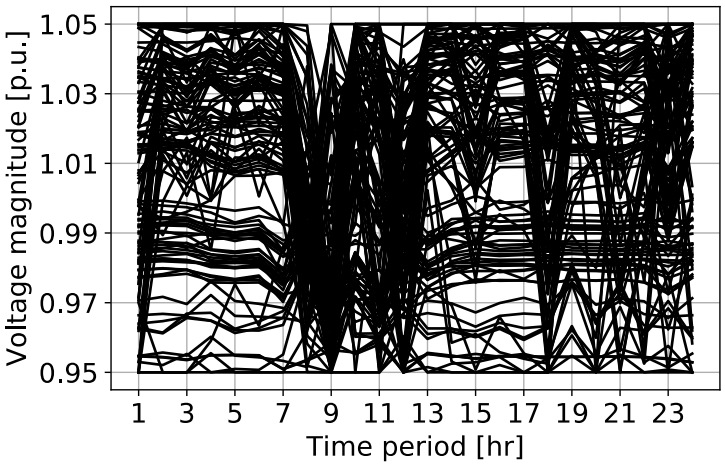

Fig. 3.49. Hourly nodal voltage profiles including frequency regulation.

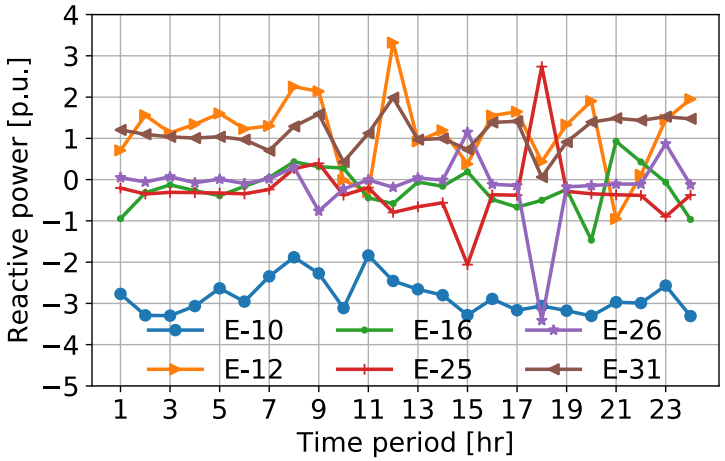

Fig. 3.50. Reactive power generation dispatches of gas-fired units for 24 hours in advance including frequency regulation.

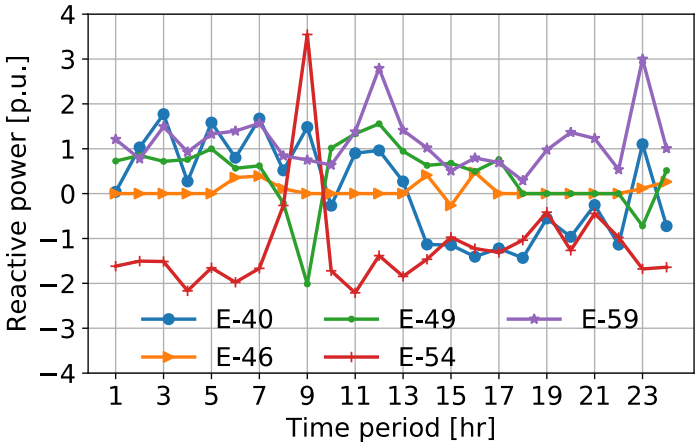

Fig. 3.51. Reactive power generation dispatches of coal-fired units for 24 hours in advance including frequency regulation.

Finally, the unified analysis of the IEEE 118-bus benchmark system and 15-node natural gas network took 175 minutes of simulation and converged to a feasible solution in 12 iterations to a mismatch tolerance of $1x10^{-3}$. The numerical test was performed using the same platform and PC equipment described in Section 3.5. This proposal solves the problem of dispatch and scheduling of thermal units, as mentioned in Section 3.5, with the aim of obtaining an optimal solution for a day in advance. In this context, the CPU time required does not affect the validity of this proposal, which includes primary security constraints.

3.8 Conclusions

Numerical results obtained from the application of the proposed methodology are reported in this chapter. The comparison between the results presented in Sections 3.2 and 3.3 demonstrates the importance of including AC constraints in the UC problem, showing how the optimal scheduling of generators and the amount of gas required for gas-fired generators are affected by reactive power generation and nodal voltage magnitude constraints. Another important result demonstrates that the use of a DC power flow-based unit commitment approach is unrealistic because it does not satisfy the requirements of

reactive power and voltage magnitude profiles throughout the electric transmission grid. On the other hand, the results associated with the four different wind/load scenarios show how these variations affect the optimality of the generators' dispatch. Lastly, the results presented in Section 3.7 show how the primary frequency regulation affects the scheduling and power dispatches, where it is important to note that the proposed approach provides a scheduling and a dispatch of the available reserves for a day in advance from a load forecast. In this context, this proposal could be applied in a control center in order to maintain the frequency within limits and to ensure the security of the system.

Chapter 4

Conclusions and future work

4.1 Conclusions

Unlike all proposals that sequentially perform the short-term scheduling of natural gas and electricity infrastructures in the context of the unit commitment study, a generalized short-term unit commitment approach where the natural gas and electricity systems are fully represented in a unified framework of analysis is proposed in this research.

Instead of decomposing the generation scheduling into two subproblems, one considering only the electric power system and another related to the feasible operation of the natural gas network according to the fuel demanded by the dispatched gas-fired units, this thesis proposes a mathematical formulation of a unit commitment problem that is integrated with a multi-period nonlinear optimal gas and AC power flows approach. This allows to better represent the existing interdependence between both energy systems in terms of their physical and operational constraints. The integration of the AC optimal power flow into this formulation allows to incorporate those constraints associated with voltage limits and the reactive power dispatches, which are not considered when a DC model is used for the electricity network.

A generalized problem is formulated with a decomposable structure based on the concepts of duplication of variables, of augmented Lagrangian relaxation and of the auxiliary problem principle, which results in two mutually coupled optimization subproblems: one associated with the unit commitment and feasible operation of the electricity network and another one related to the co-optimization of both energy systems. The application of the Lagrangian relaxation technique transforms a large-scale problem into many small problems, which allows modeling the natural gas and electricity networks in more detail. The UC and GOPF subproblems are solved by dynamic programming and nonlinear programming, respectively, in a unified framework of analysis, with the aim to obtain the optimal hourly generation scheduling. Furthermore, the addition of limits associated with both reserve

capacity and frequency deviation to the OPF problem ensures that the demand and security constraints are satisfied. In this context, the feasible operation of both energy systems is assured by performing a co-optimization of the integrated multi-energy system.

The discussed numerical examples show how constraints associated with reactive power generation and nodal voltage magnitudes affect the optimal scheduling of generators, as well as the amount of natural gas demanded by thermal units. On the other hand, these results clearly show that the DC power flow-based unit commitment approaches, which do not consider those kinds of constraints, will require a further rescheduling of units in order to satisfy the real requirements of power generation. In this case, and compared to the results obtained when considering an AC power grid, the scheduling of generators is different because some gas-fired generators are not committed for some periods of time. This difference is due to the reactive power support that must be provided by generators when the power grid is modeled in detail.

This research also includes some case studies that consider different wind and speed load profiles. As expected, the variation in the demand for electricity and natural gas results in a different programming of thermal generators, which have to modify their active power outputs to meet the demand for electricity. This, in turn, modifies the amount of natural gas that flows through the pipelines because the nodal pressure changes in the natural gas network. A similar line of reasoning is applied to the variations of the wind speed profile. For example, the effect of a high wind speed profile results in a reduction of active power generated by thermal generators, decreasing the amount of gas flowing through the natural gas infrastructure. Therefore, the proposed approach should provide gas and power system operators with a more complete and reliable tool for the short-term planning of generator scheduling, which simultaneously provides the hourly solution of the operating status and power dispatch associated with each generator as well as the hourly state of operation of both networks over the entire planning horizon.

Lastly, the results presented show how security constraints associated with primary frequency regulation affect the scheduling and power dispatches, as well as the scheduling and a dispatch of the available reserves needed to balance total generation and demand, which simultaneously prevent the system frequency from drooping excessively. The results obtained clearly demonstrate that if there is a large imbalance between power generation and

load demand, the primary regulation will act properly only if there is a sufficient number of thermal units with adequate reserve capacity margins to cope with the existing imbalance. In this context, this proposal also could be applied in order to ensure the security of the system.

4.2 Future Work

The work reported in this Thesis can be extended in the following areas:

- The efficiency of the proposed approach should be compared to the one associated with the solution obtained by using MILP- or MINLP-based optimization solvers. This comparison will permit verifying the possible application of the proposal to performing short-term unit commitment studies in energy control centers.
- Line flow limits' constraints of both electrical and natural gas networks could be included in the formulation in order to analyze how these constraints affect the optimal scheduling of generators, as well as the amount of natural gas demanded by thermal units.
- For the UC formulation proposed in this research, it might be possible to include a shadow price to limit the power generation according to the availability of natural gas.
- To develop a more flexible natural gas network, the compressors could be modeled to provide a bidirectional flow gas through the pipelines by increasing or decreasing the pressure at their corresponding terminal nodes. This re-direction of the natural gas flow could help in situations contingencies in the energy infrastructure.
- A wind cost function can be included in the proposed UC model to evaluate the interaction between multi-energy systems within an economic context of renewable generators.
- This proposal could be extended by including a formulation and solution of the short-term unit commitment problem with simultaneous primary, secondary and tertiary reserves. The regulation of secondary generation reserve, also known as automatic generation control (AGC), must be provided to regulate the area-control error under load- following conditions. On the other hand, tertiary reserves provide generation or

demand flexibility that all operational constraints such as line flow and voltage magnitude limits after a great imbalance.

Appendix A
Appendix: Systems Data

Table A.1: 5 Nodes electric power system.

NODES												
Number	Name	Type	Voltage (pu)	Angle (grad)	Load		Generation		MVAR		Shunts	
					MW	MVAR	MW	MVAR	Max	Min	G	B
1	North	3	1.050	69	0	0	65	0	120	-120	0	0
2	South	0	1.050	69	20	10	65	0	120	-120	0	0
3	Lake	0	1.000	69	45	15	0	0	0	0	0	0
4	Main	0	1.000	69	40	5	50	0	0	0	0	0
5	Elm	0	1.000	69	60	10	0	0	0	0	0	0

Table A.2: Lines of 5 nodes electric power system.

TRANSMISSION ELEMENTS					
From	To	R (p.u.)	X (p.u.)	B/2 (p.u.)	TAP
1	2	0.0200	0.0600	0.0300	0
1	3	0.0800	0.2400	0.0250	0
2	3	0.0600	0.1800	0.0200	0
2	4	0.0600	0.1800	0.0200	0
2	5	0.0400	0.1200	0.0150	0
4	5	0.0800	0.2400	0.0250	0
3	4	0.0100	0.0300	0.0100	0

Table A.3: 118 Nodes electric power system.

NODES												
Number	Name	Type	Voltage (p.u.)	Angle(grad)	Load		Generation		MVAR		Shunts	
					MW	MVAR	MW	MVAR	Max	Min	G	B
1	Riverside	2	0.955	10.67	51	27	0	0	15	-5	0	0
2	Pokagon	0	0.971	11.22	20	9	0	0	0	0	0	0
3	HickryCk	0	0.968	11.56	39	10	0	0	0	0	0	0
4	NwCarlsl	2	0.998	15.28	30	12	-9	0	300	-300	0	0
5	Olive	0	1.002	15.73	0	0	0	0	0	0	0	-0.4
6	Kankakee	2	0.990	13.00	52	22	0	0	50	-13	0	0
7	JacksnRd	0	0.989	12.56	19	2	0	0	0	0	0	0
8	Olive	2	1.015	20.77	0	0	-28	0	300	-300	0	0
9	Bequine	0	1.043	28.02	0	0	0	0	0	0	0	0
10	Breed	2	1.050	35.61	0	0	450	0	200	-147	0	0
11	SouthBnd	0	0.985	12.72	70	23	0	0	0	0	0	0
12	TwinBrch	2	0.990	12.20	47	10	85	0	120	-35	0	0
13	Concord	0	0.968	11.35	34	16	0	0	0	0	0	0
14	GoshenJt	0	0.984	11.50	14	1	0	0	0	0	0	0
15	FtWayne	2	0.970	11.23	90	30	0	0	30	-10	0	0

Number	Name	Type	Voltage (pu)	Angle (grad)	Load		Generation		MVAR		Shunts	
					MW	MVAR	MW	MVAR	Max	Min	G	B
16	N. E.	0	0.984	11.91	25	10	0	0	0	0	0	0
17	Sorenson	0	0.995	13.74	11	3	0	0	0	0	0	0
18	McKinley	2	0.973	11.53	60	34	0	0	50	-16	0	0
19	Lincoln	2	0.963	11.05	45	25	0	0	24	-8	0	0
20	Adams	0	0.958	11.93	18	3	0	0	0	0	0	0
21	Jay	0	0.959	13.52	14	8	0	0	0	0	0	0
22	Randolph	0	0.970	16.08	10	5	0	0	0	0	0	0
23	CollCrnr	0	1.000	21.00	7	3	0	0	0	0	0	0
24	Trenton	2	0.992	20.89	0	0	-13	0	300	-300	0	0
25	TannrsCk	2	1.000	27.93	0	0	220	0	140	-47	0	0
26	TannrsCk	2	1.015	29.71	0	0	314	0	1000	-1000	0	0
27	Madison	2	0.968	15.35	62	13	-9	0	300	-300	0	0
28	Mullin	0	0.962	13.62	17	7	0	0	0	0	0	0
29	Grant	0	0.963	12.63	24	4	0	0	0	0	0	0
30	Sorenson	0	0.968	18.79	0	0	0	0	0	0	0	0
31	DeerCrk	2	0.967	12.75	43	27	7	0	300	-300	0	0
32	Delaware	2	0.964	14.80	59	23	0	0	42	-14	0	0
33	Haviland	0	0.972	10.63	23	9	0	0	0	0	0	0
34	Rockhill	2	0.986	11.30	59	26	0	0	24	-8	0	0.14
35	WestLima	0	0.981	10.87	33	9	0	0	0	0	0	0
36	Sterling	2	0.980	10.87	31	17	0	0	24	-8	0	0
37	EastLima	0	0.992	11.77	0	0	0	0	0	0	0	-0.25
38	EastLima	0	0.962	16.91	0	0	0	0	0	0	0	0
39	NwLibrty	0	0.970	8.41	27	11	0	0	0	0	0	0
40	West End	2	0.970	7.35	20	23	-46	0	300	-300	0	0
41	S.Ti-n	0	0.967	6.92	37	10	0	0	0	0	0	0
42	Howard	2	0.985	8.53	37	23	-59	0	300	-300	0	0
43	S.Kenton	0	0.978	11.28	18	7	0	0	0	0	0	0
44	WMVernon	0	0.985	13.82	16	8	0	0	0	0	0	0.1
45	N.Newark	0	0.987	15.67	53	22	0	0	0	0	0	0.1
46	W.Lancst	2	1.005	18.49	28	10	19	0	100	-100	0	0.1
47	Crooksvl	0	1.017	20.73	34	0	0	0	0	0	0	0
48	Zanesvll	0	1.021	19.93	20	11	0	0	0	0	0	0.15
49	Philo	2	1.025	20.94	87	30	204	0	210	-85	0	0
50	WCambrdg	0	1.001	18.90	17	4	0	0	0	0	0	0
51	Newcmrst	0	0.967	16.28	17	8	0	0	0	0	0	0
52	SCoshoct	0	0.957	15.32	18	5	0	0	0	0	0	0
53	Wooster	0	0.946	14.35	23	11	0	0	0	0	0	0
54	Torrey	2	0.955	15.26	113	32	48	0	300	-300	0	0
55	Wagenhls	2	0.952	14.90	63	22	0	0	23	-8	0	0
56	Sunnysde	2	0.954	15.16	84	18	0	0	15	-8	0	0
57	WNwPhil1	0	0.971	16.36	12	3	0	0	0	0	0	0
58	WNwPhil2	0	0.959	15.51	12	3	0	0	0	0	0	0
59	Tidd	2	0.985	19.37	277	113	155	0	180	-60	0	0
60	SWKammer	0	0.993	23.15	78	3	0	0	0	0	0	0
61	W.Kammer	2	0.995	24.04	0	0	160	0	300	-100	0	0
62	Natrium	2	0.998	23.43	77	14	0	0	20	-20	0	0
63	Tidd	0	0.969	22.75	0	0	0	0	0	0	0	0
64	Kammer	0	0.984	24.52	0	0	0	0	0	0	0	0
65	Muskngum1	2	1.005	27.65	0	0	391	0	200	-67	0	0
66	Muskngum2	2	1.000	27.48	39	18	392	0	200	-67	0	0
67	Summer	0	1.020	24.84	28	7	0	0	0	0	0	0

Number	Name	Type	Voltage (pu)	Angle (grad)	Load		Generation		MVAR		Shunts	
					MW	MVAR	MW	MVAR	Max	Min	G	B
68	Sporn1	0	1.003	27.55	0	0	0	0	0	0	0	0
69	Sporn2	3	1.035	30.00	0	0	516.4	0	300	-300	0	0
70	Portsmth	2	0.984	22.58	66	20	0	0	32	-10	0	0
71	NPortsmt	0	0.987	22.15	0	0	0	0	0	0	0	0
72	Hillsbro	2	0.980	20.98	0	0	-12	0	100	-100	0	0
73	Sargents	2	0.991	21.94	0	0	-6	0	100	-100	0	0
74	Bellefnt	2	0.958	21.64	68	27	0	0	9	-6	0	0.12
75	SthPoint	0	0.967	22.91	47	11	0	0	0	0	0	0
76	Darrah	2	0.943	21.77	68	36	0	0	23	-8	0	0
77	Turner	2	1.006	26.72	61	28	0	0	70	-20	0	0
78	Chemical	0	1.003	26.42	71	26	0	0	0	0	0	0
79	CapitlHl	0	1.009	26.72	39	32	0	0	0	0	0	0.2
80	CabinCrk	2	1.040	28.96	130	26	477	0	280	-165	0	0
81	Kanawha	0	0.997	28.10	0	0	0	0	0	0	0	0
82	Logan	0	0.989	27.24	54	27	0	0	0	0	0	0.2
83	Sprigg	0	0.985	28.42	20	10	0	0	0	0	0	0.1
84	BetsyLne	0	0.980	30.95	11	7	0	0	0	0	0	0
85	BeaverCk	2	0.985	32.51	24	15	0	0	23	-8	0	0
86	Hazard	0	0.987	31.14	21	10	0	0	0	0	0	0
87	Pinevlle	2	1.015	31.40	0	0	4	0	1000	-100	0	0
88	Fremont	0	0.987	35.64	48	10	0	0	0	0	0	0
89	ClinchRv	2	1.005	39.69	0	0	607	0	300	-210	0	0
90	Holston	2	0.985	33.29	78	42	-85	0	300	-300	0	0
91	HolstonT	2	0.980	33.31	0	0	-10	0	100	-100	0	0
92	Saltvlle	2	0.993	33.80	65	10	0	0	9	-3	0	0
93	Tazewell	0	0.987	30.79	12	7	0	0	0	0	0	0
94	Switchbk	0	0.991	28.64	30	16	0	0	0	0	0	0
95	Caldwell	0	0.981	27.67	42	31	0	0	0	0	0	0
96	Baileysv	0	0.993	27.51	38	15	0	0	0	0	0	0
97	Sundial	0	1.011	27.88	15	9	0	0	0	0	0	0
98	Bradley	0	1.024	27.40	34	8	0	0	0	0	0	0
99	Hinton	2	1.010	27.04	0	0	-42	0	100	-100	0	0
100	Glen Lyn	2	1.017	28.03	37	18	252	0	155	-50	0	0
101	Wythe	0	0.993	29.61	22	15	0	0	0	0	0	0
102	Smythe	0	0.991	32.30	5	3	0	0	0	0	0	0
103	Claytor	2	1.001	24.44	23	16	40	0	40	-15	0	0
104	Hancock	2	0.971	21.69	38	25	0	0	23	-8	0	0
105	Roanoke	2	0.965	20.57	31	26	0	0	23	-8	0	0.2
106	Cloverdl	0	0.962	20.32	43	16	0	0	0	0	0	0
107	Reusens	2	0.952	17.53	28	12	-22	0	200	-200	0	0.06
108	Blaine	0	0.967	19.38	2	1	0	0	0	0	0	0
109	Franklin	0	0.967	18.93	8	3	0	0	0	0	0	0
110	Fieldale	2	0.973	18.09	39	30	0	0	23	-8	0	0.06
111	DanRiver	2	0.980	19.74	0	0	36	0	1000	-100	0	0
112	Danville	2	0.975	14.99	25	13	-43	0	1000	-100	0	0
113	Deer Crk	2	0.993	13.74	0	0	-6	0	200	-100	0	0
114	WMedford	0	0.960	14.46	8	3	0	0	0	0	0	0
115	Medford	0	0.960	14.46	22	7	0	0	0	0	0	0
116	KygerCrk	2	1.005	27.12	0	0	-184	0	1000	-1000	0	0
117	Corey	0	0.974	10.67	20	8	0	0	0	0	0	0
118	WHuntngd	0	0.949	21.92	33	15	0	0	0	0	0	0

Table A.4: Lines of 118 nodes electric power system.

TRANSMISSION ELEMENTS																	
From	To	R	X	B/2	TAP	From	To	R	X	B/2	TAP	From	To	R	X	B/2	TAP
1	2	0.0303	0.0999	0.0254	0	46	47	0.0380	0.1270	0.0316	0	79	80	0.0156	0.0704	0.0187	0
1	3	0.0129	0.0424	0.0108	0	46	48	0.0600	0.1890	0.0472	0	68	81	0.0017	0.0202	0.8080	0
4	5	0.0018	0.0080	0.0021	0	47	49	0.0190	0.0620	0.0160	0	81	80	0	0.0370	0	0.935
3	5	0.0241	0.1080	0.0284	0	42	49	0.0710	0.3230	0.0860	0	77	82	0.0298	0.0853	0.0817	0
5	6	0.0119	0.0540	0.0143	0	42	49	0.0715	0.3230	0.0860	0	82	83	0.0112	0.0366	0.0380	0
6	7	0.0046	0.0208	0.0055	0	45	49	0.0684	0.1860	0.0444	0	83	84	0.0625	0.1320	0.0258	0
8	9	0.0024	0.0305	1.1620	0	48	49	0.0179	0.0505	0.0126	0	83	85	0.0430	0.1480	0.0348	0
8	5	0	0.0267	0	0.985	49	50	0.0267	0.0752	0.0187	0	84	85	0.0302	0.0641	0.0123	0
9	10	0.0026	0.0322	1.2300	0	49	51	0.0486	0.1370	0.0342	0	85	86	0.0350	0.1230	0.0276	0
4	11	0.0209	0.0688	0.0175	0	51	52	0.0203	0.0588	0.0140	0	86	87	0.0283	0.2074	0.0445	0
5	11	0.0203	0.0682	0.0174	0	52	53	0.0405	0.1635	0.0406	0	85	88	0.0200	0.1020	0.0276	0
11	12	0.0059	0.0196	0.0050	0	53	54	0.0263	0.1220	0.0310	0	85	89	0.0239	0.1730	0.0470	0
2	12	0.0187	0.0616	0.0157	0	49	54	0.0730	0.2890	0.0738	0	88	89	0.0139	0.0712	0.0193	0
3	12	0.0484	0.1600	0.0406	0	49	54	0.0869	0.2910	0.0730	0	89	90	0.0518	0.1880	0.0528	0
7	12	0.0086	0.0340	0.0087	0	54	55	0.0169	0.0707	0.0202	0	89	90	0.0238	0.0997	0.1060	0
11	13	0.0222	0.0731	0.0188	0	54	56	0.0027	0.0095	0.0073	0	90	91	0.0254	0.0836	0.0214	0
12	14	0.0215	0.0707	0.0182	0	55	56	0.0049	0.0151	0.0037	0	89	92	0.0099	0.0505	0.0548	0
13	15	0.0744	0.2444	0.0627	0	56	57	0.0343	0.0966	0.0242	0	89	92	0.0393	0.1581	0.0414	0
14	15	0.0595	0.1950	0.0502	0	50	57	0.0474	0.1340	0.0332	0	91	92	0.0387	0.1272	0.0327	0
12	16	0.0212	0.0834	0.0214	0	56	58	0.0343	0.0966	0.0242	0	92	93	0.0258	0.0848	0.0218	0
15	17	0.0132	0.0437	0.0444	0	51	58	0.0255	0.0719	0.0179	0	92	94	0.0481	0.1580	0.0406	0
16	17	0.0454	0.1801	0.0466	0	54	59	0.0503	0.2293	0.0598	0	93	94	0.0223	0.0732	0.0188	0
17	18	0.0123	0.0505	0.0130	0	56	59	0.0825	0.2510	0.0569	0	94	95	0.0132	0.0434	0.0111	0
18	19	0.0112	0.0493	0.0114	0	56	59	0.0803	0.2390	0.0536	0	80	96	0.0356	0.1820	0.0494	0
19	20	0.0252	0.1170	0.0298	0	55	59	0.0474	0.2158	0.0565	0	82	96	0.0162	0.0530	0.0544	0
15	19	0.0120	0.0394	0.0101	0	59	60	0.0317	0.1450	0.0376	0	94	96	0.0269	0.0869	0.0230	0
20	21	0.0183	0.0849	0.0216	0	59	61	0.0328	0.1500	0.0388	0	80	97	0.0183	0.0934	0.0254	0
21	22	0.0209	0.0970	0.0246	0	60	61	0.0026	0.0135	0.0146	0	80	98	0.0238	0.1080	0.0286	0
22	23	0.0342	0.1590	0.0404	0	60	62	0.0123	0.0561	0.0147	0	80	99	0.0454	0.2060	0.0546	0
23	24	0.0135	0.0492	0.0498	0	61	62	0.0082	0.0376	0.0098	0	92	100	0.0648	0.2950	0.0472	0
23	25	0.0156	0.0800	0.0864	0	63	59	0	0.0386	0	0.96	94	100	0.0178	0.0580	0.0604	0
26	25	0	0.0382	0	0.96	63	64	0.0017	0.0200	0.2160	0	95	96	0.0171	0.0547	0.0147	0
25	27	0.0318	0.1630	0.1764	0	64	61	0	0.0268	0	0.98	96	97	0.0173	0.0885	0.0240	0
27	28	0.0191	0.0855	0.0216	0	38	65	0.0090	0.0986	1.0460	0	98	100	0.0397	0.1790	0.0476	0
28	29	0.0237	0.0943	0.0238	0	64	65	0.0027	0.0302	0.3800	0	99	100	0.0180	0.0813	0.0216	0
30	17	0	0.0388	0	0.96	49	66	0.0180	0.0919	0.0248	0	100	101	0.0277	0.1262	0.0328	0
8	30	0.0043	0.0504	0.5140	0	49	66	0.0180	0.0919	0.0248	0	92	102	0.0123	0.0559	0.0146	0
26	30	0.0080	0.0860	0.9080	0	62	66	0.0482	0.2180	0.0578	0	101	102	0.0246	0.1120	0.0294	0
17	31	0.0474	0.1563	0.0399	0	62	67	0.0258	0.1170	0.0310	0	100	103	0.0160	0.0525	0.0536	0
29	31	0.0108	0.0331	0.0083	0	65	66	0	0.0400	0	0.93	100	104	0.0451	0.2040	0.0541	0
23	32	0.0317	0.1153	0.1173	0	66	67	0.0224	0.1015	0.0268	0	103	104	0.0466	0.1584	0.0407	0
31	32	0.0298	0.0985	0.0251	0	65	68	0.0014	0.0160	0.6380	0	103	105	0.0535	0.1625	0.0408	0
27	32	0.0229	0.0755	0.0193	0	47	69	0.0844	0.2778	0.0709	0	100	106	0.0605	0.2290	0.0620	0
15	33	0.0380	0.1244	0.0319	0	49	69	0.0985	0.3240	0.0828	0	104	105	0.0099	0.0378	0.0099	0
19	34	0.0752	0.2470	0.0632	0	68	69	0	0.0370	0	0.93	105	106	0.0140	0.0547	0.0143	0
35	36	0.0022	0.0102	0.0027	0	69	70	0.0300	0.1270	0.1220	0	105	107	0.0530	0.1830	0.0472	0
35	37	0.0110	0.0497	0.0132	0	24	70	0.0022	0.4115	0.1020	0	105	108	0.0261	0.0703	0.0184	0
33	37	0.0415	0.1420	0.0366	0	70	71	0.0088	0.0355	0.0088	0	106	107	0.0530	0.1830	0.0472	0
34	36	0.0087	0.0268	0.0057	0	24	72	0.0488	0.1960	0.0488	0	108	109	0.0105	0.0288	0.0076	0
34	37	0.0026	0.0094	0.0098	0	71	72	0.0446	0.1800	0.0444	0	103	110	0.0391	0.1813	0.0461	0
38	37	0	0.0375	0	0.93	71	73	0.0087	0.0454	0.0118	0	109	110	0.0278	0.0762	0.0202	0
37	39	0.0321	0.1060	0.0270	0	70	74	0.0401	0.1323	0.0337	0	110	111	0.0220	0.0755	0.0200	0
37	40	0.0593	0.1680	0.0420	0	70	75	0.0428	0.1410	0.0360	0	110	112	0.0247	0.0640	0.0620	0
30	38	0.0046	0.0540	0.4220	0	69	75	0.0405	0.1220	0.1240	0	17	113	0.0091	0.0301	0.0077	0
39	40	0.0184	0.0605	0.0155	0	74	75	0.0123	0.0406	0.0103	0	32	113	0.0615	0.2030	0.0518	0
40	41	0.0145	0.0487	0.0122	0	76	77	0.0444	0.1480	0.0368	0	32	114	0.0135	0.0612	0.0163	0
40	42	0.0555	0.1830	0.0466	0	69	77	0.0309	0.1010	0.1038	0	27	115	0.0164	0.0741	0.0197	0
41	42	0.0410	0.1350	0.0344	0	75	77	0.0601	0.1999	0.0498	0	114	115	0.0023	0.0104	0.0028	0
43	44	0.0608	0.2454	0.0607	0	77	78	0.0038	0.0124	0.0126	0	68	116	0.0003	0.0040	0.1640	0
34	43	0.0413	0.1681	0.0423	0	78	79	0.0055	0.0244	0.0065	0	12	117	0.0329	0.1400	0.0358	0
44	45	0.0224	0.0901	0.0224	0	77	80	0.0170	0.0485	0.0472	0	75	118	0.0145	0.0481	0.0120	0
45	46	0.0400	0.1356	0.0332	0	77	80	0.0294	0.1050	0.0228	0	76	118	0.0164	0.0544	0.0136	0

Table A.5: 3 Nodes natural gas network.

NODES							
Number	Type	Π (PSI)	Π*max* (PSI)	Π*min* (PSI)	Temperature (ºR)	Load (MMSCF)	Source (MMSCF)
1	0	725.188	1200	0.00	520	0.00	10.00
2	1	708.668	1200	0.00	520	2.54	0.00
3	1	707.036	1200	0.00	520	5.08	0.00

Table A.6: Pipelines of 3 nodes natural gas network.

PIPELINES					
From	To	Length (Mi)	Diameter (in)	Efficiency (%)	Temperature (ºR)
1	3	49.72	23.622	100	520
1	2	55.93	23.622	100	520
2	3	62.15	23.622	100	520

Table A.7: 15 Nodes natural gas network.

NODES							
Number	Type	Π (PSI)	Π*max* (PSI)	Π*min* (PSI)	Temperature (ºR)	Load (MMSCF)	Source (MMSCF)
1	0	1000.0	1200	0.00	520	0.00	10.00
2	0	1000.0	1200	0.00	520	1.25	6.87
3	1	729.7	1200	0.00	520	3.75	0.00
4	1	737.3	1200	0.00	520	0.00	0.00
5	1	575.5	1200	0.00	520	0.00	0.00
6	1	1035.0	1200	0.00	520	0.00	0.00
7	1	607.6	1200	0.00	520	0.00	0.00
8	1	1154.4	1200	0.00	520	0.00	0.00
9	1	918.6	1200	0.00	520	0.00	0.00
10	1	951.0	1200	0.00	520	0.00	0.00
11	1	932.8	1200	0.00	520	0.00	0.00
12	1	933.8	1200	0.00	520	4.58	0.00
13	1	601.6	1200	0.00	520	1.66	0.00
14	1	600.8	1200	0.00	520	3.75	0.00
15	1	600.0	1200	0.00	520	0.00	8.00

Table A.8: Pipelines of 15 nodes natural gas network.

PIPELINES					
From	To	Length (Mi)	Diameter (in)	Efficiency (%)	Temperature (ºR)
1	3	80.5	19.56	90	520
2	4	80.3	19.56	90	520
3	4	55.9	19.56	90	520
3	5	81.1	19.62	90	520
4	7	87.9	19.62	90	520
6	9	93.5	19.62	90	520
8	11	99.7	16.69	90	520
10	13	93.5	16.69	90	520
12	14	97.9	16.69	85	520
13	14	86.6	16.69	90	520
13	15	79.7	16.69	90	520
14	15	83.5	16.69	85	520

Table A.9: 15 Pipelines natural gas network.

COMPRESSORS				
From	To	Efficiency (%)	Compression ratio	Temperature (ºR)
5	6	83	1.6	520
7	8	84	1.8	520
9	10	83	1.3	520
11	12	84	1.8	520

Bibliography

[Alabdulwahab 2015] A. Alabdulwahab, A. Abusorrah, X. Zhang, M. Shahidehpour, "Coordination of interdependent natural gas and electricity infrastructures for firming the variability of wind energy in stochastic day-ahead scheduling", IEEE Trans Sust Energy, Vol. 6, pp. 606-615, March 2015.

[Alabdulwahab 2017] A. Alabdulwahab, A. Abusorrah, X. Zhang, M. Shahidehpour, "Stochastic security-constrained scheduling of coordinated electricity and natural gas infrastructures", IEEE Syst J., Vol. 11, pp. 1674-1683, September 2017.

[Alvarez 2002] C. Alvarez, A. J. Conejo, "Control de frecuencia y de tensiones", Análisis y operación de sistemas de energía eléctrica, McGraw-Hill, pp. 217-219, 2002.

[An 2003] S. An, Q. Li, T. Gedra, "Natural gas and electricity optimal power flow", In: Proc of the IEEE PES Trans and Dist Conf and Exp, pp. 138-143, September 2003.

[Badakhshan 2015] S. Badakhshan, M. Kazemi, M. Ehsan, "Security-constrained unit commitment with flexibility in natural gas transmission delivery", J. Nat. Gas Science and Engineering, Vol. 27, pp. 632-640, November 2015.

[Bai 2015] Y. Bai, H. Zhong, Q. Xia, C. Kanf, L. Xie, "A decomposition method for network-constrained unit commitment under wih AC power flow constraints", Energy, Vol. 88, pp. 595-603, August 2015.

[Baldick 1995] R. Baldick, "The generalized unit commitment problem", IEEE Trans Power Syst., Vol. 10, pp. 465-475, February 1995.

[Batut 1992] J. Batut, A. Renaud, “Daily generation scheduling optimization with transmission constraints: a new class of algorithms”, IEEE Trans Power Syst., Vol. 7, pp. 982-989, August 1992.

[Belloni 2003] A. Belloni, A. L. Diniz, M. E. P. Maceira and C. A. Sagastizabal, “Bundle relaxation and primal recovery in unit commitment problems-the Brazilian case”, Annals of Operations Research, Vol. 120, pp. 21-44, April 2003.

[Biskas 2014] P. N. Biskas ; N. G. Kanelakis, “Co-optimization of electricity day-ahead market and steady-state natural gas system using Augmented Lagrangian”, *11th International Conference on the European Energy Market (EEM14), IEEE 2014*, May 28-30, 2014.

[Biskas 2018] P.N. Biskas, N.G. Kanelakis, A. Papamatthaiou, I Alexandridis, “Coupled optimization of electricity and natural gas systems using augmented Lagrangian and an alternating minimization method”, Int J Electr Power Energy Syst., Vol. 80, pp. 202-218, September 2016.

[Bragin 2016] M.A. Bragin, P.B. Luh, J.H. Yan, G.A. Stern, “Natural gas and electricity optimal power flow”, In: Proc of the IEEE PES General Meeting, pp. 1-5, July, 2016.

[Castillo 2016] A. Castillo, C. Laird, C.A. Silva-Monroy, J.P. Watson, R.P. O'Neill, “The unit commitment problem with AC optimal power flow constraints”, IEEE Trans Power Syst., Vol. 31, pp. 4853-4866, November 2016.

[Chaudry 2014] M. Chaudry, N. Jenkins, Qadrdan M. Qadrdan, J. Wu, “Combined gas and electricity network expansion planning”, Appl Energy, Vol 113, pp. 1171-1187, January 2014.

[Clegg 2015] S. Clegg, P. Mancarella, "Integrated Electrical and Gas Network Flexibility Assessment in Low-Carbon Multi-Energy Systems", IEEE Transactions on Sustainable Energy, Volume: 7, no. 2, pp. 718-731, April 2016.

[Cohen 1980] G. Cohen, "Auxiliary problem principle and decomposition of optimization problems", J Optim Theory and Appl., Vol. 32, pp. 277-305, November 1980.

[Correa-Posada 2015] C.M. Correa-Posada, P. Sánchez-Martín, "Security-constrained unit commitment with dynamic gas constraints", In: Proc of the IEEE Power & Energy Society General Meeting, pp. 1-5, 2015.

[Damavandi 2011] M.Y. Damavandi, I. Kiaei, M.K. Sheikh-El-Eslami, H. Seifi, "New approach to gas network modeling in unit commitment", Energy, Vol. 36, pp. 6243-6250, 2011.

[Goldfarb 1999] D. Goldfarb, R. Polyak,K. Scheinberg and I. Yuzefovich, "A modified barrier-augmented Lagrangian method for constrained minimization", Comp. Optimization and Appl., Vol. 14, pp. 55-74, 1999.

[Guan 1996] X. Guan, R. Baldick, W. Liu, "Integrating power system scheduling and optimal power flow", In: Proc of the 12th Power Syst Comp Conf., pp. 717-23, 1996.

[He 2017] Y. He, M. Shahidehpour, Z. Li, C. Guo and B. Zhu, "Robust constrained operation of integrated electricity-natural gas system considering distributed natural gas storage", IEEE Trans Sust. Energy, Vol. 99, pp. 1-10, 2017.

[Kariniotakis 2006] G.N. Kariniotakis, I. Marti, T. S. Nielsen, G. Giebel, J. Tambke, I. Waldl, J. Usaola, R. Brownsword, G. Kallos, U. Focken, I. Sanchez,

N. Hatziargyriou, A.M. Palomares and P. Frayssinet, “Advanced short-term forecasting of wind generation-Anemos”, IEEE Trans Power Syst. 2006; invited paper to Special Section on Power Syst Performance Issues Associates with Wind Energy.

[Knowles 2010] D. Knowless, “Lagrangian Duality for Dummies”, November 2010.

[Liu 2009] C. Liu, M. Shahidehpour, Y. Fu, Z. Li, “Security-constrained unit commitment with natural gas transmission constraints’, IEEE Trans Power Syst., Vol. 24, pp. 1523-1536, August 2009.

[Liu 2010] C. Liu, M. Shahidehpour, J. Wang, “Application of augmented Lagrangian relaxation to coordinate scheduling of interdependent hydrothermal power and natural gas systems”. IET. Gen., Trans. Dist., Vol. 4, pp. 1314-1325, December 2010.

[Liu 2011] C. Liu, M. Shahidehpour, J. Wang, “Coordinated scheduling of electricity and natural gas infrastructures with a transient model for natural gas flow”, Chaos: Interdiscipl J Nonlin Sci., Vol. 21, June 2011.

[Martinez-Mares 2012] A. Martinez-Mares, C.R. Fuerte-Esquivel, “A unified gas and power flow analysis in natural gas and electricity coupled networks”, IEEE Trans Power Syst., Vol. 27, pp. 2156-2166, November 2012.

[Moritz 2007] S. Moritz, “A mixed-integer approach for the transient case of gas network optimization”, PhD Thesis, Technischen Universitat Darmstadt, 2007.

[Murillo-Sánchez 1997] C. Murillo-Sánchez, R.J. Thomas, Thermal unit commitment including optimal AC power flow constraints. In: Proc of the Hawaii Int Conf on Syst Sci., pp. 81-88, 1997.

[Murillo-Sánchez 2000] C. Murillo-Sánchez, R.J. Thomas, "Parallel processing implementation of the unit commitment problem with full AC power flow constraints", In: Proc of the Hawaii Int Conf on Syst Sci, pp. 1-9, 2000.

[Murillo-Sánchez 2001] C. Murillo-Sánchez and R. Thomas, "Thermal unit commitment with a nonlinear AC power flow network model," in The Next Generation of Electric Power Unit Commitment Models. Norwell, MA, USA: Kluwer Academic, 2001, Ch. 5.

[Godinez-Fernández 2019] Godinez-Fernández S.A. Head of the department of financial transmission rights, CENACE, personal communication with Dr. Fuerte-Esquivel, July 15, 2019.

[Power System Test Case Archive] Power Systems Test Case Archive. [Online], Available: http://www.ee.washington.edu/research/pstca/

[Qadrdan 2014] M. Qadrdan, J. Wu, N. Jenkins, J. Ekanayake, "Operating strategies for a GB integrated gas and electricity network considering the uncertainty in wind power forecasts', IEEE Trans Sust Energy. Vol. 5, pp. 128-138, January 2014.

[Reipin 2018] I. Riepin, T. Mobius, F. Müsgens, "Integrated Electricity and Gas Market Modeling-Effects of Gas Demand Uncertainty" In: Proc of the IEEE 15th Int Conf on the European Energy Market, Lodz, Poland, September 2018.

[Restrepo 2005] J. Restrepo, ""Unit Commitment with Primary Frequency Regulatio Constraints in Electric Power Systems", M. E. dissertation, department of Electrical and Computer Engineering, McGill University, Montreal, Quebec, Canada, February 2005.

[Shahidehpour 2005] M. Shahidehpour, Y. Fu, T. Wiedman, "Impact of natural gas infrastructure on electric power systems", In: Proc of the IEEE, Vol. 93, pp. 1042-1056, May 2005.

[Stagg 1968] G.H Stagg, A.H. El-Abiad, "Computer Methods in Power System Analysis", McGraw-Hill, New York, NY, 1968.

[Takigawa 2012] F.Y.K. Takigawa, E.L. da Silva, E.C. Finardi and R.N. Rodrigues, "Solving the hydrothermal scheduling problem considering network constraints", Electr. Power Syst. Res., Vol. 88, pp. 89-77, July 2012.

[Tao 1998] W.Q. Tao, H.C. Ti, "Transient analysis of gas pipeline network", Chemical Eng. J., Vol. 69, pp. 47-52, 1998.

[Wood 1996] A. J. Wood, B.F. Wollenberg, "Power Generation Operation and Control", 2nd ed., NY: Wiley, 1996.

[Zhang 2016] X. Zhang, M. Shahidehpour, A. Alabdulwahab, A. Abusorrah, "Hourly electricity demand response in the stochastic day-ahead scheduling of coordinated electricity and natural gas networks", IEEE Trans Power Syst., Vol. 31, pp. 592-601, 2016.

[Zhao 2017] B. Zhao, A.J. Conejo amd R. Sioshansi, "Unit commitment under gas-supply uncertainty and gas-price variability", IEEE Trans Power Syst., Vol. 32, pp. 2394-2405, May 2017.